63-3-3

FTD-TT-62-768

402 800

TRANSLATION

STABILIZATION OF A FLAME AND THE DEVELOPMENT OF THE COMBUSTION PROCESS IN TURBULENT FLOW
(SELECTED PARTS)

FOREIGN TECHNOLOGY DIVISION

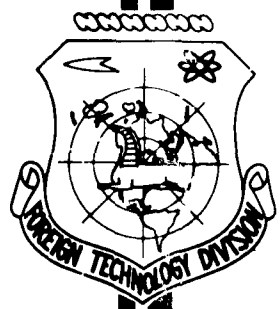

AIR FORCE SYSTEMS COMMAND

WRIGHT-PATTERSON AIR FORCE BASE

OHIO

UNEDITED ROUGH DRAFT TRANSLATION

STABILIZATION OF A FLAME AND THE DEVELOPMENT OF THE COMBUSTION PROCESS.IN TURBULENT FLOW (SELECTED PARTS)

English Pages: 141

SOURCE: Russian Book, Stabilizatsiya Plameni i Razvitiye Protessa Sgoraniya v Turbulentnom Potoke, Oborongiz, Moskva, 1961, pp. 31-148

S/5752
S/262-62-0-6

PREPARED BY:

TRANSLATION SERVICES BRANCH
FOREIGN TECHNOLOGY DIVISION
WP-AFB, OHIO.

TABLE OF CONTENTS

INFLUENCE OF TURBULENCE PARAMETERS ON THE VELOCITY OF FLAME PROPAGATION

Candidate of Technical Sciences G.M. Gorbunov

The development of air-breathing jet engines has obliged us to organize new work on the study of the combustion of atomized liquid fuel in a rapidly moving stream. However, the exceeding complexity of the real working combustion process in which the final results are influenced by several factors which are difficult to differentiate, has made it necessary in the overwhelming majority of cases to simplify the problem by carrying out the investigation on a previously prepared homogeneous mixture. This pertains in equal degree to theoretical as well as to experimental work.

Without going into a detailed analysis of the theories in which an attempt is made to explain the mechanism whereby the flame propagation velocity increases in a turbulent stream, we can merely note that based on the premises used by the authors of the various theories in the analysis of the turbulent flame, all the theoretical investigations can be broken up into three main groups.

In the theoretical investigations of the first group the authors reach the conclusions that in the case of a large-scale turbulence the main influence on the magnitude of the turbulent flame-front propagation velocity u_t is exerted by the mean square pulsating component of the velocity w', and to a lesser degree by the excess-air coefficient α. The latter quantity influences u_t not directly, but via the normal combustion velocity u_n. Experimental results obtained by the adherents

of this theory are usually generalized by means of an experimental formula of the form

$$u_t = A(w')^n (u_n)^m,$$

where A is a constant factor greater than unity while n and m are constant coefficients, with $n \gg m$ and $(m + n) = 1$.

The magnitude of the turbulence scale l does not exert any influence on u_t, if this scale exceeds appreciably the width of the laminar flame front. The values of the constant coefficients A, n, and m obtained by various authors differed, owing to differences in the methods used to determine the principal quantities. It is characteristic that the coefficient A assumed values between 2.5 and 5.3 in the experimental formulas. Some authors attributed the last circumstance to the fact that in the mechanism where the flame jumps from the hot gases back to the fresh mixture a decisive influence is exerted not by the batches whose velocity is close to the mean square pulsating velocity, but the fastest moving batches, whose pulsating velocity is two, three, and more times larger than the average pulsating velocity. These high-speed batches indeed determine the jumping of the flame back to the fresh mixture, and consequently, the rate of advance of the forward boundary of the combustion zone – the flame front.

In the theoretical investigations of the second group, the growth in the turbulent combustion velocity u_t with increasing turbulence is attributed to a growth in the turbulent exchange coefficient $D_t = w'l$ or to a growth in the Reynolds number $Re = Hw/\nu$, where H is the characteristic dimension of the stream. Replacing the values of H and w in the Reynolds number by the geometrical similarity criterion (the Strouhal number $Sh = H/l$) and by the kinematic similarity criterion (intensity of turbulence $\varepsilon = w'/w$), we obtain

$$Re = \frac{Sh\, lw'}{\varepsilon\nu} \approx \text{const}\, lw'.$$

Thus, according to these theories, the turbulent combustion velocity u_t should depend both on the pulsating velocity component w' and on the turbulence scale $\underline{l}$.

Finally, the third group includes theories whose authors believe that the principal factor accelerating the transport of the flame is autoturbulization in the flame itself.

In various experimental investigations, set up for the purpose of verifying theories, and also to obtain experimental values of u_t as functions of the mixture composition and the characteristics of the turbulence, different procedures were employed.

In most studies of the flame characteristics in a moving turbulent stream of a homogeneous mixture, the flame front surface was assumed to be the forward boundary of the flame. The definition of this boundary was carried out on the basis of the start in the change of temperature, total head, and one of the gas components, determined by gas analysis, direct and shadow photography of the flame, or measurement of the ionization current.

Experimental investigations of the dependence of u_t on the turbulence parameters are usually carried out within the core of a free turbulent jet in direct or inverted cones (see Fig. 1). Measurements of the turbulence intensity show* that the values of ε increase both from the axis toward the boundaries of the core of the jet, and along the core of the jet. Therefore in determining u_t by the use of the relation of V.A. Mikhel'son ($u_t = w \cos \varphi$) or the ratio of the areas $u_t = wF_0/F_{kon}$, it is necessary to refer the value of u_t to that value of w', which actually prevailed in the region where the flame front was situated.

If, for example, we confine ourselves to the measurement of turbulence on the axis of the jet behind the nozzle (see Fig. 1a), and

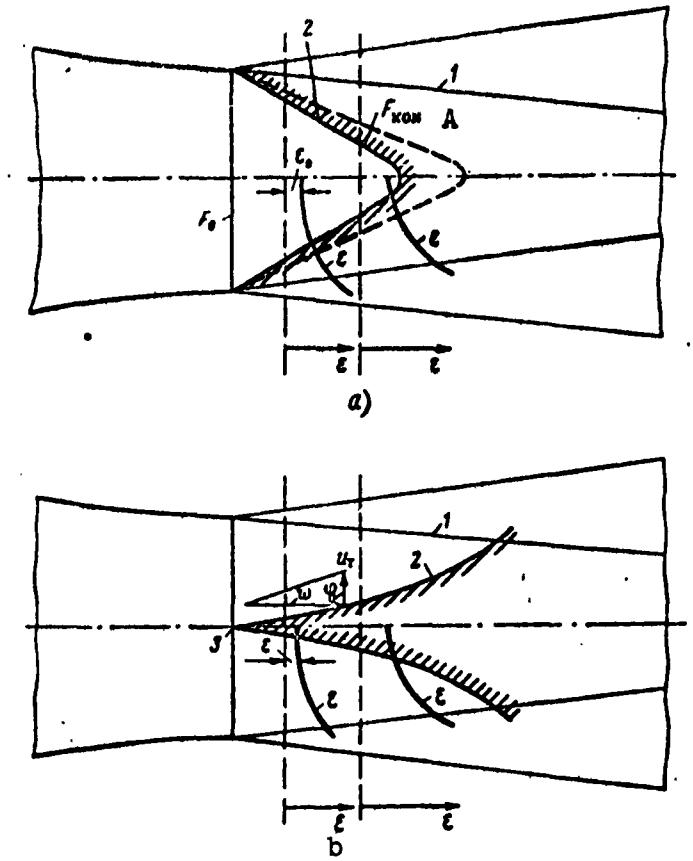

Fig. 1. Illustrating the determination of u_t in a free turbulent jet. a) Direct cone; b) inversed cone; 1) core of jet; 2) flame front; 3) igniting burner. A) Cone.

the value of the turbulent velocity u_t determined from the direct cone is referred to $w'_0 = \varepsilon_0 w$, then, other conditions being equal, the value of the constant coefficient A_0 in the experimental formula for the determination of u_t will be larger than the true value A. Let us consider this by means of an example.

Let the determination of u_t be carried out at two velocities at the exit from the nozzle. For these velocities, w_1 and w_2, we determine u_{t1} and u_{t2}, respectively: $w'_{01} = \varepsilon_0 w_1$ and $w'_{02} = \varepsilon_0 w_2$. The data obtained are plotted (Fig. 2a) on a logarithmic scale and we obtain A_0 and

$$n_0 = \frac{\lg u_\tau - \lg A_0}{\lg w'_0} = \operatorname{tg} \alpha_0.$$

The theoretical formula will have the form

$$u_{\tau 0} = A_0 (w'_0)^{n_0}.$$

But in fact the flame front is located in regions where $\varepsilon > \varepsilon_0$. Let us assume that $n = 1$; then as the velocity is increased (other conditions being equal) the flame front will remain in a fixed position. It is known that for natural turbulence the intensity of the turbulence ε at any point of the core of the jet is independent of the stream velocity w. Then at the point where the flame front exists the condition $w' = kw'_0$ will always be satisfied, where $k > 1$. Were the same velocities u_{t1} and u_{t2} to be referred to the true values of the pulsating velocities w'_1 and w'_2, we would obtain the true value of the coefficient A, which is less than A_0:

$$u_t = A(w')'.$$

Inasmuch as $u_{t0} = u_t$, we get $A_0(w')_0 = A(w')$ and

$$A = A_0 \frac{w'_0}{w'} = A_0 \frac{w'_0}{kw'_0} = \frac{A_0}{k}.$$

According to the data of most investigators, however, $n < 1$.

In this case when the velocity increases from w_1 to w_2, the flame front occupies the position indicated dotted in Fig. 1a, and goes over to those portions of the core, where the values of ε and w' are greater than in the first position.

After determining from the Mikhel'son relation or from the ratio of the areas the values of the turbulent velocities for two stream velocities, $(u_{t1})_n$ and $(u_{t2})_n$, as well as the true values of the pulsating components w'_1 and w'_2, and again using logarithmic coordinates, we can determine the true values of A_n and $n = \tan \alpha_n$ (see Fig. 2b). Were the obtained values of the flame velocities $(u_{t1})_n$ and $(u_{t2})_n$ to be referred to the pulsating velocities on the jet axis, w'_{01} and w'_{02},

we would obtain values A_0 and $n_0 = \tan \alpha_0$ different from the real ones (see Fig. 2b).

The foregoing examples show that to obtain correct data it is necessary to refer the combustion velocity to the values of the pulsation velocities at the points where u_t is determined, as was indeed done in the present work.

A comparison of the results of the measurement of u_t by different authors, other conditions being equal, indicates that there are considerable discrepancies in the values of u_t, reaching 30 or 50% and even more.

In the present work we undertook to ascertain the degree to which a particular method of determining the forward boundary of the combustion zone influences the experimentally determined value of u_t, and whether other characteristics of the turbulent stream (in addition to w') exert any influence on the velocity of turbulent propagation of the flame front u_t. In particular, the task was to check whether the character of the spectrum of the turbulent stream influences the value of u_t. In the case of artificial turbulization of the stream, usually produced by passing the stream through grids with various geometric parameters, one can conceive of cases when two streams are obtained with identical value of the average pulsating velocity component w', but with different spectrum of pulsation velocities. If in one of these streams the number of pulsations with velocity exceeding the average one (w') by several times is larger than in the other, then in such a stream the turbulent flame should propagate with greater velocity, although the values of w', $\underline{l}$, and u_n will be the same in either case.

The principal diagram of the setup on which the experiments were carried out is shown in Fig. 3. The flow of air delivered to the ex-

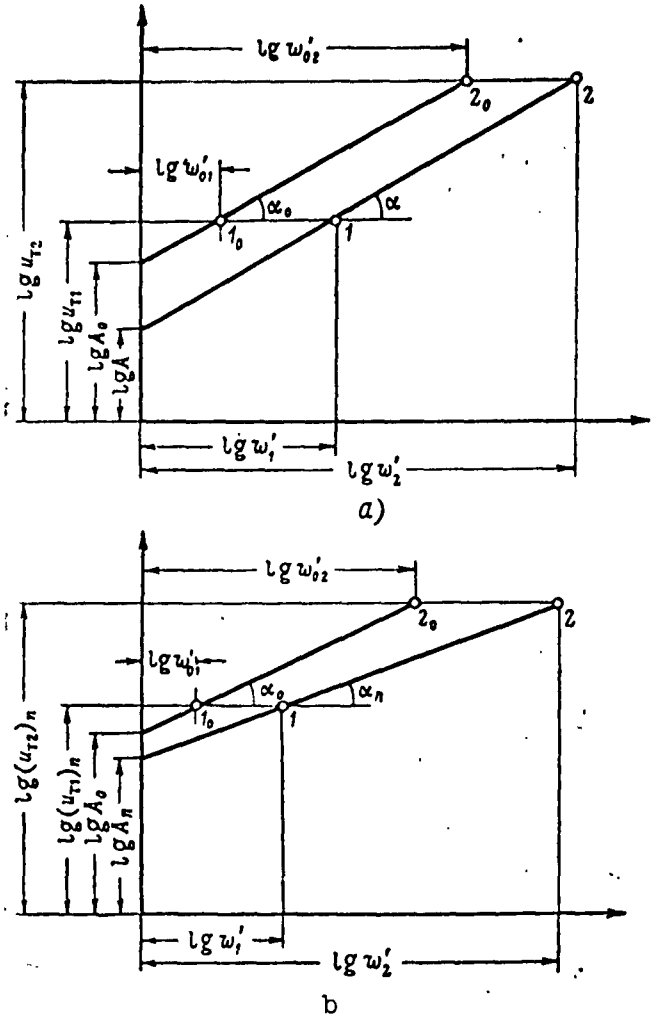

Fig. 2. The dependence $u_t = f(w')$ in logarithmic coordinates.

perimental stand was measured by a usual gasdynamic method. The fuel, B-70 gasoline, was introduced into the mixing chamber by centrifugal nozzles. To ensure good pulverization of the fuel, depending on the required consumption, one, two, or more nozzles were turned on, so that the pressure of the fuel ahead of the nozzles was not less than 10 atm. The mixture was then fed through a 15-meter tube, where the fuel drops were completely evaporated, something monitored many times by means of special apparatus (the OMK instrument). The fuel consump-

tion was measured by a volume method.

At the exit from the mixing tubes, depending on the required velocity, nozzles were installed with inlet aperture diameters of 280 or 154 mm. The nozzles were profiled in accordance with the recommendations of Ye. Vitoshinskiy and made of sheet material by a pressure method.

To ignite the homogeneous mixture, a burner with an outlet hole diameter 1.5 mm, operating with a gasoline-air mixture with oxygen added, was installed 50 mm away from the rake of the nozzle, opposite its center. The igniting burner was fed from a special generator.

The turbulizing grids were secured to the rake of the nozzle. Before carrying out the combustion experiments, experiments were made to determine the characteristics of the turbulence in the core of the jets for different nozzles and for different turbulizing grids (see the first article of the present collection).

All the main investigations were carried out in the core of the jet, and the measurements were made in a horizontal plane coinciding with the axis of the jet. To install the instruments, a special coordinate unit was constructed, which made it possible to place the sensitive elements of the instruments at any point of the investigated plane with accuracy ± 0.5 mm. The coordinates of the position of the sensitive element were measured against special scales of the coordinate unit. In addition, the coordinate unit was provided with a device (electrical path marker), which made it possible to record on a loop oscillograph the longitudinal displacement of the instrument. The coordinate unit was rigidly connected to the nozzle during the time of the experiment.

In carrying out the basic experiments, the following measurement apparatus was used:

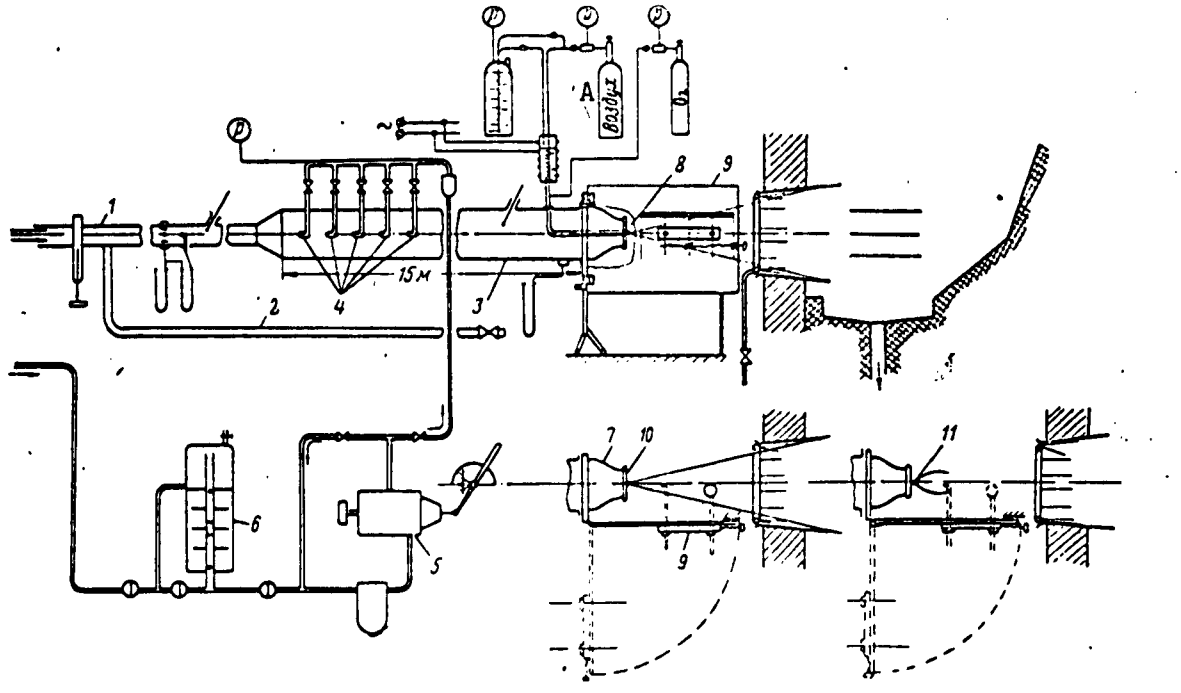

Fig. 3. Schematic diagram of the setup. 1) Air duct; 2) air bypass; 3) mixing chamber; 4) nozzles; 5) fuel pump; 6) volume flow meter for fuel; 7) profiled nozzle; 8) igniting burner; 9) panel with coordinate unit; 10) turbulizing grid; 11) stabilizer. A) Air.

1) instrument for measuring the ionization of the gas, consisting of a transducer, amplifier, path marker, and recorder (MPO-2 loop oscillograph). The transducer was of the two-electrode type, with a gap of 1 mm between copper electrodes;

2) small-size total-head fitting with water-cooled housing. The receiver tube had a diameter of about 1.5 mm;

3) platinum-rhodium/platinum thermocouple with U-shaped open junction. The diameter of the electrodes was 0.3 mm. The place of the electrode junction was stripped to the initial diameter of the wires;

4) instrument for determination of the local fuel concentration (OMK), based on the well-known property of the magnetic susceptibility of oxygen. The instrument made it possible to determine the loss of oxygen in a gasoline-air mixture as the latter is burned up. The cool-

ing gas sampler had an inlet aperture 3 mm in diameter;

5) standard "Kiev" camera for flame photography. The photography was with a neutral filter, using an exposure of 2 seconds. Along with the flame, ruled scales were photographed so as to determine the dimensions of the photographed torch of the flame.

When working with so-called "inverted cones," in view of the heat released in the combustion zone, the initial current lines along which it is necessary to investigate the variation of the different gas parameters become curved. To determine the mutual placement of the current lines for a given combustion mode of the flame, the following procedure was used.

In five sections (Fig. 4), at a specified operating condition, measurements were made of the temperature field, the total pressure heads, and the static pressures. The currents were measured every 10 or 5 mm, in the zone of the greater gradient of the measured quantity. The velocity fields were plotted from these data. The specific gravities of the gas γ_1 at the measurement points were calculated.

Every 5 mm from the axis of the torch, in the direction of the radius, calculations were made of the current density

$$dG/dF = w\gamma.$$

The values of the flow per unit length of the segment were calculated

$$\frac{dG}{dr} = \frac{dG}{dF} 2\pi r,$$

where r is the distance from the axis to the limit of the segment.

The following quantity was determined

$$\left(\frac{dG}{dr}\right)_{cp} = \frac{\left(\frac{dG}{dr}\right)_k + \left(\frac{dG}{dr}\right)_{k+1}}{2},$$

where k is the serial number of the flow division boundary; the flow rate of gas on the chosen segment

$$\Delta G = \left(\frac{dG}{dr}\right)_{cp} \Delta r$$

and the flow of gas in the entire section

$$G_n = \Delta G_1 + \Delta G_2 + \ldots + \Delta G_n,$$

where n is the number of elementary segments.

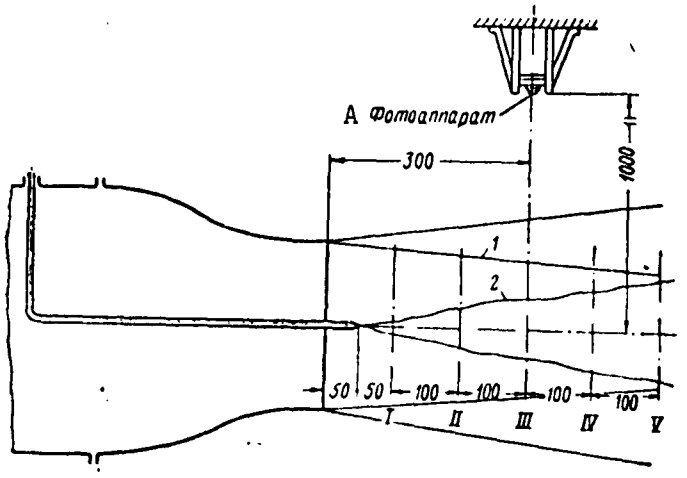

Fig. 4. Diagram of jet and torch of the flame. 1) Limits of the core of the jet; 2) outer limits of the torch of the flame. A) Camera.

Curves of G = f(r) were plotted for each of the sections in which the measurements were made, and were then combined on a single graph (Fig. 5).

By drawing a horizontal line through the flow curves, it is easy to determine from the points of intersection the radii of the points in sections I, II, etc., through which the lines of equal flow, i.e., the current lines will pass.

The coordinates of the current lines determined in this manner for various preselected operating modes have shcwn that the current lines within the core of the jet are quite close to straight lines, which make for each mode a separate small angle with the jet axis. This circumstance has made it possible to use for the investigation of the parameters of the flow along the current lines the same coordinate

unit, but in this case the entire panel with the coordinate-unit plate was inclined at an appropriate angle relative to the initial position so that the receiving element of the instrument followed the current line exactly as the coordinate unit was displaced longitudinally.

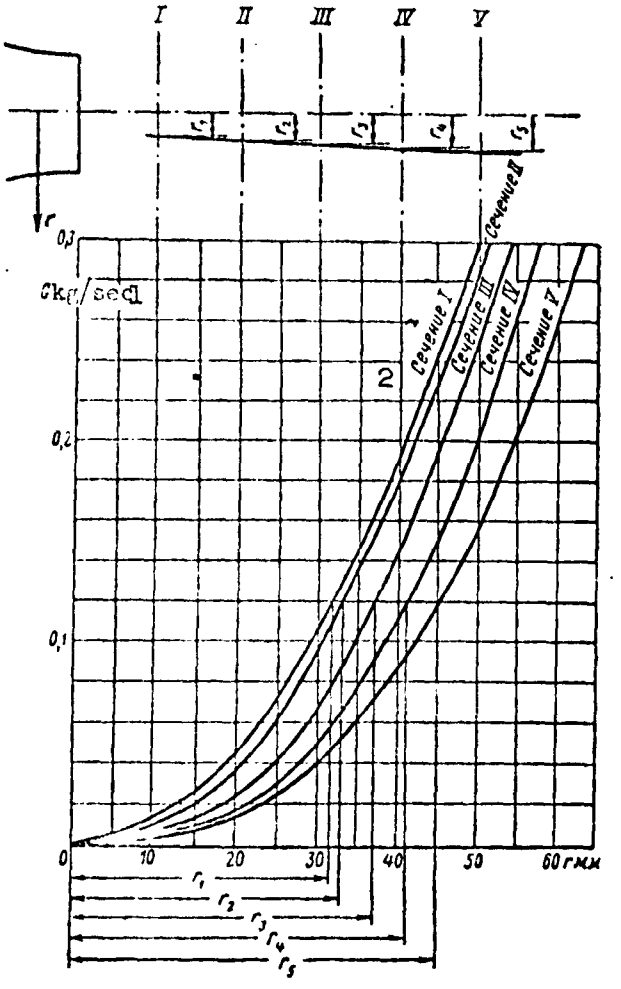

Fig. 5. Variation of gas flow along the radius of the jet (and the torch of the flame) at different sections. 1) kg/sec; 2) section.

An investigation of the turbulence characteristics (see the first article of the present collection) made it possible to choose for the study turbulent streams such as would permit separation of the independent variables of interest to us. For experiments with a flame, a

large nozzle (BS) was chosen with a free exhaust (S) and with two grids "2" and "5." The parameters of the turbulent flows in section II are listed in Table 1.

TABLE 1

2 Параметр	1 Объект		
	БС-С	БС-2	БС-5
$\varepsilon\%$	~5	6,53	6,5
l мм	~125	~1,7	~1,6
$\omega_{ср}\frac{1}{сек.}$ 3	~100	~625	~680
$w' = f(\omega)$	4 Фиг. 6	Фиг. 7	Фиг. 8

1) Object; 2) parameter; 3) sec; 4) Fig.

The intensity magnitudes and the transverse turbulence scales for the grids are presented with corrections for the length of the filament, introduced by the Dryden method.

Figures 6, 7, and 8 show the spectra of the pulsation velocities. If it is assumed that the variation of the velocity at a given point of the turbulent stream follows a sinusoidal law, then the pulsation frequency n can be regarded as the number of pulsations. The largest pulsation velocity corresponds to a frequency of 66 cps for BS-S, 100 cps for BS-2, and 140 cps for BS-5.

Thus, it can be assumed that for the same intensity of turbulence in the streams BS-2 and BS-5, the stream of BS-5 will contain a larger number of pulsations with maximum pulsating velocity component.

Figure 9 shows by way of an example the results of experiments on the investigation of the parameters of the gas over the sections of a turbulent torch and over several current lines for BS-S.

The values of the total pressure head, the temperature, and oxygen content were measured along the current lines No. 1, 4, and 2 every 3 mm. In addition, the variation of the ionization current was recorded

on an oscillograph and the torch was photographed with long exposure (1.5-2 sec).

The front of the flame can be assumed to be the geometric locus of the points on the longitudinal section of the torch, at which one of the measured quantities (i.e., T^*, Δp^*, etc.) begins to change in value.

In the lower part of Fig. 9 are plotted the positions of the flame fronts as determined by the start of the temperature rise, the drop in the total pressure head, the start of the ionization-current bursts, the change in the oxygen, and the start of visible glow on the photograph, all as determined by the performed measurements. The boundaries of the flame, determined by various methods, do not agree with one another.

Let us disregard pulsations in the stream and let us consider the average motion of a particle along the current line.

If a particle of fresh mixture moves along the current line (we choose for further analysis the central current line No. 4), then at some point in it there will be observed an increase in temperature, corresponding to a position of the flame front as determined by the start of the rise in temperature; on further motion, glow will begin in this particle, as can be determined by photography; at the same place one observes the first bursts in the ionization current and finally by the start of the decrease in the oxygen (based on gas analysis).

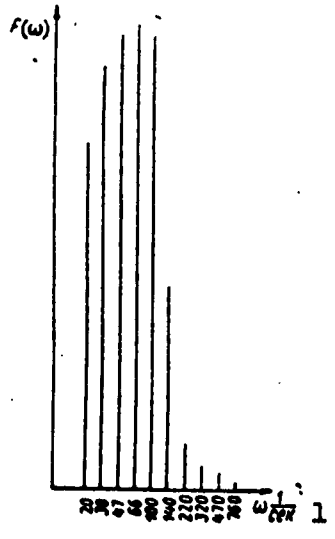

Fig. 6. Spectrum of pulsation velocities in free jet. 1) sec.

Whereas in the direction transverse to the torch axis the distance between the ex-

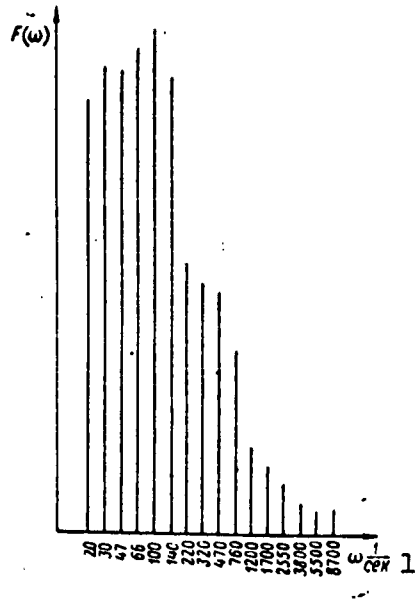

Fig. 7. Spectrum of pulsation velocities behind grid "2." 1) sec.

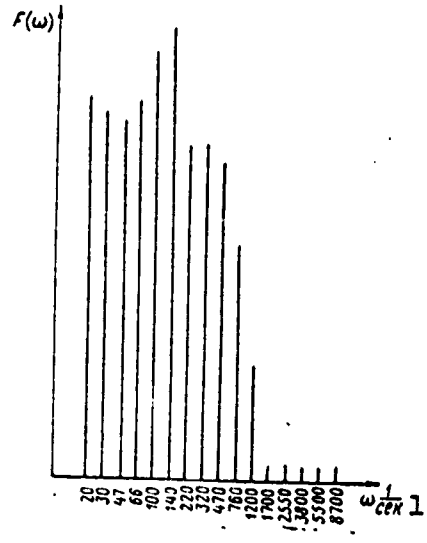

Fig. 8. Spectrum of pulsation velocities behind grid "5." 1) sec.

treme positions of the flame fronts, determined by the starts of the changes in T*, I, Δp*, etc., amounts in the initial sections to several millimeters (in section IV this quantity amounts to about 25 mm), along the current lines this quantity amounts to about 100 mm. If it is assumed that the velocity along the current line remains constant, then the value of u_t determined by the Mikhel'son law will depend only on the value of the angle between the current line and the tangent to the given flame front at the point of intersection. It is quite obvious that the largest value of u_t should be obtained when this quantity is determined in accordance with the forward front of the flame (in accordance with the temperature), and the smallest value should be obtained when the determination is based on the flame front as determined by the variation of the oxygen concentration. It is necessary to bear in mind here that the intensity of the turbulence along the current lines does not remain constant.

Figure 10 shows, in accordance with the data obtained in Fig. 9,

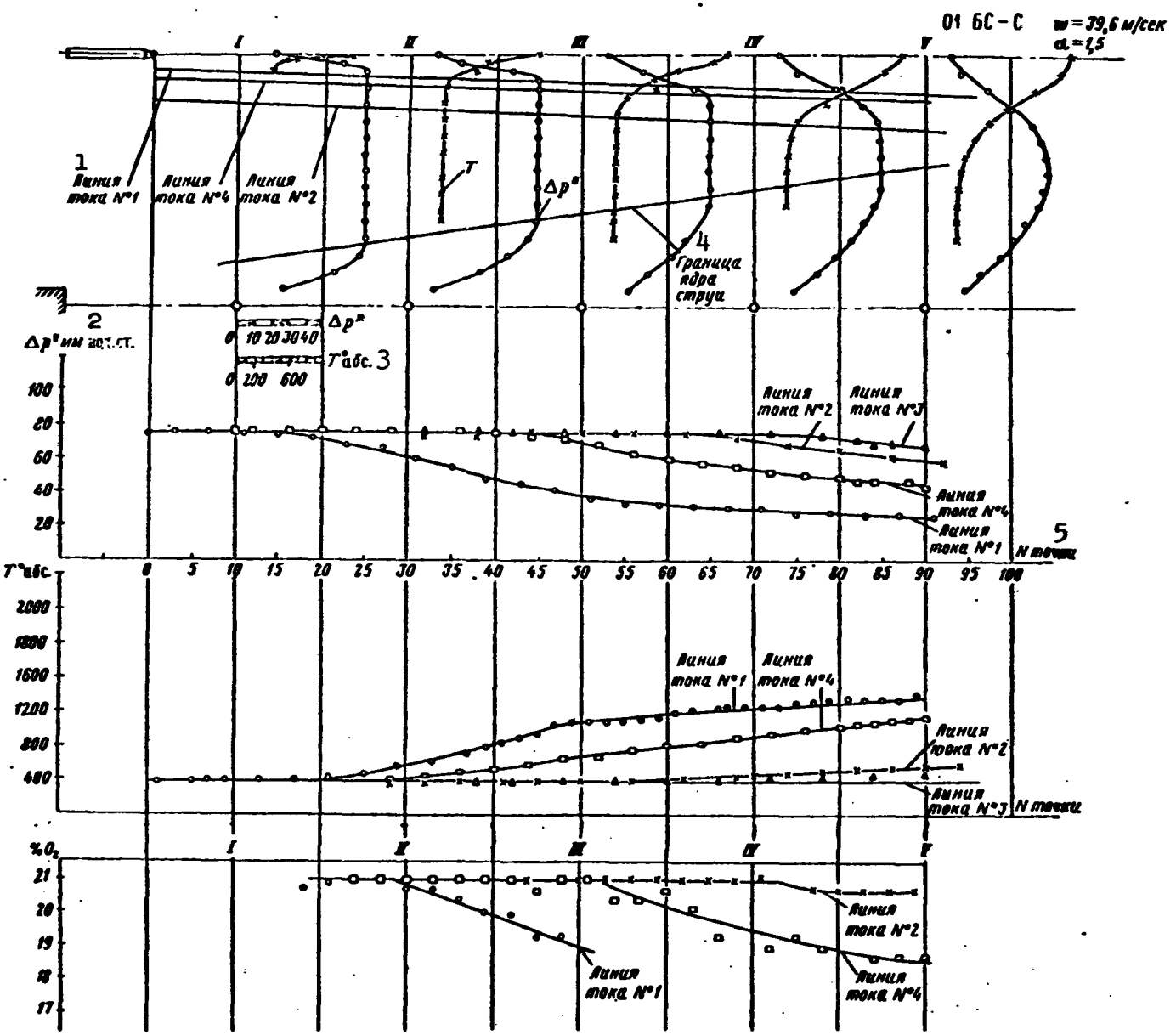
01 БС-С
w = 79,6 м/сек
α = 1,5
I
II
III
IV
V
1
Линия тока N°1
Линия тока N°4
Линия тока N°2
T
Δp°
4
Граница ядра струи
2
Δp° мм вод.ст.
Δp°
0 10 20 30 40
T°абс. 3
0 200 600
100
80
60
40
20
Линия тока N°2
Линия тока N°3
Линия тока N°4
Линия тока N°1
5
N точки
0 5 10 15 20 25 30 35 40 45 50 55 60 65 70 75 80 85 90 95 100
T°абс.
2000
1800
1600
1200
800
400
Линия тока N°1
Линия тока N°4
Линия тока N°2
Линия тока N°3
N точки
%O2
21
20
19
18
17
Линия тока N°2
Линия тока N°1
Линия тока N°4

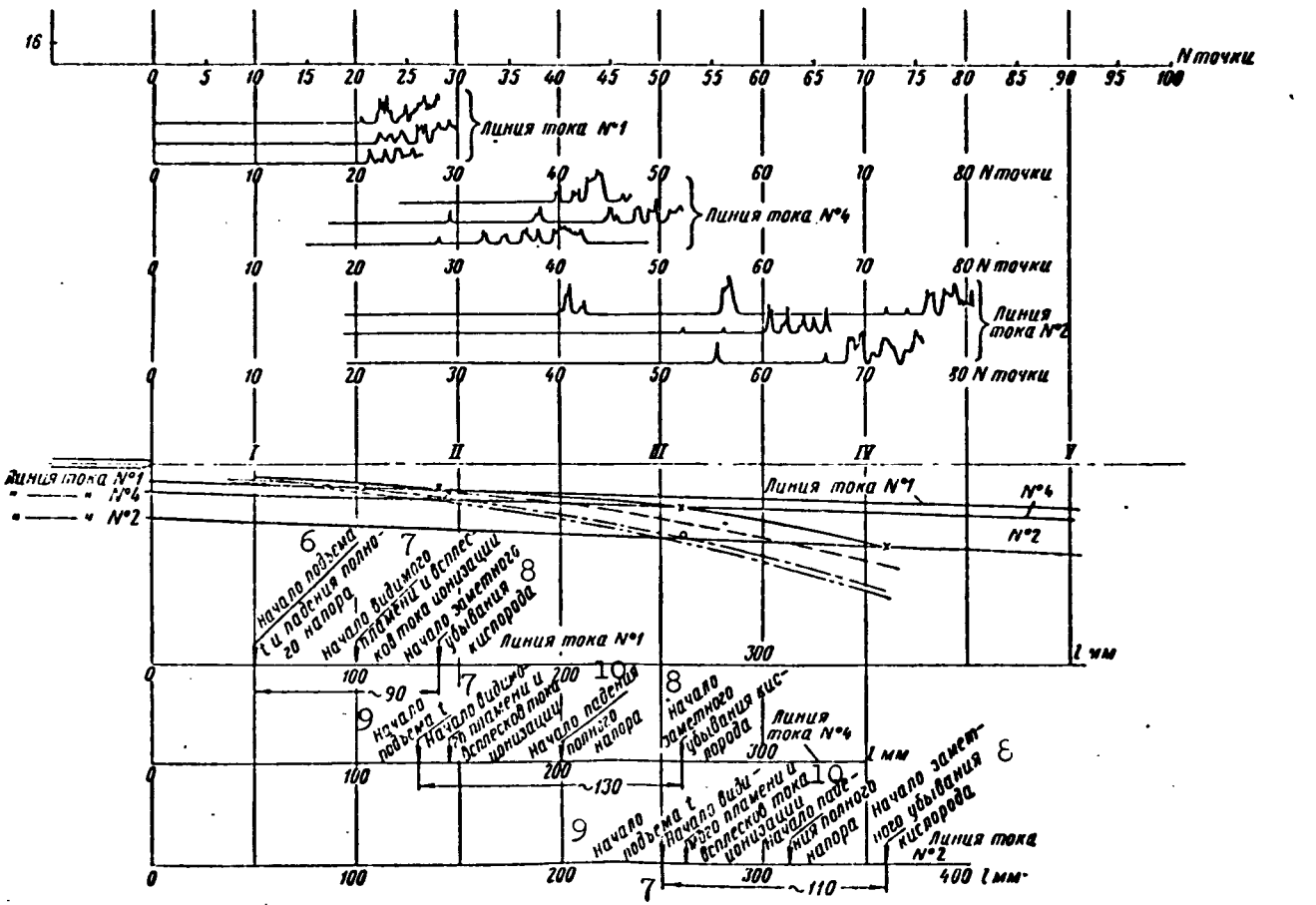

Fig. 9. Results of experiment on the determination of the forward boundary of the combustion zone (the flame front), for different current lines, using measurements of the total pressure head, the temperature, the oxygen contents, the gas ionization, and direct photography. 1) Current line; 2) mm water; 3) absolute; 4) boundary of core of jet; 5) number of point; 6) start of rise in t and of drop of total pressure head; 7) start of visible flame and ionization-current bursts; 8) start of noticeable decrease in oxygen; 9) start of rise in t; 10) start of drop in total pressure head.

the values of u_t as a function of w'. The values of w' for the corresponding points of the stream were chosen without account of autoturbulization (see Fig. 6a of the first article of the present collection). It is quite understandable that from two or three points it is impossible to determine correctly the slope of the curve $u_t = f(w')$ on the given section. At the same time, the data of Fig. 10, as well as logical reasoning, lead to the conclusion that the experimental values of u_t are the smaller, the closer to the axis the conditional flame surface is determined. Thus, for example, in the present case the values of u_t, determined in accordance with the front constructed on the basis of the variation of the oxygen content, are considerably smaller than the values of u_t determined from the front constructed on the basis of the drop in total pressure head, photography, or temperature fields.

Taken by itself, the disagreement between the starts of the changes in T*, the ionization, Δp^*, and the oxygen-content in the turbulent stream, in which the mechanism whereby the matter (concentration) is transported is the same as the mechanism of heat transfer, is little likely, but this fact was confirmed in experiments made by different authors.

The explanation must be sought probably in the following.

Deep in the turbulent torch of the flame, where the increase in the average temperature of the mixture reaches 100-300°, intensive burning up of the fuel begins. If one moves from this point deep into the torch along the current line or along the radius of the torch, it is there that the maximum temperature gradient is observed. The chemical composition of the mixture also begins to change noticeably. Obviously, an instrument which measures the variation of the oxygen concentration along the current line will note the start of the change at

a point corresponding to the sensitivity threshold of the instrument. When the instruments TI and OMK were used, the point where the change in $O_2(\alpha)$ began corresponded to a temperature rise by 100-300°.

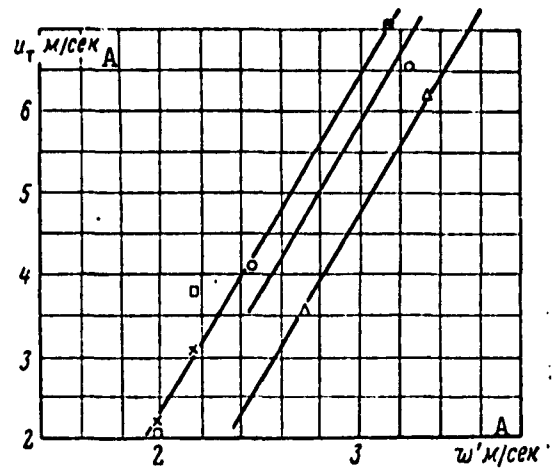

Fig. 10. Dependence $u_t = f(w')$, determined from measurements of different parameters. □) Determined from start of rise in temperature; X) from visible boundary of torch on the photograph; o) from start of drop in total pressure; Δ) from start of decrease in oxygen content. A) m/sec.

However, hot batches of gas are ejected from this zone to the periphery of the torch, where they can be detected by an ionization transducer. Their luminosity is sufficiently high to be recorded on photographic film with long exposure. But the relative mass of the hot batches is small here, and the instruments employed do not detect changes in the concentration.

At a certain distance from the torch axis, the ejected batches either burn up completely, or cease to burn as a result of mixing with fresh mixture and reduction in the reaction rate resulting from the drop in temperature. In this case the torch does not glow and all the ionization transducer records are very rare bursts. The thermocouple, on the other hand, notes an increase in temperature.

A similar change in the parameters was obtained also in other experiments by us.

From the physical point of view, the most correct way to determine the forward boundary of the combustion zone would be to measure the ionization current, but methodological difficulties arise here, too, for it is not known which of the bursts are accidental and which are reliable.

For an open torch, a very convenient method is to photograph the torch. The flame front determined on the photograph practically coincides with the front determined by measuring the ionization current (if one takes the average position of the individual bursts, see Fig. 9).

In the later experiments u_t was determined either from the "temperature" flame front, or from the front obtained on the photograph.

It must be noted that, independently of the method used to determine the flame front, the method wherein u_t is determined by the angle between the direction of the current line and the tangent to the flame front is inaccurate. Even under most careful reduction of the experimental data and when a geodetic protractor is used a large spread in the values of u_t is obtained.

The experimental data presented show that the choice of the method for determining the flame front predetermines also the values obtained for u_t. Thus, the difference in the values of u_t, obtained by different authors, may be attributed to the choice of different procedures for determining the main quantities.

Let us return to the question of the influence of the frequency spectrum of the stream and the turbulence scale on the values of u_t.

The procedure outlined above (with allowance for the deviations of the current lines) was used to determine the values of u_t at con-

stant value of the excess-air coefficient ($\alpha = 1.25$) in section II behind a large nozzle without a grid (BS-S) and with grids "2" and "5" (the position of the flame front was determined by noting the start of the temperature rise). Table 2 lists the data obtained.

TABLE 2

2 Параметр	1 Объект		
	БС-С	БС-2	БС-5
3 w' м/сек	2,3	3,12	2,86
u_t м/сек	5,76	8,5	11,4
l мм	125	1,7	1,6
$w' = f(\omega)$	4 Фиг. 6	Фиг. 7	Фиг. 8

1) Object; 2) parameter; 3) m/sec; 4) Fig.

The data presented show that u_t is apparently influenced by the frequency spectrum.

Indeed, for BS-5 the value of w' (with account of the correction for the length of the thermoanemometer filament) is less than for BS-2. The scales are approximately the same. On the other hand, the value of u_t is 34% larger for BS-5 than for BS-2.

Comparison of Figs. 7 and 8 shows that the frequency spectrum for BS-5 has larger values of pulsation velocity components in the region of medium frequencies than the frequency spectrum for BS-2.

This probably explains the larger value of u_t for BS-5 compared with its value for BS-2. It can be assumed that in the BS-5 jet there is a larger number of pulsations having larger pulsating velocity components (larger than the mean square value w'). This is what causes the faster transport of the flame, i.e., the larger values of u_t. In the case of BS-S the larger values of the pulsating velocity components are concentrated in the low-frequency part of the spectrum and u_t has a smaller value than for BS-2 and BS-5.

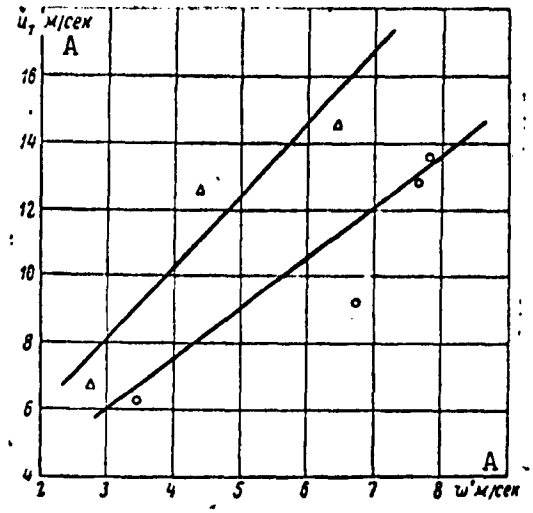

Fig. 11. Dependence $u_t = f(w')$ behind grids with different frequency spectra. Δ) Grid "5"; O) grid "2." A) m/sec.

The turbulence scale apparently does not influence u_t. The scale in the case of BS-S is approximately 75 times larger than for BS-5, but u_t for BS-S is almost half that of BS-5 for nearly equal values of w'. The main influence on the value of u_t (apart from w') is exerted by the frequency spectrum.

Experiments on the determination of the influence of the frequency spectrum of the stream on the value of u_t were carried out with the same grids "2" and "5" using a small nozzle (MS-2 and MS-5). The procedure used to determine the main quantities remained the same. The results of the experiments, shown in Fig. 11, confirm that the values of the turbulent flame-front propagation velocities u_t behind grid "5," which gives larger values of the pulsating velocities in the high-frequency part of the spectrum than grid "2," turn out to be larger.

Thus, the value of u_t, other conditions being equal, depends on the frequency spectrum of the turbulent stream, something not accounted for in any of the investigations known to us. In connection with the influence of the frequency spectrum, the structure of the formula em-

ployed in many papers for the turbulent velocity, namely

$$u_\tau = A(w')^n (u_n)^m$$

is not sufficiently universal.

Manuscript Page No.

[Footnote]

3 See Figs. 6-10 in the first article of the present collection.

Manuscript Page No.

[List of Transliterated Symbols]

1 т = t = turbulentnyy = turbulent

1 н = n = normal'nyy = normal

3 кон = kon = konus = cone

10 ср = sr = srednyy = average

INVESTIGATION OF PROPAGATION AND STABILIZATION OF A FLAME BEHIND A TROUGH-SHAPED STABILIZER

Candidate of Technical Sciences E.L. Solokhin

One of the main requirements imposed on ramjet combustion chambers is the maintenance in them of a stable combustion process over a sufficiently wide range of velocities, pressures, temperatures, and excess-air coefficients. The range of variation of these parameters is determined by the type and purpose of the engine.

Stable combustion in ramjet chambers is guaranteed by installing in them various poorly streamlined bodies, behind which a backflow zone is produced, filled with hot gases which ensure continuous ignition of the fresh combustible mixture.

However, neither the experimental nor the theoretical papers have dealt sufficiently with the structure of the backflow zone, the mechanism of exchange between this zone and the active stream, and their response to various parameters.

The insufficiency of the experimental data from which to judge the physical picture of the phenomenon makes it difficult to develop a rigorous theory of flame stabilization behind poorly streamlined bodies, so that the following was undertaken in the present work:

1) accumulation of experimental data on the variation of the dimensions of the backflow zone behind poorly streamlined trough-shaped stabilizers for a wide variation of stream parameters (velocity, turbulence, mixture composition α), and on the influence of the stabilizer dimensions;

2) investigation of the time-averaged temperature field, fuel concentration, ionization, and turbulence in the backflow zone at modes close to lean flameout;

3) attempts to explain the exchange mechanism between the backflow zone and the active stream and the influence of the stream parameters on the flameout characteristics of the stabilizers.

An experimental study of the stream behind a stabilizer was carried out starting from the following notions. The backflow zone is the result of turbulent exchange between the gas located in the feed region of the body and the active stream. Instruments placed in the backflow zone indicate a positive velocity head in some definite direction. The latter indicates that there exists in the backflow zone a definite stream direction, which prevails over the direction of the mass transport. This enables us to determine lines which delineate equal flows ("jets"), between which constant turbulent mass exchange, energy exchange, etc. take place. These lines can be determined by starting from the flow equation, so as to analyze further the changes of the gas parameter along the "jets."

The diagram of such a flow is shown in Fig. 1. Let us consider this diagram. Behind the stabilizer is formed a circulation zone, which encompasses both the backflow zone and that part of the forward stream which is adjacent to the backflow zone. The per-second flow of gas through the forward stream of the circulation zone (c) is equal to the per-second flow of gas through the backflow zone. Beyond the boundaries of the circulation zone is located the active stream (a).

An experimental investigation of the flow of gas was carried out in an initial portion of a blunted axially symmetrical turbulent jet of a homogeneous gasoline-air mixture.

Since the purpose of the investigation was to determine the pre-

flameout modes with a lean mixture, we first plotted the characteristics of the lean flameout behind the stabilizers employed. In the investigation of the flow, the excess-air coefficient was always set equal to $\alpha = 0.9\alpha_{sr}$.

Wherever possible, a comparison was made of the values of the individual stream parameters, obtained in one and the same mode by different methods. Thus, temperatures measured with thermocouples and calculated from the results of gas analysis were compared (see Fig. 13 below); the pressures were obtained with a thermoanemometer and compared with those obtained after processing the fields of the temperatures, static pressures, and total heads; the dimensions of the backflow zone, measured by means of a special fitting and obtained from processing of the velocity fields were also compared (see Fig. 17 below). The agreement of the results was found to be quite satisfactory.

1. EXPERIMENTAL SETUP AND OBJECTS OF INVESTIGATION

The experiments were carried out with the setup shown in Fig. 3 of the second article of the present collection.

To obtain in the jet turbulence with different characteristics, grids were used, the characteristics of which are presented in the first article of the present collection.

The construction of the stabilizers employed is shown in Fig. 2. The spread angle of the stabilizers was chosen to be 60°, and the heights 2h were, respectively, 60, 30, 20, and 10 mm. The stabilizers were secured to the nozzle by means of aerodynamic posts at a distance of 22 mm from the outer boundaries of the nozzle, so that no atmospheric air should have entered into the backflow zone. A check has shown that this actually was the case.

In the preliminary experiments it was established that the intensity of the turbulence changes with distance from the rake of the noz-

zle, and therefore all the stabilizers were installed with their rakes at an equal distance from the nozzle, thus guaranteeing formation of backflow zones in stabilizers of different size at identical turbulence intensity.

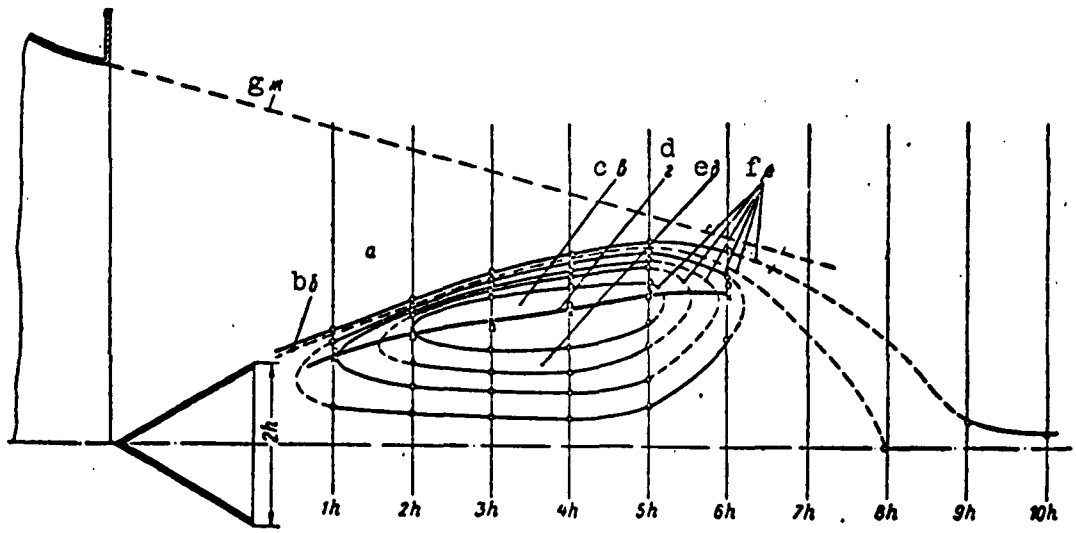

Fig. 1. Diagram showing flow of gas behind the stabilizer. a) Active stream; b) boundary of circulation zone; c) forward stream of circulation zone; d) boundary of backflow zone; e) backward flow of circulation zone (backflow zone); f) lines delineating the "jets" of equal flows (current lines); g) boundary of core of free jet.

The cross sections for the measurement of the stream characteristics in the backflow zone behind the stabilizers were located at distances 1h, 2h, 3h, etc. Thus, independently of the dimensions of the stabilizers, the number of investigated sections in the backflow zone remained approximately the same.

The apparatus used for the measurement of pressures, temperatures, fuel concentrations, ionization current, and also the procedure for processing the experimental data were the same as in [1].

2. RESULTS OF THE EXPERIMENTS

Figure 3 shows the flameout characteristics with lean mixture plotted behind different stabilizers with the velocity of the incident stream ranging from 30 to 190 m/sec. The curves divide the field of

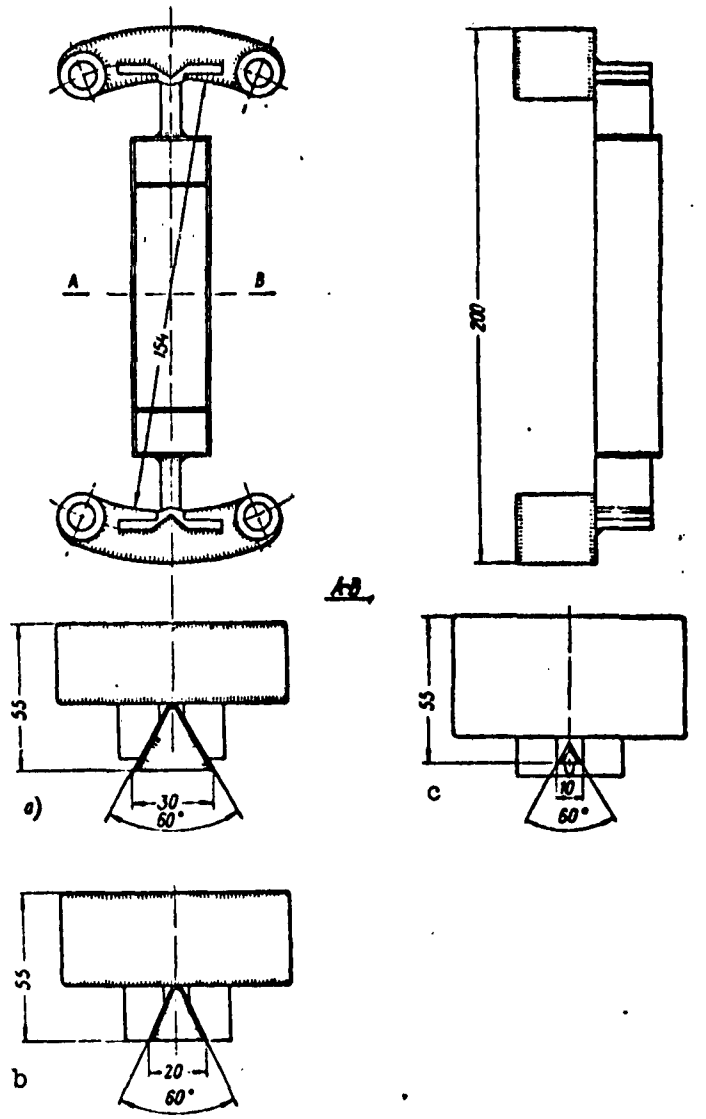

Fig. 2. Construction of stabilizers. a) Stabilizer with 2h = 30 mm; b) stabilizer with 2h = = 20 mm; c) stabilizer with 2h = 10 mm.

the drawing into two regions: upper – above the curve, in which the combustion is impossible under the given conditions, and lower – region of stable combustion. The stability of the combustion deteriorates both with increasing velocity of the incoming stream and with increasing dimensions of the stabilizers.

Figure 4 shows the dependence of α_{sr} on the initial stream turbulence. With increasing initial turbulence, α_{sr} decreases.

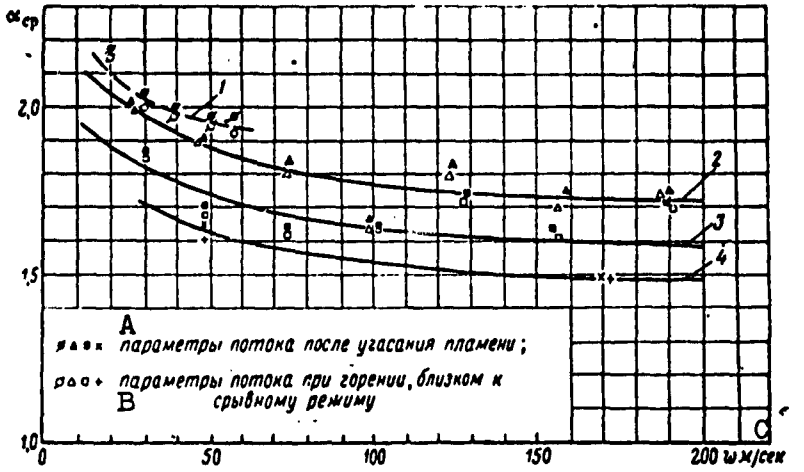

Fig. 3. Flameout characteristics of stabilizers of different dimensions. 1) Stabilizer with 2h = 60 mm; 2) stabilizer with 2h = 30 mm; 3) stabilizer with 2h = 20 mm; 4) stabilizer with 2h = 10 mm. A) Stream parameters after extinction of flame; B) stream parameters during combustion close to flameout mode; C) m/sec.

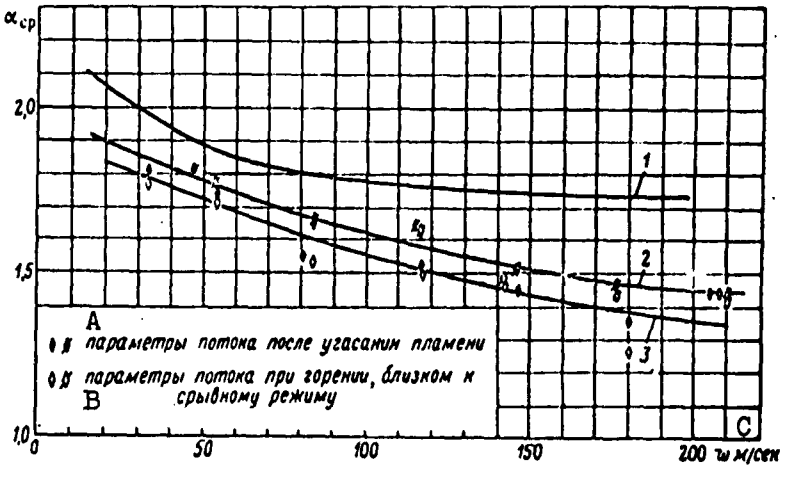

Fig. 4. Variation of flameout characteristics of stabilizer with 2h = 30 mm as a function of the initial stream turbulence. 1) In free jet at the rake of the stabilizer $\varepsilon \approx 2.5\%$; 2) behind grid No. 5, at the rake of the stabilizer at $\varepsilon \approx 10\%$; 3) behind grid No. 2, at the rake of the stabilizer $\varepsilon \approx 15\%$. A) Stream parameters after extinction of flame; B) stream parameters during combustion close to flameout mode; C) m/sec.

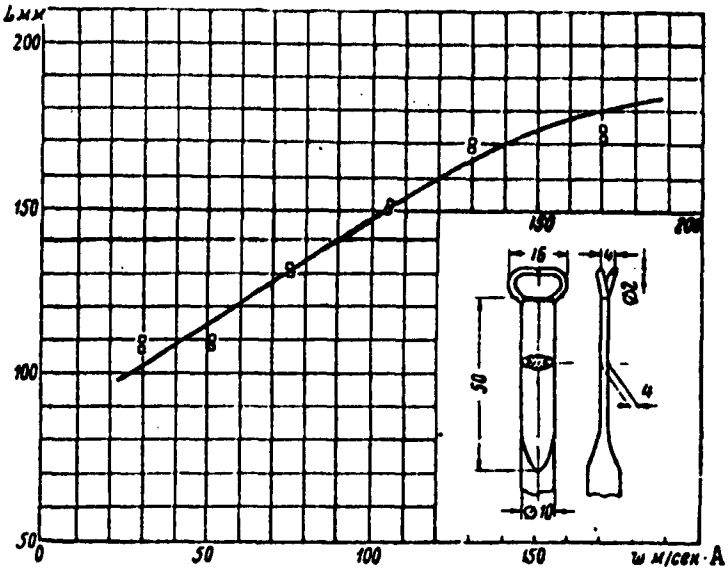

Fig. 5. Variation in the length of the backflow zone behind a stabilizer with 2h = 30 mm as a function of the velocity of the incoming stream in a free jet at near-flameout mode ($\alpha = 0.9\alpha_{sr}$). A) m/sec.

The measurement of the dimensions of the backflow zone was made by means of a fitting, the construction of which is shown in Fig. 5. Both tubes of the fitting were connected to an alcohol differential manometer. It was assumed that when the drop on the manometer is equal to zero, both tubes are on the boundary between the backflow zone and the forward stream.

The width of the backflow zone was measured in cross sections spaced a distance h apart, i.e., a distance equal to half the stabilizer height. In each section two points were fixed, in one of which the pressure drop was positive and in the other negative. Usually in determining the width of the backflow zone a displacement of the fitting by 1 mm near the boundary of the zone caused an appreciable change in the value and in the sign of the pressure drop. In determining the length of the zone, the distance between points with positive and negative pressure head amounted to 3-5 mm.

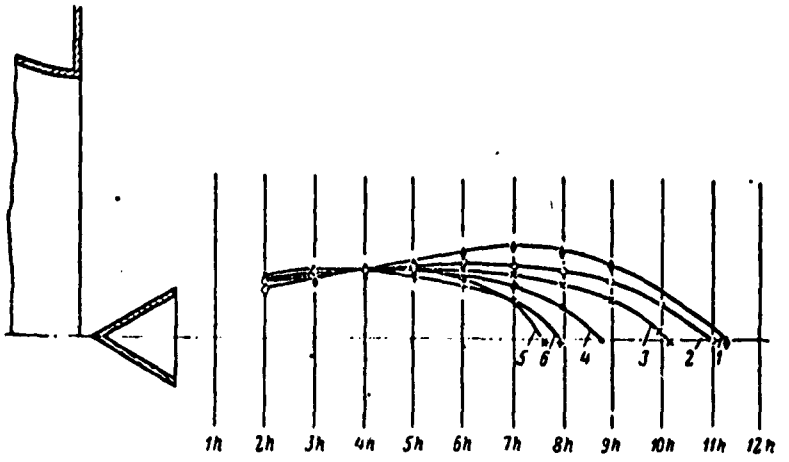

Fig. 6. Dimensions of the backflow zone during combustion, as a function of the velocity of the incoming stream. (Stabilizer with 2h = 30 mm, $\alpha = 0.9\alpha_{sr}$, in free jet.) 1) w = 170 m/sec, $\alpha = 1.44$; 2) w = 130 m/sec, $\alpha = 1.50$; 3) w = = 105 m/sec, $\alpha = 1.53$; 4) w = 74.5 m/sec, α = = 1.59; 5) w = 50.9 m/sec, $\alpha = 1.69$; 6) w = = 29.9 m/sec, $\alpha = 1.69$.

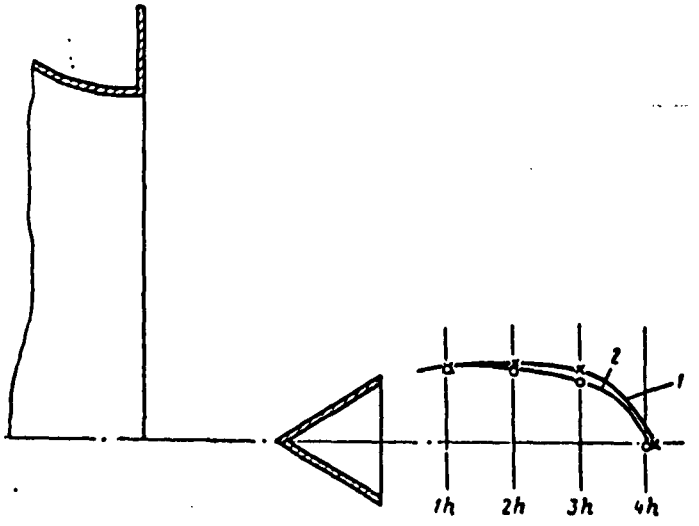

Fig. 7. Dimension of backflow zone as a function of the velocity of the incoming stream in the absence of combustion. (Stabilizer with 2h = 30 mm, $\alpha = \infty$, in free jet.) 1) w = 184 m/sec; 2) w = 34.5 m/sec.

It was shown above that the characteristics of lean flameout varied monotonically relative to the velocity, the initial turbulence of the stream, and the stabilizer dimensions. We therefore chose the

following sequence of investigation. On one stabilizer, at a constant initial turbulence, we investigated the variation of the dimensions of the backflow zone as a function of the velocity of the incoming stream; then, at a constant velocity and at a constant stabilizer dimension, we investigated the variation of the backflow zone with changing initial turbulence of the stream, and finally, at constant velocity and constant initial stream turbulence we investigated the variation of the backflow zone as a function of the stabilizer dimensions.

Figure 6 shows the dimensions of the backflow zone for different incoming-stream velocities. With increasing incoming-stream velocity in combustion, the length and width of the backflow zone increase continuously and at a velocity w = 170 m/sec its width was 30% larger and its length was 45% larger than at a velocity 30 m/sec (the Reynolds number increased by a factor 5.7).

In the absence of combustion, the dimensions of the backflow zone were considerably smaller and hardly changed with variation of the velocity of the incoming stream (Fig. 7).

The gas velocity in the backflow zone increased with increasing stream velocity (Fig. 8): in the absence of combustion the increase was proportional to the velocity of the incoming stream ($u_x \sim w$); in the case of combustion the increase was less intense ($u_g \sim w^{0.6}$).

Figure 9 shows the dimensions of the backflow zone behind various stabilizers. It was natural to assume that with increasing stabilizer dimensions the length and width of the backflow zone would increase in proportion to the height of the stabilizer. However, a reduction of the experimental results in dimensionless coordinates (Fig. 10) has shown that this assumption did not turn out to be correct. Whereas the dimensionless length at near-flameout modes was approximately the same for all tested stabilizers, the dimensionless maximum width fluctuated

between 2.1h for the stabilizer with 2h = 60 mm to 1h for the stabilizer with 2h = 10 mm.

Figures 11 and 12 show the dimensions of the backflow zone with changing initial turbulence and excess-air coefficient and at constant stream velocity. No appreciable difference was observed in the dimensions of the backflow zone in the indicated ranges of variation of the initial turbulence and the excess-air coefficient.

Thus, it follows from the foregoing that the laws governing the variation of the dimensions of the backflow zones behind a V-shaped stabilizer are different in combustion than in a cold stream.

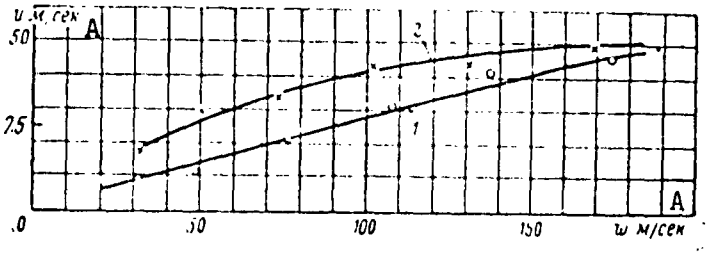

Fig. 8. Variation of axial velocity $\underline{u}$ in the backflow zone on the velocity of the incoming stream. (Stabilizer with 2h = 30 mm in the free jet.) 1) $\alpha = \infty$; 2) $\alpha = 0.9\alpha_{sr}$. A) m/sec.

The experimental data shown in Figs. 13, 14, 15, and 16 give an idea of the temperature distribution, the fuel concentration, the axial velocity, and the ionization current in the circulation zone behind the stabilizer during combustion.

The velocity and temperature fields were used to plot the lines of equal flow (Fig. 17). The equal-flow lines, as well as the first "jet" of the active stream 0-0 are shown in Figs. 13, 14, and 16.

From an examination of the temperature fields and the fuel-concentration fields (see Figs. 13 and 14) it follows that the temperature deep in the backflow zone is constant at near-flameout modes, and the fuel concentration is close to zero. Consequently, deep in the

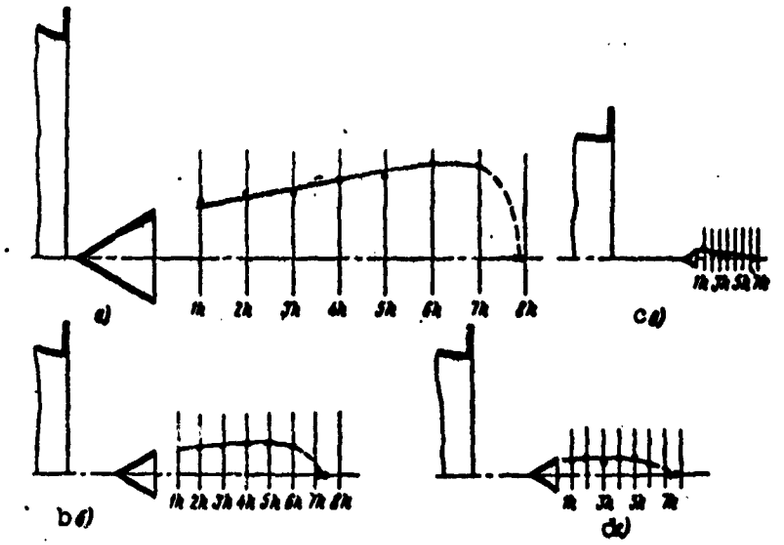

Fig. 9. Dimensions of backflow zone in free jet as a function of the size of the stabilizer. a) Stabilizer with 2h = 60 mm, α = 1.74, w = 50 m/sec; b) stabilizer with 2h = 30 mm, α = 1.69, w = 50.9 m/sec; c) stabilizer with 2h = 10 mm, α = 1.48, w = 48.3 m/sec; d) stabilizer with 2h = 20 mm, α = 1.53, w = 49.7 m/sec.

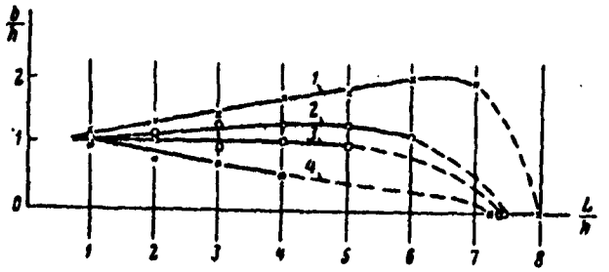

Fig. 10. Dimensions of backflow zone in dimensionless coordinates. 1) Stabilizer with 2h = 60 mm, α = 1.74, w = = 50 m/sec; 2) stabilizer with 2h = 30 mm, α = 1.69, w = 50.9 m/sec; 3) stabilizer with 2h = 20 mm, α = 1.53, w = = 49.7 m/sec; 4) stabilizer with 2h = = 10 mm, α = 1.48; w = 48.3 m/sec; b) current width of backflow zone; h) half the height of the stabilizer; L) current length of backflow zone.

backflow zone there is no combustion. On the other hand, the presence of ionization current in that region (see Fig. 16) can be attributed

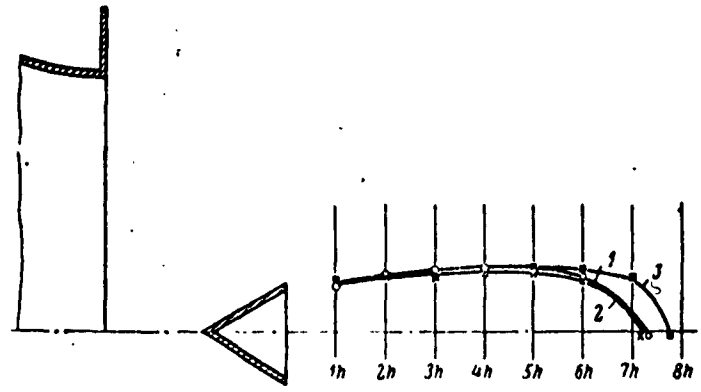

Fig. 11. Dimensions of backflow zone as a function of the initial turbulence of the stream at the rake of the stabilizer (stabilizer with z_1 = 30 mm). 1) $\varepsilon \approx 2.5\%$, $\alpha = 1.69$, $w = 50.9$ m/sec; 2) $\varepsilon \approx 10\%$, $\alpha = 1.61$, $w = 50$ m/sec; 3) $\varepsilon \approx 15\%$, $\alpha = 1.57$, $w = 50$ m/sec.

to two factors: first, the afterburn of the individual unit batches of mixture, and second, as shown by the investigations of [5], ionization current can be observed in the combustion products behind the flame front.

In the backflow zone, at its boundary with the active stream (see current line IV in sections 4h, 3h, and 2h of Figs. 13, 14, and 16), an increase takes place in the fuel concentration and a decrease in the temperature, while the magnitude of the ionization-current bursts increases compared with the central part of the backflow zone.

This indicates that the combustion process engulfs a small external region of the backflow zone. The mixture enters there because of the high intensity of exchange with the active stream.

The variation in the fuel-concentration fields begins somewhat closer to the stream axis, than the variation of the temperature. Such mutual placement of the temperature and fuel-concentration fields in combustion was observed by many investigators. Its cause has not yet been explained.

It is interesting to trace the variation of the gas temperature

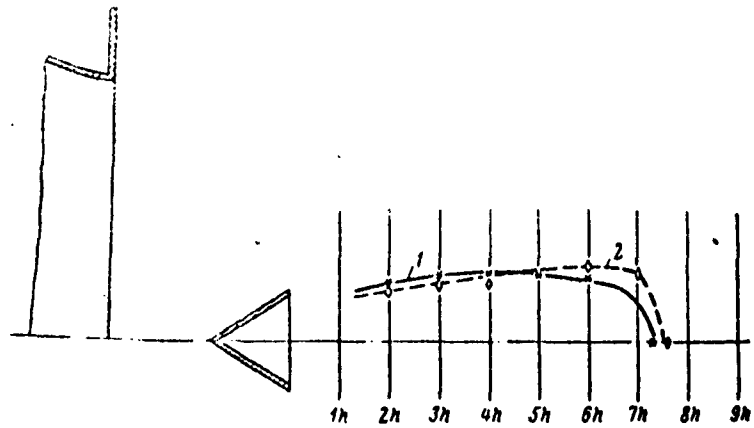

Fig. 12. Dimensions of backflow zone as a function of the excess-air coefficient α in the free jet (stabilizer with 2h = 30 mm). 1) α = = 1.67, w = 50.7 m/sec; 2) α = 1.05, w = 49.5 m/sec.

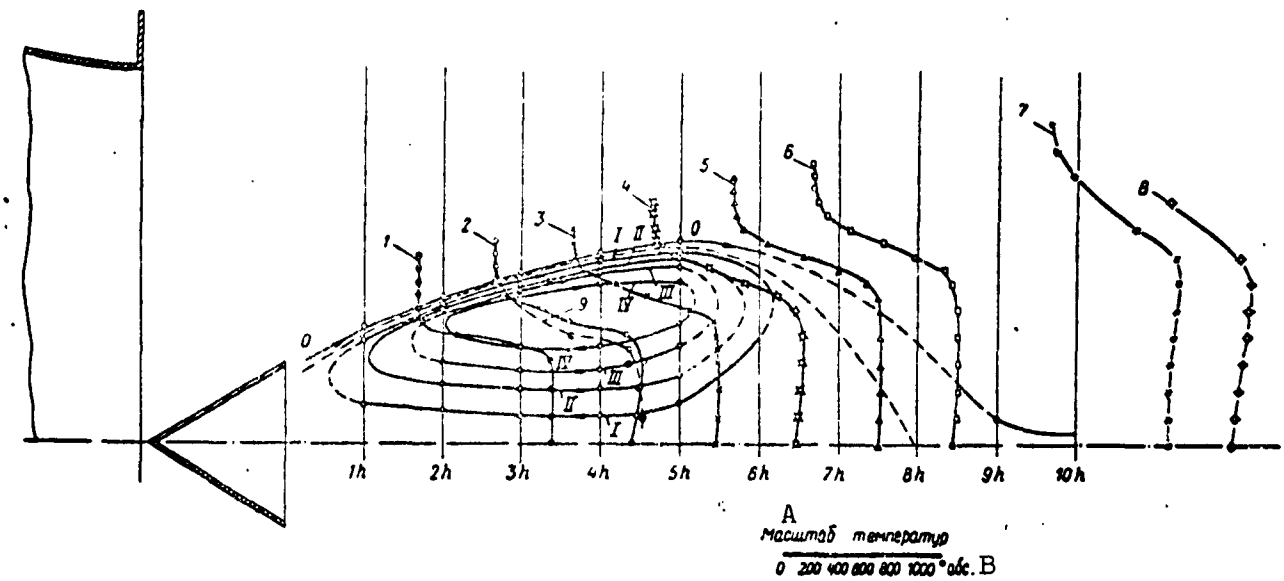

Fig. 13. Temperature fields in the circulation zone behind the stabilizer with 2h = 60 mm at near-flameout mode, w = 50 m/sec, α = 1.74. 1) For section 1h; 2) for section 2h; 3) for section 3h; 4) for section 4h; 5) for section 5h; 6) for section 6h; 7) for section 9h; 8) for section 10h; 9) for section 2h as obtained by gas analysis. 0, I-IV) current lines. A) Temperature scale; B) absolute.

and the fuel concentration along the lines that delineate equal flows. Inside the backflow zone the gas temperature is constant over the volume, and the fuel concentration is close to zero. The situation is en-

tirely different in the direct stream of the circulation zone. Figure 18 shows the variation of the gas temperature along the current lines in the direct stream of the circulation zone. From the stabilizer rake to section 3h the gas becomes cooler in the direct flow of the circulation zone (lines I-I, II-II, III-III) and transfers heat to the active stream (in the construction of Fig. 18 it was arbitrarily assumed that the current line II on Fig. 13 is tangent to the section 1h).

It is characteristic that the active-stream gas layer adjacent to the circulation zone (line 0-0 on Fig. 18) is heated up to section 5h by merely 100° and its temperature remains practically constant in the section 2h-4h, which can be attributed to the constant removal of heat into the active stream.

Starting with section 3h the temperature begins to rise in the direct stream of the circulation zone as a result of the combustion of the individual batches of the fresh mixture, which enter there as a result of turbulent exchange. Between sections 5h and 6h begins a process of combustion in the active stream. The start of the combustion can be observed by comparing plots of the variation of the fuel concentration, gas temperature, and ionization current.

Figure 19 shows plots of the variation of the temperature and fuel concentration along the current lines, from which it is seen that a sharp change in these quantities occurs beyond the section 5h. What causes this radical change, an increase in the turbulent exchange or the combustion process? This question can be answered directly by examining the plots of the ionization current (see Fig. 16), the rise of which along the current line 0-0 is determined over the interval between sections 5h and 6h. Consequently, at near-flameout lean modes the start of the combustion of the mixture in the active stream occurs at the end of the backflow zone.

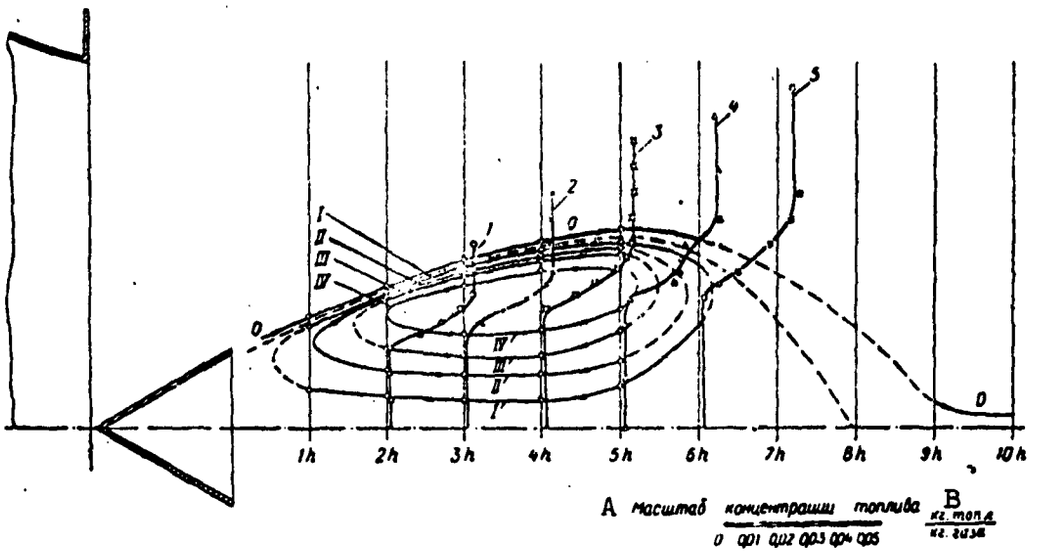

Fig. 14. Fuel concentration fields in the circulation zone behind the stabilizer with 2h = 60 mm at near-flameout mode; w = 48.9 m/sec, α = = 1.81. 1) For section 2h; 2) for section 3h; 3) for section 4h; 4) for section 5h; 5) for section 6h; 0, I-IV) current lines. A) Fuel concentration scale; B) kg of fuel per kg of gas.

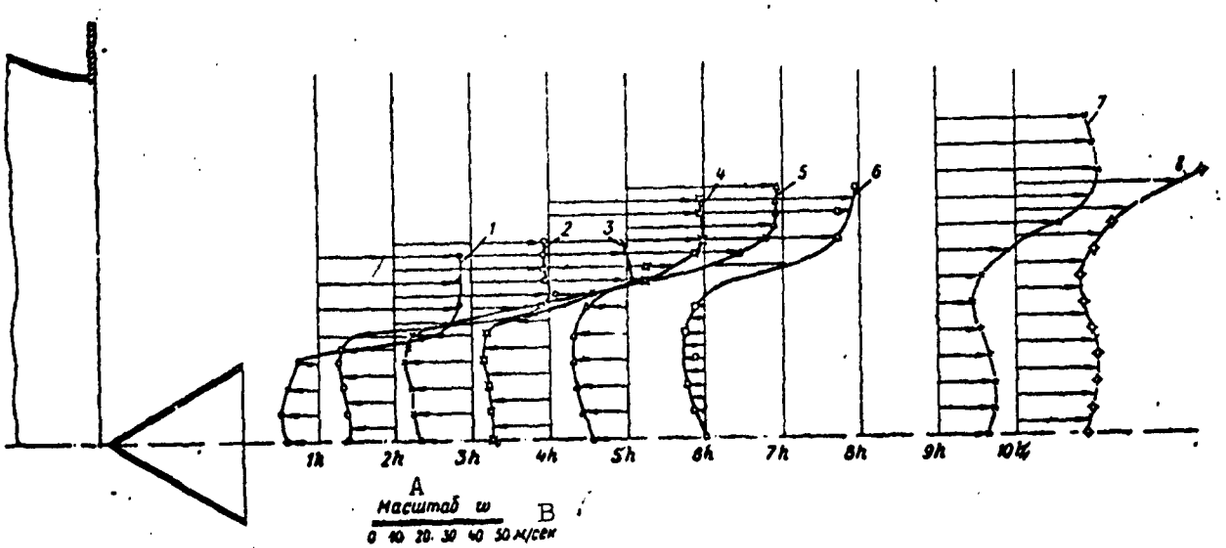

Fig. 15. Fields of axial velocity in the circulation zone behind the stabilizer with 2h = 60 mm at near-flameout mode, w = 50 m/sec, α = = 1.74. 1) For section 1h; 2) for section 2h; 3) for section 3h; 4) for section 4h; 5) for section 5h; 6) for section 6h; 7) for section 9h; 8) for section 10h. A) Scale of $\underline{w}$; B) m/sec.

The start of the mixture combustion in the active stream was registered by three methods in one and the same place, so that it can

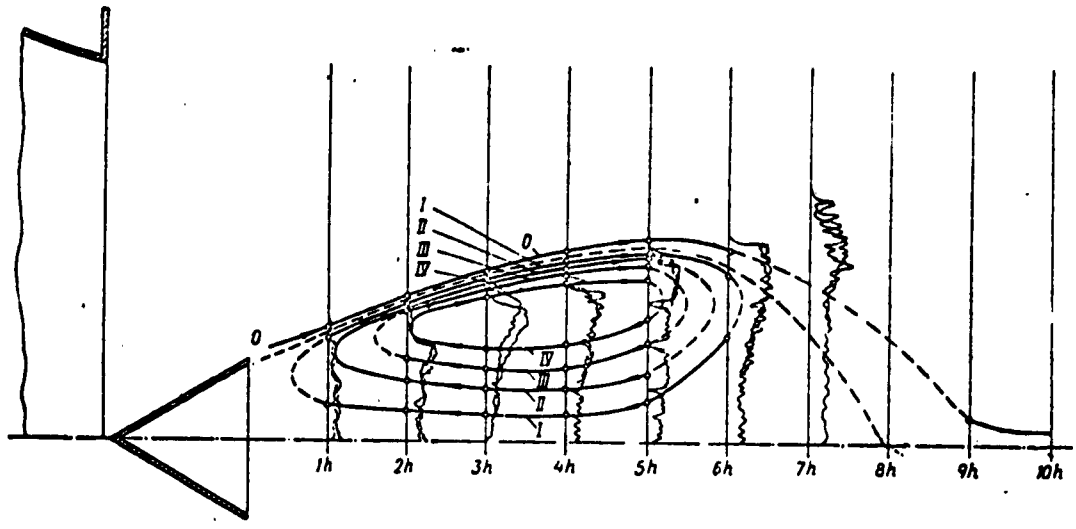

Fig. 16. Ionization-current fields in the zone of circulation behind the stabilizer with 2h = 60 mm at near-flameout mode, w = 50 m/sec, α = 1.74. 0, I-IV) Current lines.

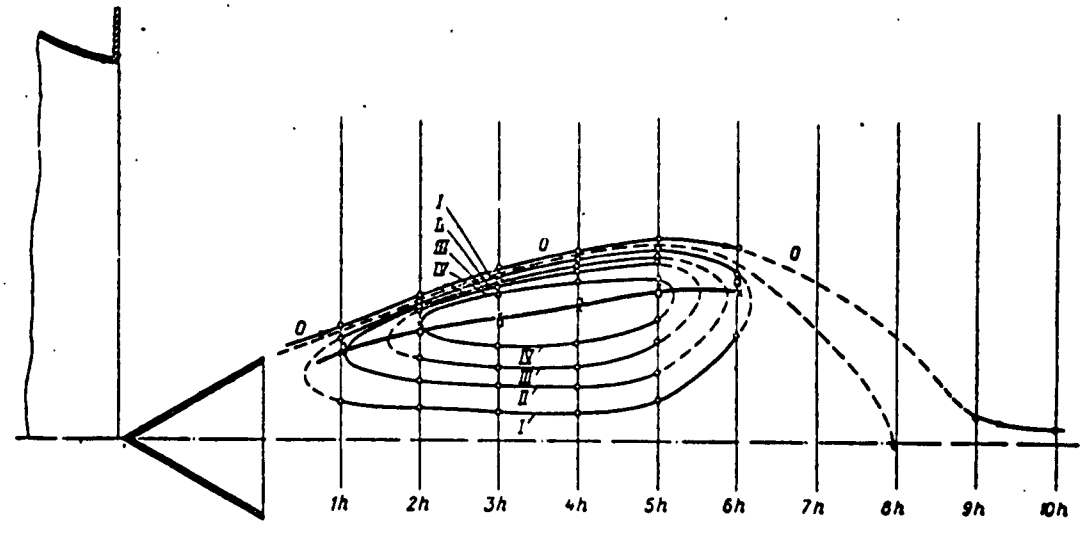

Fig. 17. Lines of equal flows in the circulation zone behind the stabilizer with 2h = 60 mm at near-flameout mode, w = 50 m/sec, α = 1.74. x) Boundary of backflow zone, calculated from the velocity fields; o) boundary of backflow zone obtained by measuring with a special fitting. [Line of equal flows delineates the flow of 0.05 kg/sec·m. The maximum gas flow in the backflow zone occurs at the section 4h (center of the zone) and amounts to 0.25 kg/sec·m.]

henceforth be determined from the place where an abrupt change takes place in any one quantity, say the temperature.

Figure 19 shows also a plot of the variation of the temperature

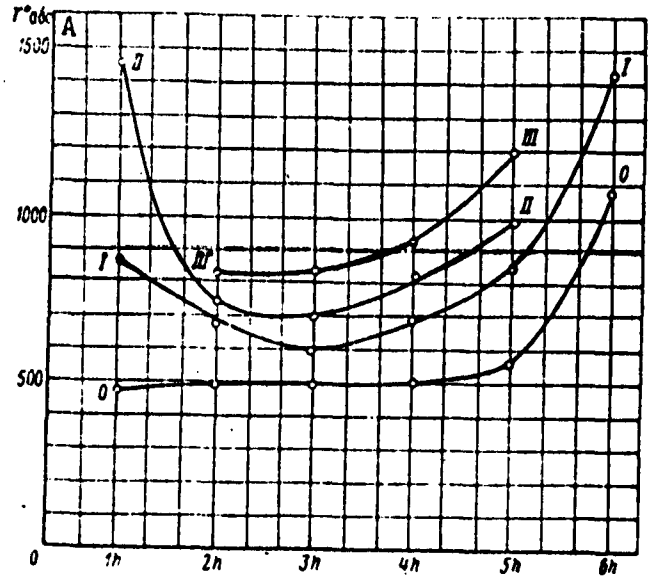

Fig. 18. Variation of gas temperature along the current lines I-I, II-II, III-III in the direct stream of the circulation zone and in the first "jet" of the active stream 0-0 (stabilizer with 2h = = 60 mm, w = 50 m/sec, α = 1.74). A) Absolute.

along the current line 0-0 for the mode with w = 51.0 m/sec and α = = 1.34. The place where the gas temperature rises abruptly lies in this case between sections 4h and 5h. This indicates that when the mixture becomes enriched the point of flame stabilization in the active stream moves closer to the stabilizer.

At the present time there are no sufficiently reliable methods developed for the determination of the characteristics of stream turbulence in the presence of combustion. The experiments were therefore limited to a measurement of the turbulence characteristics in the cold stream behind the stabilizer and at individual points of the backflow zones during combustion – in the points where the combustion process, in accordance with the curves which show the variation of the fuel concentration (see Fig. 14), has practically terminated. In the latter case the stream was colored with NaCl vapor, photographed through a

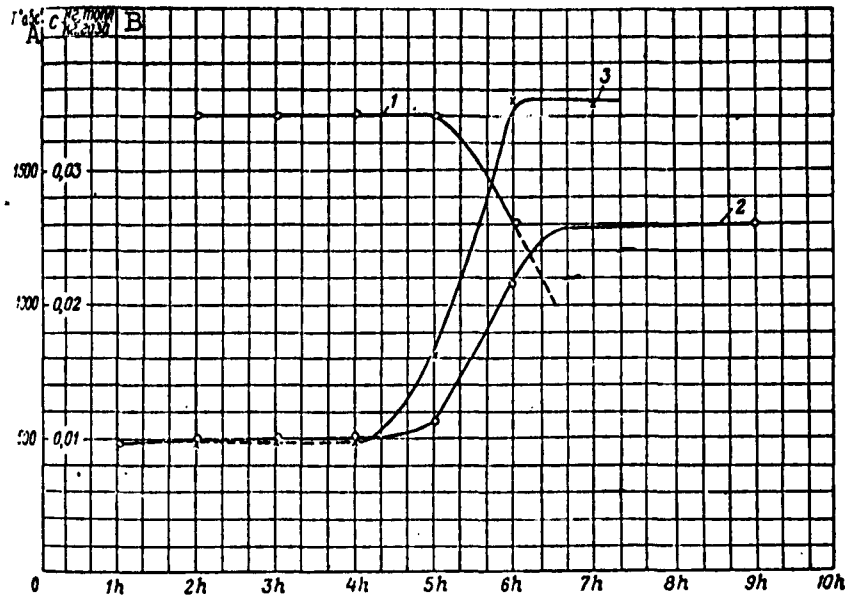

Fig. 19. Variation in gas temperature and fuel concentration along the 0-0 current line behind the stabilizer with 2h = 60 mm. 1) Variation of fuel concentration in the mode $\alpha = 1.81$, $w = 48.9$ m/sec; 2) variation of gas temperature in the mode $\alpha = 1.74$, $w = 50$ m/sec; 3) variation of gas temperature in the mode $\alpha = 1.34$, $w = 51.0$ m/sec. A) Absolute; B) kg of fuel per kg of gas.

light filter, and the limits of propagation of the coloring were compared with the turbulence-intensity table obtained for direct hot streams.

Figure 20 shows plots of the distribution of the turbulence intensity ε behind a stabilizer with 2h = 60 mm in the presence of grids "2" and "5" and also in a free jet. The curves show the limits of the backflow zone, and in the case of flow around the stabilizer without grids it also shows the limit of the constant-velocity core of the direct stream.

An examination of the curves indicates the following:

1) behind the stabilizer, in the backflow zone, the intensity of the turbulence turns out to be 45-50% and is practically independent of the value of the initial stream turbulence (more accurately, it

even decreases somewhat with increasing initial stream turbulence);

2) in the direct stream, on the boundary with the backflow zone, a region is produced where the turbulence is larger than in the backflow zone, and the higher the initial turbulence of the stream the broader this region, starting with the section 2h.

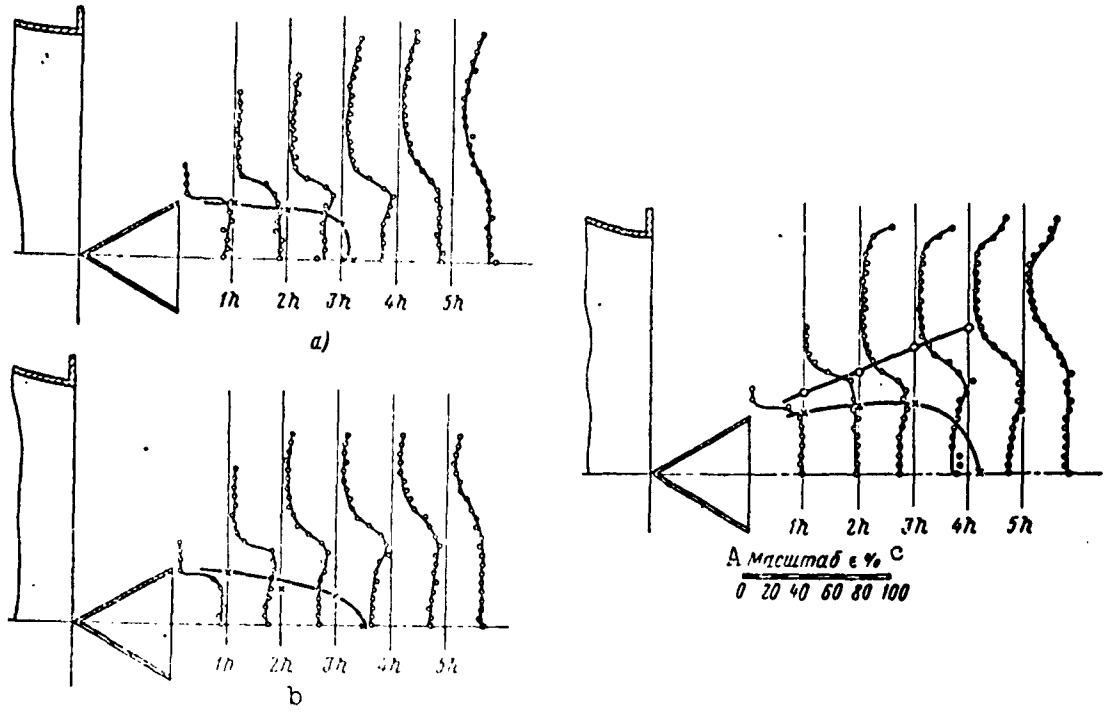

Fig. 20. Intensity of turbulence in the case of flow of a cold stream around a stabilizer with 2h = 60 mm. a) w = 50 m/sec, grid "5"; b) w = = 50 m/sec, grid "2"; c) w = 50 m/sec in free jet; x) boundary of backflow zone; 0) boundary of constant velocities. A) Scale.

Figure 21 shows plots of the distribution of the average frequencies ω_{sr} and the Euler turbulence scales L calculated with their aid. In the backflow-zone points the turbulence scales are considerably smaller (by a factor 10-12) than in the unperturbed direct stream.

The intensity of exchange in a turbulent stream can be characterized by a turbulent-exchange coefficient

$$D = \underline{l}w',$$

where $\underline{l}$ is the reduced mixing path and w' is the pulsation velocity.

In A. Prandtl's "Mechanics of Viscous Liquids" (see [2]) it is shown that a proportional relationship exists between the turbulence scale and the mixing path, and a formula obtained during the investigation of a free jet is presented.

Assuming that the mixing path is proportional to the turbulence scale in our case, too, we can calculate the ratio of the turbulent-exchange coefficients on the axis of the backflow zone to the coefficients at other points of the stream, $D_i/D_{z.o.sk}$.

The distribution of this ratio behind the stabilizer with 2h = 60 mm is shown in Fig. 22. In the region of increased turbulence, the ratio of the turbulent-exchange coefficients reaches 20, whereas in the direct stream with natural turbulence it has approximately the same magnitude as in the backflow zone.

The boundary of the direct stream with natural turbulence is located farther away from the stabilizer axis (see Figs. 20 and 21) than the boundary of the constant-velocity stream. Consequently, in the direct stream the coefficient of turbulent exchange increases with increasing distance from the backflow zone, and its maximum is located on the boundary between the circulation zone and the active stream.

Figure 23 shows the distribution of the intensity of turbulence behind stabilizers of different dimensions with 2h = 60-10 mm.

The absolute width of the region of increased turbulence decreases with decreasing stabilizer dimensions.

At individual points of the backflow zone, as was already mentioned above, measurement was made of the intensity of turbulence during combustion by coloring the stream with NaCl vapor. The results of the measurement have shown that inside the backflow zone the turbulence intensity during combustion is approximately 40%, i.e., it has approximately the same magnitude as in the case of a cold blast.

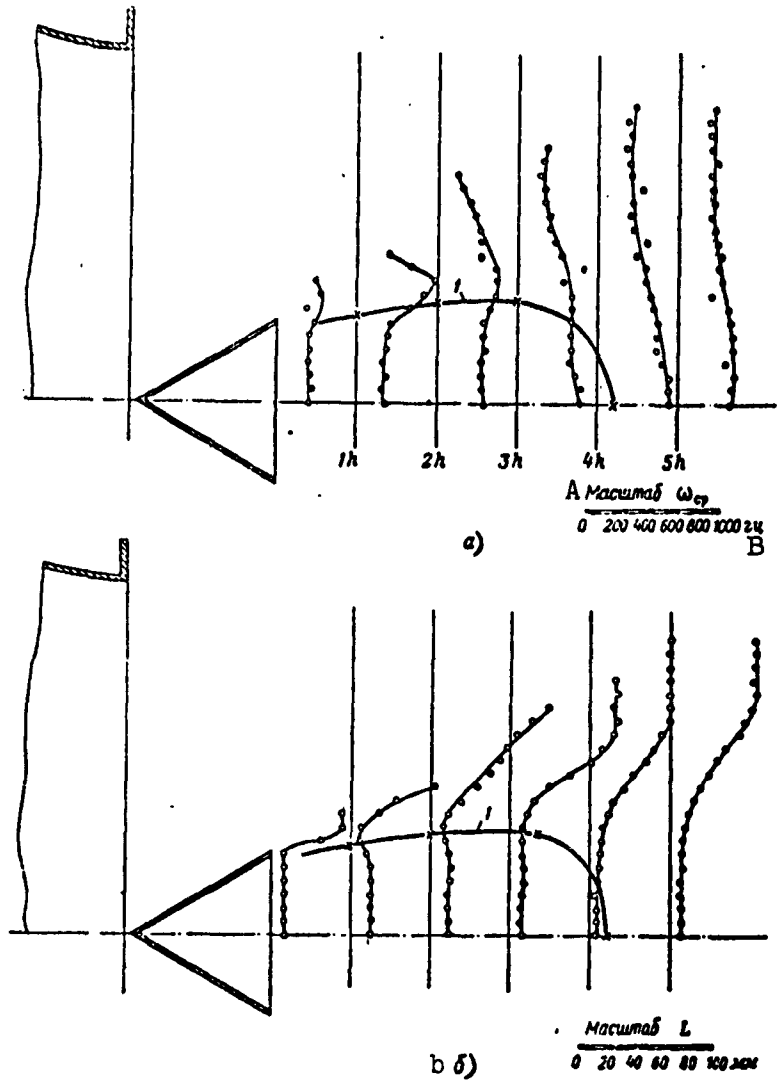

Fig. 21. Average frequencies and turbulence scales in flow of a cold stream around a stabilizer with 2h = 60 mm. a) Average frequencies ω_{sr}; b) turbulence scales L; 1) limit of backflow zone. A) Scale of ω_{sr}; B) cps.

After introducing the coloring in the backflow zone, the glow extended only up to the stabilizer and along the boundary of the circulation zone. This indicates that the greater part of the NaCl vapor does not return to the backflow zone but is carried out in the active stream. In other words, an intense exchange is observed in the region of the direct stream adjacent to the backflow zone also in the case of

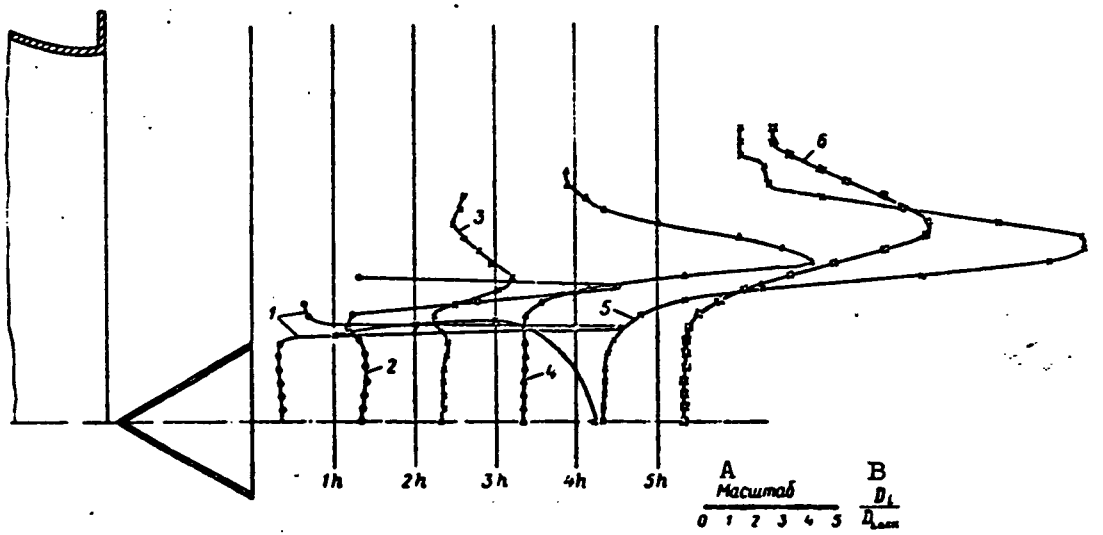

Fig. 22. Ratio of local coefficient of turbulent exchange to the coefficient of turbulent exchange on the axis of the backflow zone in the case of flow of a cold stream in a free jet around a stabilizer with 2h = 60 mm. 1) for section 0h; 2) for section 1h; 3) for section 2h; 4) for section 3h; 5) for section 4h; 6) for section 5h. A) Scale of; B) $D_i/D_{z.o.sk}$.

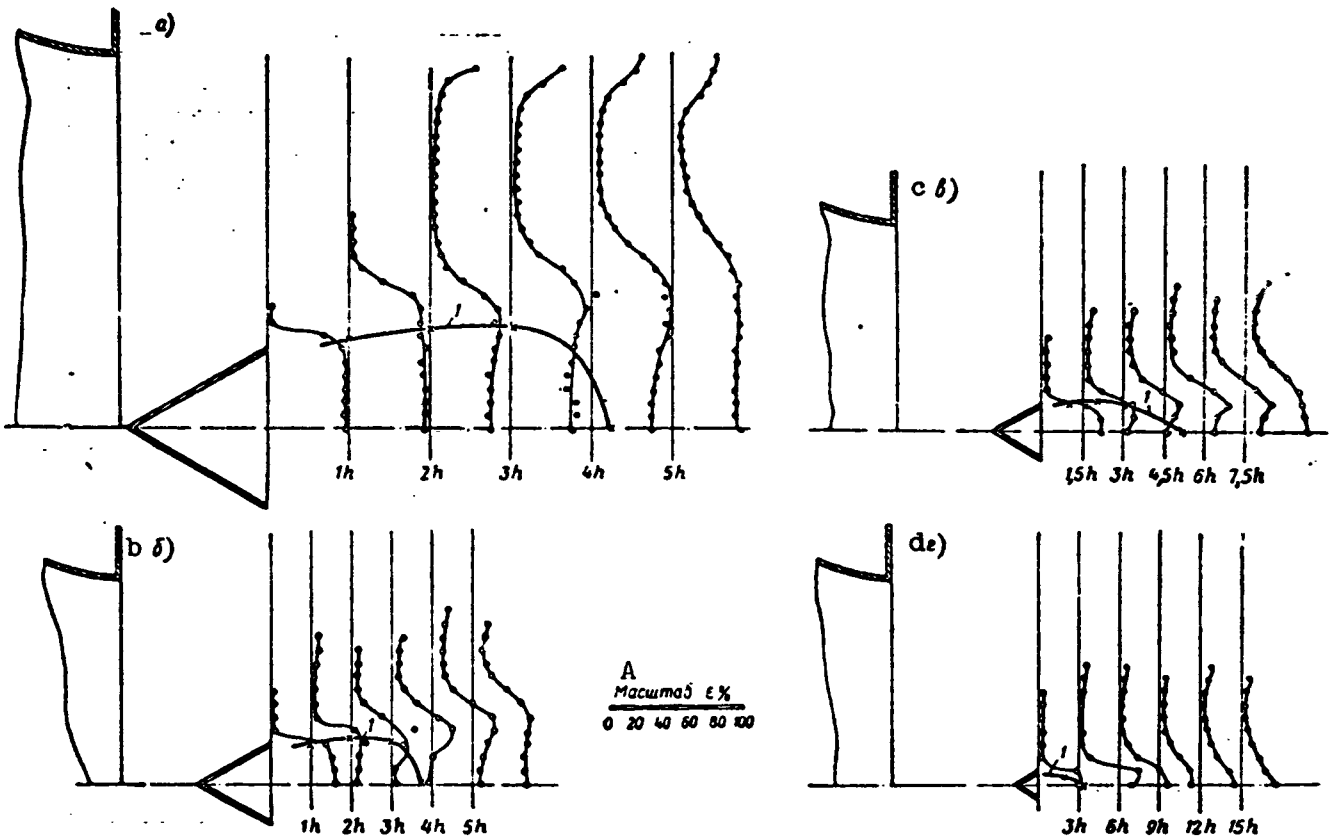

Fig. 23. Intensity of turbulence behind stabilizers of different dimensions in the case of flow of a cold stream in a free jet. a) Stabilizer with 2h = 60 mm; b) stabilizer with 2h = 30 mm; c) stabilizer with 2h = 20 mm; d) stabilizer with 2h = 10 mm; 1) limit of backflow zone. A) Scale of.

combustion.

The agreement between the values of the turbulence intensities inside the backflow zone during combustion and when cold gas is blown and the statements just made concerning the distribution of the glow of the NaCl vapor enables us to assume that the distribution of the turbulence characteristics, namely the turbulence intensity, scale, and turbulent-exchange coefficient among the cross sections is probably the same in combustion as in the case of a cold blast.

CONCLUSION

The experimental material analyzed above enables us to broaden somewhat our representation of the stabilization of flames behind poorly streamlined bodies.

When a stabilizer is installed in the stream of a gasoline-air mixture, a backflow zone is produced behind the stabilizer, and is filled with hot combustion products during the combustion.

The hot gas proceeds from the backflow zone into the direct stream of the circulation zone, which is located in a region with higher turbulent-exchange coefficients. The region with higher values of the turbulent-exchange coefficient D encompasses also the direct active stream. From the direct stream of the circulation zone there is an intense removal of heat into the active stream. The temperature of the gases emerging from the backflow zone decreases here appreciably.

Owing to the turbulent exchange, the individual batches of fresh mixture enter into layers of the direct stream of the circulation zone, where they are gradually ignited. Their ignition occurs after a sufficient degree of heating. Therefore in segments close to the stabilizer no release of heat in the direct stream of the circulation zone is observed (or else the intensity of heat supply is much lower than that of heat removal).

The burning individual batches of fresh mixture raise the gas temperature in the direct stream of the circulation zone in sections located far from the stabilizer, and this causes ignition of the batches in the adjacent layers of the active stream.

Thus, at near-flameout modes the combustion process of a mixture in the active stream begins at a considerable distance from the stabilizer (on the order of 6h).

If the mixture is enriched, then the temperature in the backflow zone increases and all the above-described combustion processes in the fresh-mixture batches occur much more rapidly. The start of the combustion of the mixture in the active stream shifts closer to the stabilizer.

To the contrary, when the mixture becomes leaner, the gas temperature in the backflow zone decreases and the start of the mixture combustion in the active stream shifts farther away from the stabilize..

As the mixture becomes even leaner, an instant arises when the heat obtained from the backflow zone becomes insufficient to ignite the mixture in the active stream. The combustion of the mixture in the active stream terminates. However, combustion can still occur in the direct stream of the circulation zone, and as a result a high temperature can be maintained in the backflow zone (such cases were observed experimentally).

With still greater reduction in the fuel supply, the batches that enter into the circulation zone did not have time to ignite and burn. A cascade process occurs wherein the temperature decreases in the backflow zone and flameout occurs.

Thus, it must be assumed that the mechanism whereby a flame is stabilized behind a poorly streamlined body consists of two processes: the removal of heat from the circulation zone into the active stream

and the resultant decrease of the temperature in this zone, with simultaneous heating of the individual batches of fresh mixture entering into the circulation zone to the ignition temperature. This model of flame stabilization behind a poorly streamlined body makes it possible to explain the flameout characteristics of stabilizers of various dimensions upon variation of velocity and initial turbulence of the stream.

Let us consider the influence of the stabilizer dimensions on the flame stabilization. From the flame stabilization scheme described above it follows that in order to heat the fresh mixture of the active stream it is necessary for a certain time to elapse, and in the presence of a velocity a certain distance is also necessary. The question arises why a small poorly streamlined body is capable of stabilizing the flame. The answer to this question can be obtained by considering the propagation of the increased turbulence-intensity zone behind stabilizers of different dimensions (see Fig. 23). A small stabilizer excites a narrow zone with increased turbulence intensity. Consequently, in order to heat up the active stream to the ignition temperature less heat is necessary, which can be supplied over a shorter segment of path.

As was already shown, the dimensions of the backflow zone change during combustion not in proportion to the dimensions of the stabilizer (see Fig. 10). In the case of a large stabilizer the dimensions of the zone are relatively larger, and consequently the conditions for the flame stabilization are better. Indeed, as shown by experiment, the flameout occurs at leaner mixtures with increasing stabilizer dimensions.

The relative dimensions of the backflow zone can influence the stabilization conditions in the following fashion. An increase in the transverse cross section of the backflow zone causes a similar increase

in the heat stored in it. An increase in the length and width of the backflow zone increases the time of exchange between the circulation zone and the active stream.

The initial turbulence of the stream influences the stabilization conditions in the following fashion. With increasing natural turbulence of the stream, the turbulence behind the stabilizer becomes practically constant. Consequently, an increase in the initial stream turbulence leads only to an increase in the heat removal into the active stream, i.e., to a deterioration in the flame stabilization conditions. Indeed, as shown by experiments, when the initial turbulence increases the flameout occurs at richer mixtures, i.e., at higher temperatures in the backflow zone.

The influence of the initial stream velocity on the stabilization conditions is manifest in the following. The dimensions of the backflow zone and the gas velocity in it change during combustion not in proportion to the velocity of the incoming stream, but much slower (see Figs. 5 and 8). Consequently, the stabilization conditions become worse with increasing velocity of the incoming stream, as a result of which flameout occurs for richer mixtures.

The results obtained in the experimental part of the work enable us to draw the following basic conclusions.

1) The backflow zone behind a trough-like stabilizer increases during combustion with increasing velocity of the incoming stream and with increasing stabilizer dimensions. In the case when cold gas is blown through, the dimensions of the backflow zone are practically independent of the stream velocity and are determined only by the stabilizer dimensions. A change in the turbulence of the incoming stream (up to 15.0%) and in the excess-air coefficient (in the range $\alpha = 1.07$-1.6) does not exert an appreciable influence on the dimensions of the back-

flow zone.

2) Near the boundary of the circulation zone and the active stream, a region is observed where the turbulent-exchange coefficient is larger. The turbulence intensity during combustion and in the case of a cold blast has approximately the same value in the backflow zone and is practically independent of the initial stream turbulence.

3) With increasing stabilizer dimension, the flameout characteristics improve. An increase in the stream velocity and in the initial stream turbulence deteriorate these conditions.

4) The point of flame stabilization (the start of ignition of the fresh mixture) at near-flameout modes is located at a considerable distance from the stabilizer.

5) The presented model of flame stabilization of a homogeneous mixture behind a poorly streamlined body is close to the scheme proposed by J. Williams.

Manuscript Page No.

[List of Transliterated Symbols]

26 cp = sr = srednyy = average

32 r = g = goreniye = combustion

43 з.о.ск. = z.o.sk. = zona obratnoy skorosti = backflow zone

INFLUENCE OF THE TURBULENCE PARAMETERS ON THE COMBUSTION OF A HOMOGENEOUS GASOLINE-AIR MIXTURE BEHIND A STABILIZER UNDER CONDITIONS OF A CLOSED STREAM

Candidate of Technical Sciences V.P. Solntsev

The requirements imposed on jet-engine chambers (short length, high combustion completeness, small hydraulic resistance) are contradictory and to satisfy them most completely it is necessary to make a thorough study of the factors that influence the combustion process.

For a purposeful selection of some particular type of stabilizer it is necessary to know the influence of the form and dimension of the poorly streamlined body on the fuel combustion process.

In addition, inasmuch as several stabilizers are installed in the chamber, it is necessary to study the laws governing the burning of the fuel under conditions where turbulent trails of neighboring stabilizers interact.

Recently several theoretical and experimental papers were published, in which the distribution of fuel concentration over the sections of the chamber and problems in the gasdynamic structure of the stream are considered [1], [4].

So far no work has been done on the study of the turbulence parameters and their influence on the combustion under combustion-chamber conditions, whereas the turbulence parameters exert a direct influence on such very important combustion characteristics as the rate of propagation of the turbulent flame front and the width of the combustion zone.

The task of the present work is to investigate the turbulence parameters behind a poorly streamlined body, the influence of the form and dimensions of the stabilizer on these parameters, and also the influence of the parameters themselves on the combustion of a homogeneous gasoline-air mixture under the conditions of a closed flow behind the stabilizer.

1. INVESTIGATION PROCEDURE

Determination of the Flame Front Propagation Velocity

The flame front propagation velocity u_t was assumed numerically equal to the normal component (relative to the front) of the velocity vector of the incoming stream.

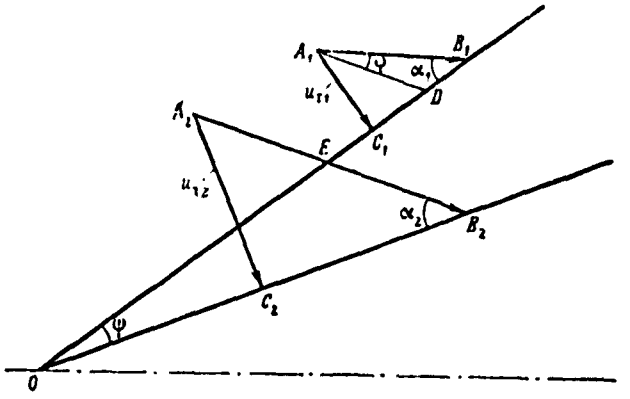

Fig. 1. Showing the dependence of u_t on w'.

With such a definition, the flame front propagation velocity can be calculated from the formula

$$u_t = w \sin \alpha$$

where w is the stream velocity at the point under consideration and α is the angle between the velocity vector and the tangent to the flame-front surface at the point under consideration.

In Fig. 1 the line OB_1 denotes the position of the flame front at a stream velocity w_1, to which the segment A_1B_1 corresponds in the figure; A_1C_1 is the normal component of the velocity vector, numerically

equal to the flame front propagation velocity u_{t1}. It can be assumed that in the general case when the velocity of the incoming stream is increased a change can take place both in the position of the front and in the direction of the velocity vector.

The line OB_2 on Fig. 1 corresponds to the new position of the front, and the segment A_2B_2 corresponds to the new increased value of the velocity w_2.

$$A_2C_2 \perp OB_2 \text{ and } A_2C_2 = u_{t2}.$$

The symbol ψ denotes the change in the slope of the front, while φ denotes the change in the angle of the velocity vector.

It follows from the triangle $A_1B_1C_1$ that

$$u_{n1} = w_1 \sin \alpha_1.$$

On the basis of several theoretical and experimental papers [3, 5, 6], the dependence of u_t on w' can be expressed in the form

$$u_{n1} = B(w_1')^a.$$

Analogously, for the case of an increasing velocity we have:

$$u_{n2} = w_2 \sin \alpha_2; \quad u_{n2} = B(w_2')^a.$$

Dividing the expressions u_{t1} by the corresponding expressions for u_{t2}, we obtain

$$\frac{u_{n1}}{u_{n2}} = \frac{w_1}{w_2} \frac{\sin \alpha_1}{\sin \alpha_2}; \quad \frac{u_{n1}}{u_{n2}} = \left(\frac{w_1'}{w_2'}\right)^a.$$

Equating the right halves of the equations

$$\left(\frac{w_1'}{w_2'}\right)^a = \frac{w_1}{w_2} \frac{\sin \alpha_1}{\sin \alpha_2},$$

we determine the exponent a

$$a = \frac{\lg \frac{w_1}{w_2} + \lg \frac{\sin \alpha_1}{\sin \alpha_2}}{\lg \left(\frac{w_1'}{w_2'}\right)},$$

but

$$w_1 = \frac{w_1'}{\varepsilon_1}; \quad w_2 = \frac{w_2'}{\varepsilon_2}$$

and

$$a = \frac{\lg\left(\frac{w_1'}{w_2'}\right) + \lg\left(\frac{\sin\alpha_1}{\sin\alpha_2}\right) + \lg\left(\frac{\varepsilon_2}{\varepsilon_1}\right)}{\lg\left(\frac{w_1'}{w_2'}\right)};$$

$$a = 1 + \frac{\lg\left(\frac{\sin\alpha_1}{\sin\alpha_2}\right) + \lg\left(\frac{\varepsilon_2}{\varepsilon_1}\right)}{\lg\left(\frac{w_1'}{w_2'}\right)}.$$

Let us express α_2 in terms of α_1, φ, and ψ:

$$\angle A_1DB_1 = 180^\circ - (\varphi + \alpha_1);$$
$$\angle OEB_2 = \angle A_2EB_1 = \angle A_1DB_1 = 180^\circ - (\varphi + \alpha_1);$$
$$\alpha_2 = 180^\circ - (\angle OEB_2 + \psi);$$
$$\alpha_2 = \alpha_1 + \varphi - \psi,$$

and the final expression for a assumes the form

$$a = 1 + \frac{\lg\left\{\frac{\sin\alpha_1}{\sin[\alpha_1 + (\varphi - \psi)]}\right\} + \lg\left(\frac{\varepsilon_2}{\varepsilon_1}\right)}{\lg\left(\frac{w_1'}{w_2'}\right)}.$$

Let us analyze the expression obtained.

We put

$$\frac{\lg\left\{\frac{\sin\alpha_1}{\sin[\alpha_1 + (\varphi - \psi)]}\right\} + \lg\left(\frac{\varepsilon_2}{\varepsilon_1}\right)}{\lg\left(\frac{w_1'}{w_2'}\right)} = A.$$

In our analysis we start from the following considerations:

1) $w_2 > w_1$ and $w'_2 > w'_1$, consequently,

$$\lg\left(\frac{w_1'}{w_2'}\right) < 0.$$

2) When $\psi = 0$ we have $\varepsilon_2 = \varepsilon_1$ and $\log(\varepsilon_2/\varepsilon_1) = 0$, which is valid when ε is independent of the velocity.

3) When $\psi > 0$ we have $\varepsilon_2 > \varepsilon_1$ and $\log(\varepsilon_2/\varepsilon_1) > 0$.

The case $\psi < 0$ is not real when $w_2 > w_1$.

The statement that when $\psi > 0$ we have $\varepsilon_2 > \varepsilon_1$ is valid for the case when we investigate combustion behind a stabilizer. In the case of investigations in the core of a free jet with a point-like ignition

source we get $\varepsilon_2 < \varepsilon_1$ when $\psi > 0$.

Let us consider the possible values of a for different values of φ and ψ:

1) $\varphi = \psi = 0$.

In this case

$$\lg\left(\frac{\varepsilon_2}{\varepsilon_1}\right)=0, \quad \lg\left\{\frac{\sin\alpha_1}{\sin[\alpha_1+(\varphi-\psi)]}\right\}=0$$

and $a = 1$.

2) $\varphi = \psi \neq 0$.

$$\lg\left(\frac{\varepsilon_2}{\varepsilon_1}\right)>0, \quad \lg\left\{\frac{\sin\alpha_1}{\sin[\alpha_1+(\varphi-\psi)]}\right\}=0,$$

$A < 0$ and $a < 1$.

3) $\varphi < \psi = 0$.

$$\lg\left(\frac{\varepsilon_2}{\varepsilon_1}\right)=0, \quad \lg\left\{\frac{\sin\alpha_1}{\sin[\alpha_1+(\varphi-\psi)]}\right\}>0,$$

$A < 0$ and $a < 1$.

4) $\varphi < \psi$.

$$\lg\frac{\varepsilon_2}{\varepsilon_1}>0, \quad \lg\left\{\frac{\sin\alpha_1}{\sin[\alpha_1+(\varphi-\psi)]}\right\}>0,$$

$A < 0$ and $a < 1$.

5) $\varphi > \psi = 0$.

$$\lg\left(\frac{\varepsilon_2}{\varepsilon_1}\right)=0, \quad \lg\left\{\frac{\sin\alpha_1}{\sin[\alpha_1+(\varphi-\psi)]}\right\}<0,$$

$A > 0$ and $a > 1$.

6) $\varphi > \psi$.

$$\lg\left(\frac{\varepsilon_2}{\varepsilon_1}\right)>0, \quad \lg\left\{\frac{\sin\alpha_1}{\sin[\alpha_1+(\varphi-\psi)]}\right\}<0.$$

The case $\varphi > \psi$ when $\psi \neq 0$ is the most complicated. It is obvious that a can assume the values $a > 1$, $a = 0$, and $a < 1$, depending on the ratio of the absolute values

$$\left|\lg\left(\frac{\varepsilon_2}{\varepsilon_1}\right)\right| \text{ and } \left|\lg\left\{\frac{\sin\alpha_1}{\sin[\alpha_1+(\varphi-\psi)]}\right\}\right|.$$

$$\text{for} \left| \lg\left(\frac{\varepsilon_2}{\varepsilon_1}\right) \right| > \left| \lg\left\{\frac{\sin\alpha_1}{\sin[\alpha_1+(\varphi-\psi)]}\right\} \right|$$
$$a < 1.$$

$$\text{for} \left| \lg\left(\frac{\varepsilon_2}{\varepsilon_1}\right) \right| = \left| \lg\left\{\frac{\sin\alpha_1}{\sin[\alpha_1+(\varphi-\psi)]}\right\} \right|$$
$$a = 1.$$

$$\text{for} \left| \lg\left(\frac{\varepsilon_2}{\varepsilon_1}\right) \right| < \left| \lg\left\{\frac{\sin\alpha_1}{\sin[\alpha_1+(\varphi-\psi)]}\right\} \right|$$
$$a > 1.$$

Consequently, if the front position and the direction of the velocity vector do not change when the velocity of the incoming stream increases, then

$$u_t \sim w'.$$

If the angle by which the velocity vector changes is equal to the angle of inclination of the flame front or is smaller than this angle, then $u_t \sim (w')^a$, where

$$a < 1.$$

If the position of the flame front does not change with increasing velocity of the incoming stream, and the angle of the velocity vector changes (with $\varphi > 0$), then

$$u_t \sim (w')^a, \text{ where } a > 1.$$

If the angle through which the velocity vector has changed is larger than the angle of inclination of the flame front, then the value of a depends on the ratio of the absolute values

$$\lg\left(\frac{\varepsilon_2}{\varepsilon_1}\right) \text{ and } \lg\left\{\frac{\sin\alpha_1}{\sin[\alpha_1+(\varphi-\psi)]}\right\}.$$

This is the only case when it is impossible to determine directly the value of a from data on the change in the position of the front and on the change in the direction of the velocity vector with increasing velocity of the incoming stream, and it becomes necessary to carry out an additional analysis.

It follows from the foregoing analysis that the investigation of

the dependence of u_t on w' can be broken up into three stages:

1) an investigation of the influence of the velocity of the incoming stream on the intensity of the turbulence;

2) an investigation of the influence of the velocity of the incoming stream on the position of the flame front;

3) an investigation of the influence of the velocity of the stream on the direction of the velocity vector.

Influence of the Turbulence Parameters on the Width of the Flame Front

In examining the dependence of the width of the flame front on the turbulence parameters, we shall start from the combustion time, obtained in [5] under the assumption that turbulent pulsations participate in the combustion of each batch:

$$\tau \sim \frac{l}{w'},$$

where l is the turbulence scale and w' is the pulsating velocity component.

We define the width of the flame front as the length of the combustion zone along the current line.

Such a definition of the width of the flame front is most convenient when it comes to determining the necessary length of the combustion chamber:

$$\delta_\tau = w_{cp}\tau_{cp},$$

where w_{sr} is the average velocity along the current line and τ_{sr} is the average combustion time along the current line.

Using the proportional relationship for τ indicated above, we obtain

$$\delta_\tau \sim w_{cp}\frac{l}{w'}, \quad \delta_\tau \sim \frac{l}{\varepsilon}.$$

Recognizing that

$$l_{cp} = k\frac{w_{cp}}{\omega_{cp}},$$

where ω_{sr} is the average frequency of the turbulent pulsations, we express δ_t in terms of ω_{sr}:

$$\delta_t \sim w_{sr}/\omega_{sr}\varepsilon.$$

To check the obtained dependences of the flame front width on the turbulence parameters it was necessary to investigate the following:

1) the influence of the velocity of the incoming stream on the turbulence intensity;

2) the influence of the stream velocity on the average frequency of the turbulent pulsations;

3) the influence of the stream velocity on the flame front width.

2. EXPERIMENTAL SETUP

A diagram of the experimental setup is shown in Fig. 3 of the second article of the present collection.

The length of the mixing chamber is chosen to satisfy the conditions for complete evaporation of the fuel, which was calculated by the procedure of D.N. Vyrubov [2].

The mixing chamber was terminated with a transition piece, on the end of which was installed the combustion chamber, which comprised a tube of rectangular cross section measuring 200 x 175 mm (Fig. 2). Through quartz windows 1 installed in the upper part of the chamber it was possible to observe the combustion process. The ignition of the mixture was with the aid of a starting unit, consisting of a spark plug and a nozzle; the starting unit was installed in the lower part of the chamber.

The measurements were made with a measuring baffle 4 having 17 apertures spaced 25 mm apart.

The stabilizers 2 were secured in the chamber in such a way, that the forward edges (on the side of the chamber) of the different stabilizers were located always in one cross section. The walls of the

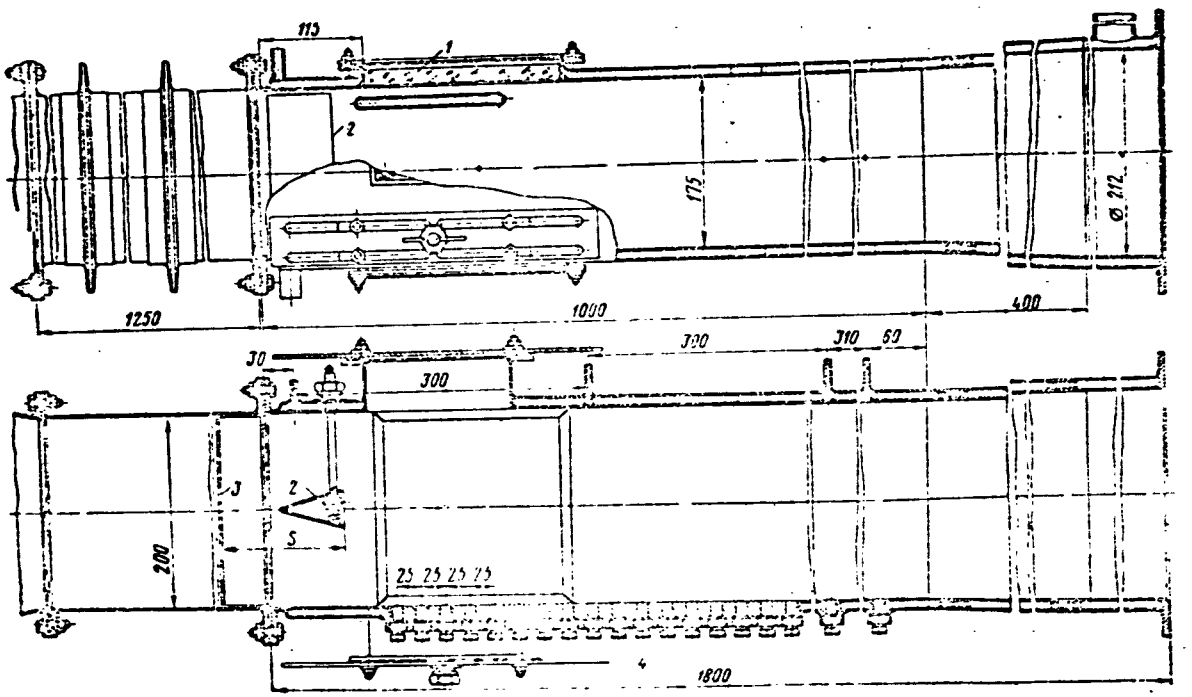

Fig. 2. Combustion chamber. 1) Viewing window; 2) stabilizer; 3) turbulizing grid; 4) measuring baffle.

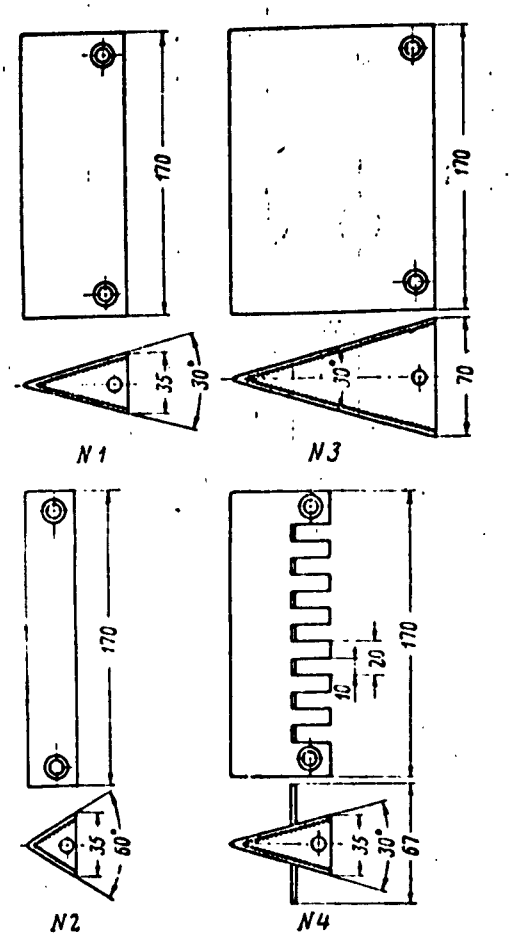

Fig. 3. Stabilizers.

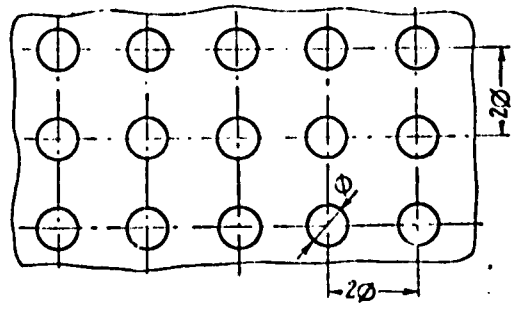

Fig. 4. Turbulizing grids.

1 № решетки	1	2	3	4	5
2 Диаметр	5	10	15	20	25

1) Grid number; 2) diameter.

chamber were water cooled.

Figure 3 shows different stabilizers, behind which the combustion process was investigated. The heights of the stabilizers were equal to the height of the combustion chamber. All the stabilizers were made closed on top and bottom and differed in their aperture angle β and in their width 2h.

Stabilizer No. 4 differed from stabilizer No. 1 in the fact that its side walls were cut at intervals of 10 mm to a depth of 20 mm, bent at the cuts, and installed perpendicular to the stream.

The turbulizing grids, which were used in the experiments, are shown in Fig. 4.

In the present work the investigations were carried out only behind single stabilizers, installed on the chamber axis. The static pressure in the chamber exceeded slightly atmospheric pressure, and differed from the latter because of the hydraulic and thermal resistances of the chamber. The air temperature ahead of the mixing chamber was maintained at 125°C.

The investigations were carried out with a homogeneous gasoline-air mixture at three stream velocities: $w = 35$, 50, and 70 m/sec. The excess-air coefficient in all the modes was $\alpha = 1.5$, except for one in which $\alpha = 1$.

The measurement cross sections, in which the temperature, velocities, concentrations, ionization, intensity, and frequency characteristics of the turbulence were measured, were located at distances 100, 200, 300, 450, and 660 mm from the leading edge of the stabilizer. The measurements of these quantities were made with apparatus described in [4] and in the first article of the present collection.

3. RESULTS OF THE EXPERIMENTS

Investigation of the Flame-Front Structure

In the investigations of the flame-front structure, we measured the temperatures, concentrations, and ionization current over the sections of the torch. The experiments were made behind stabilizers 1 and 2 at a stream velocity $w = 50$ m/sec and at an excess-air coefficient $\alpha = 1.5$. The results of the experiments are shown in Fig. 5. The quantity $\Delta\alpha_{t.p}$ shows the change in the increase of the excess-air coefficient determined from the fuel and the combustible additives (see [4]).

In all the sections of the chamber, the start of intense ionization lagged somewhat the start of the change in temperature. In many cases the start of intense ionization was preceded by individual bursts of ionization current, which appeared at approximately the location where the temperature begins to change.

Figure 6 shows data on the investigation of the ionization in the flame by the "shooting through" method. In all the photographs the wall of the chamber from which the transducer was moved was located to the right. Under the photograph of the ionization current one can see the readings of the path marker and below that the readings of the time marker.

Figure 6a shows photographs of the ionization current, obtained in the investigation of the combustion process behind stabilizer No. 1. The first two photographs were made in a section located 50 mm away from the stabilizer. The photographs show clearly outlined boundaries of the flame front. The next three photographs pertain to a section located 100 mm away from the stabilizer.

The first two photographs do not show the individual bursts of ionization current ahead of the flame front.

According to the path-marker data, the start of the front on both

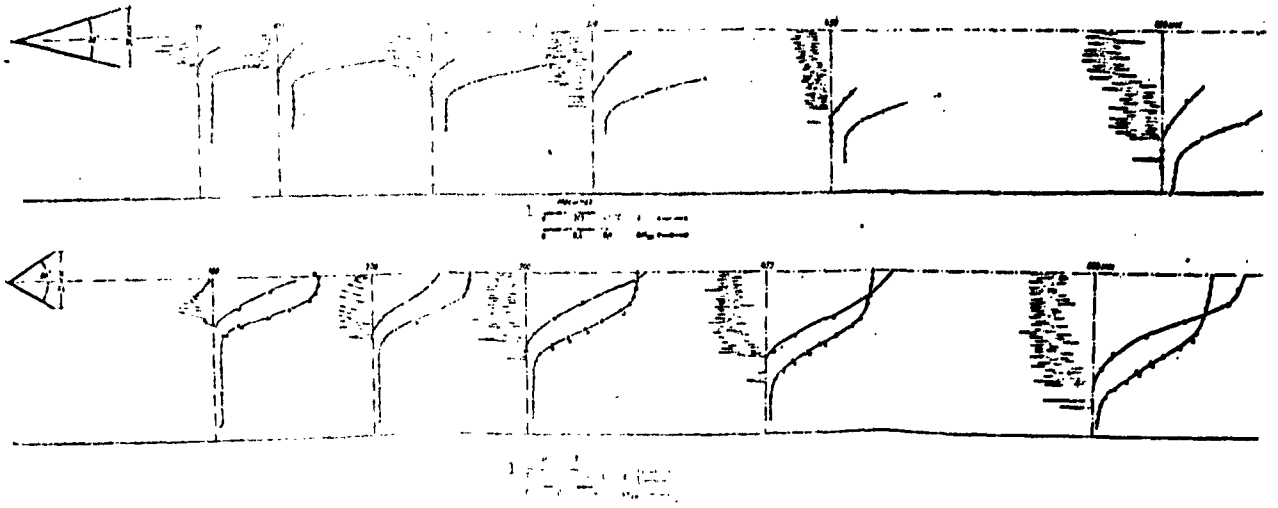

Fig. 5. Structure of flame front. 1) Scale.

photographs is 81-82 mm away from the wall. On the third photograph we see an individual burst of ionization current, located 73 mm away from the wall, and the start of the intense ionization is located (as in the first two photographs) at a distance of 82 mm.

The photographs obtained behind stabilizer No. 2 are shown in Fig. 6b. The first and second photographs pertain to the 100-mm section. The photographs do not show the individual bursts of ionization current. The third photograph was taken at the 200-mm section. It shows an individual burst and the intense ionization begins only 8 mm away from it. On the fourth photograph, which pertains to the 600-mm section, the individual ionization-current burst is located 13 mm away from the start of the intense ionization.

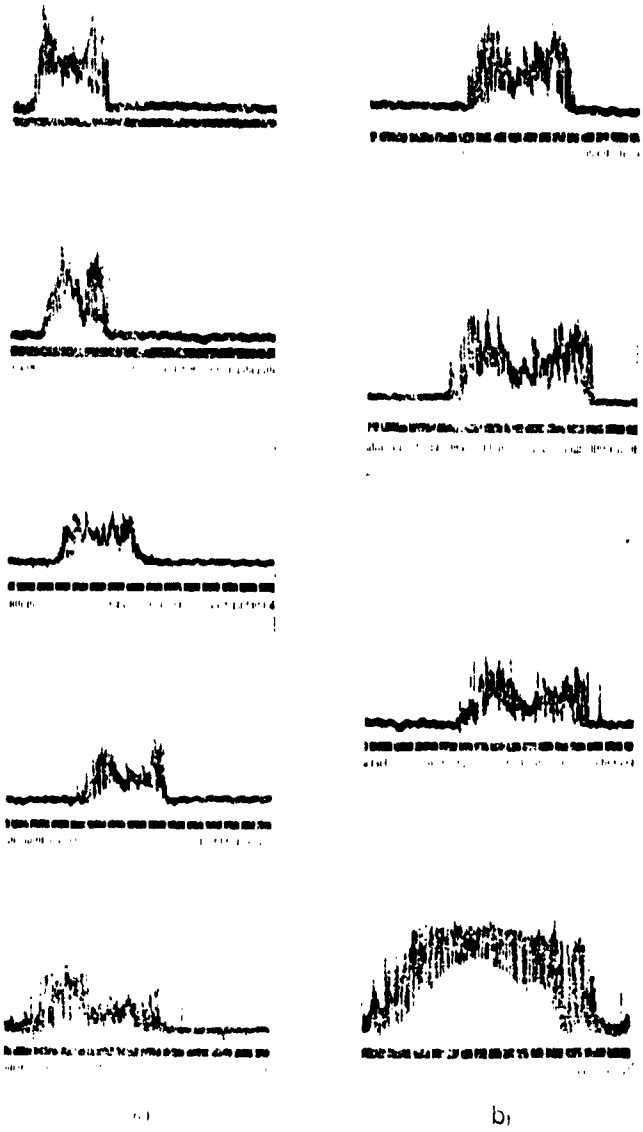

Fig. 6. Variation of ionization current over the sections of the torch. ($2h = 35$ mm, $w = 50$ m/sec, $\alpha = 1.5$.) a) $\beta = 30°$; b) $\beta = 60°$.

In all the sections of the chamber, there is a certain lag in the start of the change in the concentration as compared with the start in the change of temperature (see Fig. 5). The start of the change in concentration is in satisfactory agreement with the start of the intense ionization. The difference between the start in the change in tempera-

ture and the start in the change of concentration or of the intense ionization cannot be attributed to the error in the temperature measurement due to radiation.

Calculation of the possible increase in the thermocouple temperature, due to radiation of the flame, shows that in the case of a chromel-copel thermocouple the maximum error under the experimental conditions could reach 22°. The maximum error in measurements with a platinum-platinum-rhodium thermocouple was 2°.

In fixing the forward boundary of the flame front, an important factor is not the maximum possible error in the temperature measurement, but the increase in the error as the temperature approaches the flame front. Calculation shows that even in the case of a chromel-copel thermocouple this error reaches only 2.7°.

With the mechanism whereby burnout occurs in the turbulent flame front still unexplained, it is difficult to choose with any justification a correct method for determining the leading boundary of the front. In the following investigations the leading boundary of the flame front was determined both from the start of the change in concentration and the start of intense ionization, and also from the start of the change in temperature, so that it was possible to ascertain the effect that the procedure used to determine the flame front position has on the dependence of u_t and δ_t on the turbulence parameters.

Influence of Turbulence Parameters on the Flame Front Propagation Velocity

Figure 7 shows the results of an investigation of the turbulence intensity behind stabilizer No. 1 at a stream velocity w = 30 m/sec.

At a distance of 100 mm from the stabilizer, the turbulence intensity changes appreciably over the section of the chamber. Having an

increased value at the wall (owing to the influence of the wall itself), the turbulence intensity decreases somewhat and begins to increase noticeably upon penetrating into the turbulent trail behind the stabilizer, reaching a value $\varepsilon = 21\%$ on the chamber axis. The attainment of the maximum value of ε on the chamber axis can be attributed to the small dimensions of the stabilizer, as the result of which the turbulent "whiskers" merge already at a distance of 100 mm away from the stabilizer. With increasing distance from the stabilizer, the unevenness in the turbulence intensity over the cross section decreases. This equalization is the result of both the decrease in the maximum value of ε on the chamber axis, and the increase in the minimum value of the turbulence intensity at the sections of the chamber. As a result of which, at a distance of 660 mm away from the stabilizer, the turbulence intensity, remaining practically constant over the cross section, exceeds by approximately three times the value of the initial turbulence.

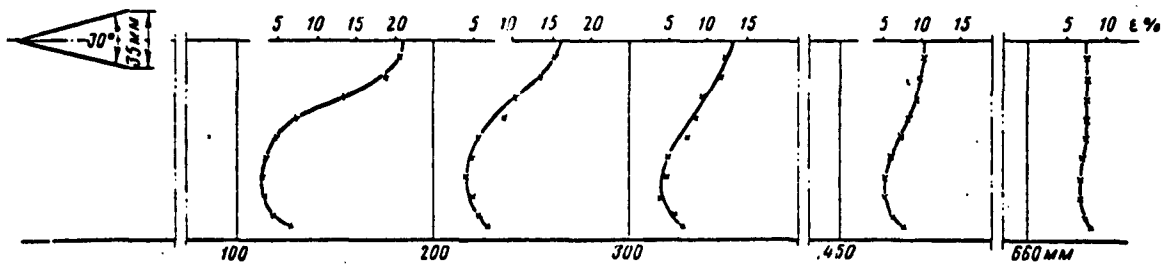

Fig. 7. Variation of turbulence intensity over the sections of the chamber.

An investigation of the influence of the velocity of the incoming stream on the turbulence intensity was made behind stabilizers 1 and 2. The results of the investigation, shown in Fig. 8, lead to the conclusion that behind the stabilizers, under conditions of a closed stream, the turbulence intensity does not depend on the stream velocity. A certain scatter in the experimental points is obviously due to the inaccuracy of the experiment. This can be seen from an examination of the

variation of the turbulence intensity along the chamber axis behind stabilizer No. 1.

At a distance of 100 mm from the stabilizer, the maximum value of ε is obtained at a velocity $w = 50$ m/sec. In the 200-mm section, the maximum value of ε is attained already at a velocity 70 m/sec, and the values of ε at $w = 35$ m/sec and $w = 50$ m/sec coincide. When the distance from the stabilizer is 300 mm, the maximum value of ε corresponds already to $w = 35$ m/sec. In the sections located 450 and 660 mm away from the stabilizer, the values of the turbulence intensity are practically the same for all three velocities.

In investigations of the influence of the turbulence parameters on the combustion process, the pulsating component of the velocity w' was varied by changing the stream velocity.

Figures 9 and 10 show the results of an investigation of the influence of the velocity of the incoming stream on the flame front position. The experiments were carried out behind stabilizer No. 1. From the data shown in Fig. 9 it is seen that the start of the temperature rise coincides fairly well at all stream velocities.

The variation of the increment in the excess-air coefficient $\Delta\alpha_{t.p}$ over the sections of the chamber, determined from the fuel and combustible additives, and also the change in the oxygen concentration, is shown on Fig. 10. In all sections of the chamber, the start of the change in $\Delta\alpha_{t.p}$ and in the concentration of the oxygen also coincides for all stream velocities.

The results of the investigations of the influence of the velocity of the incoming stream on the flame front position behind stabilizer No. 1 at an excess-air coefficient $\alpha = 1$ are shown in Fig. 11a. In this case, too, the change in velocity of the incoming stream did not influence the start of the change in temperatures in all sections of

the chamber.

Analogous investigations were carried out behind stabilizer No. 2. From the data of these investigations, shown in Fig. 11b, it is seen that the points of all three modes in each section of the chamber fitted satisfactorily a single curve.

On the basis of the experimental data obtained we can conclude that the flame front position, independently of how it is determined, whether it be from the start of the change in temperature or from the start in the change of the excess-air coefficient, which coincides with the start of the ionization intensity, does not change with changing velocity of the incoming stream.

Consequently, the angle ψ in the formula for the determination of the exponent of w' is equal to zero.

An investigation of the influence of the stream velocity on the direction of the velocity vectors was carried out behind stabilizer No. 1. The results of the investigations are shown in Fig. 12.

In the overwhelming majority of points, the directions of the velocity vectors coincide for all three stream velocities. The small deviations that arise (essentially at points located near the chamber axis) are apparently the results of inaccuracy in the experiment.

The results obtained show that the velocity of the incoming stream does not influence the direction of the velocity vectors behind the stabilizer.

From the formula for the exponent of w'

$$a = 1 + \frac{\lg\left\{\frac{\sin\alpha_1}{\sin[\alpha_1 + (\varphi - \psi)]} + \lg\frac{z_2}{z_1}\right\}}{\lg\left(\frac{w_1'}{w_2'}\right)}$$

it is seen that inasmuch as $\psi = 0$ and $\varphi = 0$, we have

$$\lg\left\{\frac{\sin\alpha_1}{\sin[\alpha_1 + (\varphi - \psi)]}\right\} = 0.$$

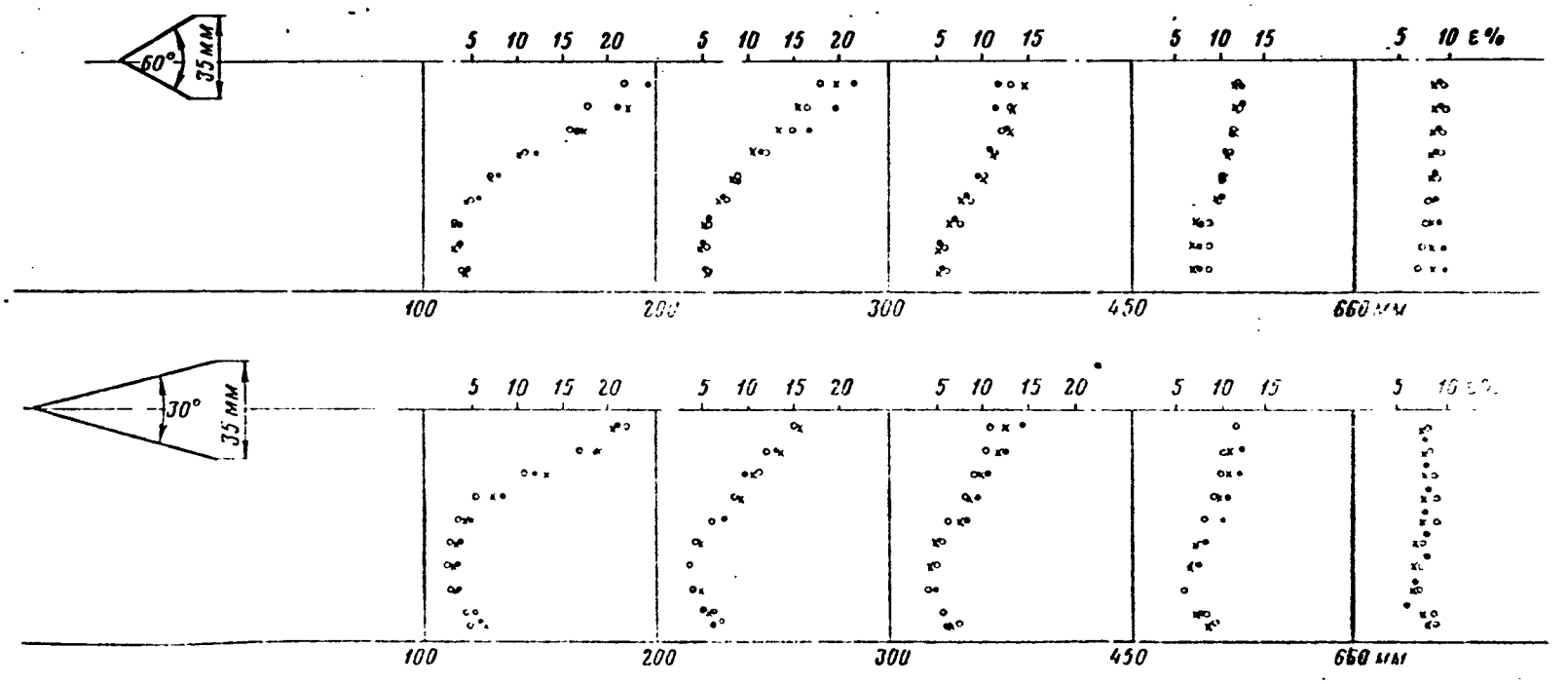

Fig. 8. Dependence of the intensity of the turbulence on the stream velocity. ●) w = 35 m/sec; 0) w = 50 m/sec; x) w = 70 m/sec.

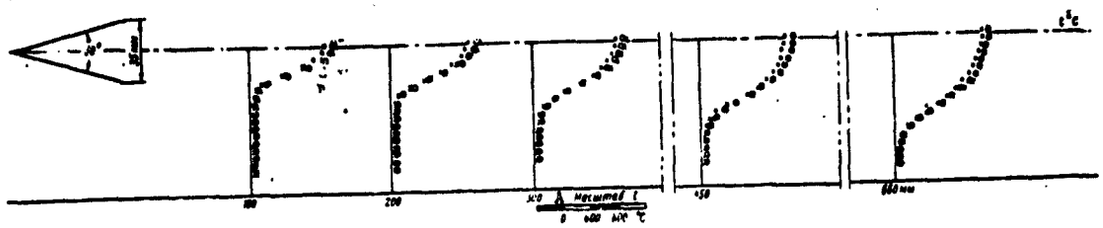

Fig. 9. Temperature fields. ●) w = 37 m/sec, α = 1.58; O) w = 50 m/sec, α = 1.5; x) w = 70 m/sec, α = 1.5. A) Scale of.

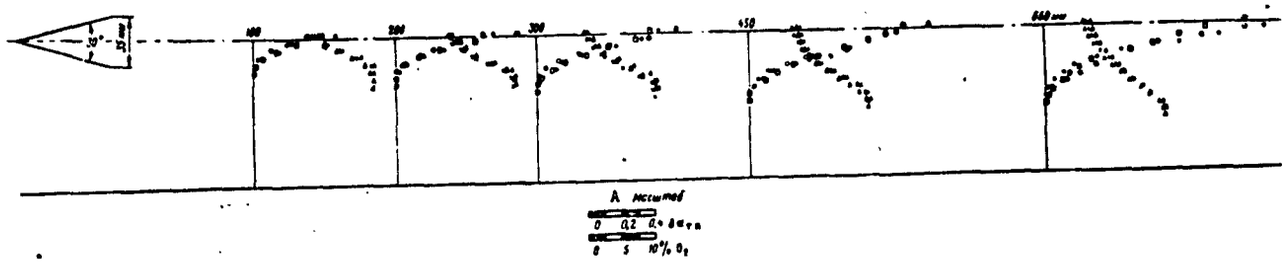

Fig. 10. Change in the increment of the excess-air coefficient $\Delta\alpha_{t.p}$ and in the concentration of the oxygen O_2 over the sections of the chamber.

●, x — $\Delta\alpha_{T.n}$, O_2 } w=37 м/сек, α=1,58; O, ▲ — $\Delta\alpha_{T.n}$, O_2 } w=50 м/сек, α=1,5; □, △ — $\Delta\alpha_{T.n}$, O_2 } w=70 м/сек, α=1,5.
B B B

A) Scale of; B) m/sec.

From the invariance of the turbulence intensity and of the front position under variations in the stream velocity it follows that $\varepsilon_1 = \varepsilon_2$, which leads to the vanishing of the second logarithm:

$$\lg\left(\frac{\varepsilon_2}{\varepsilon_1}\right) = 0.$$

The entire fraction vanishes and we obtain from the formula:

$$a = 1.$$

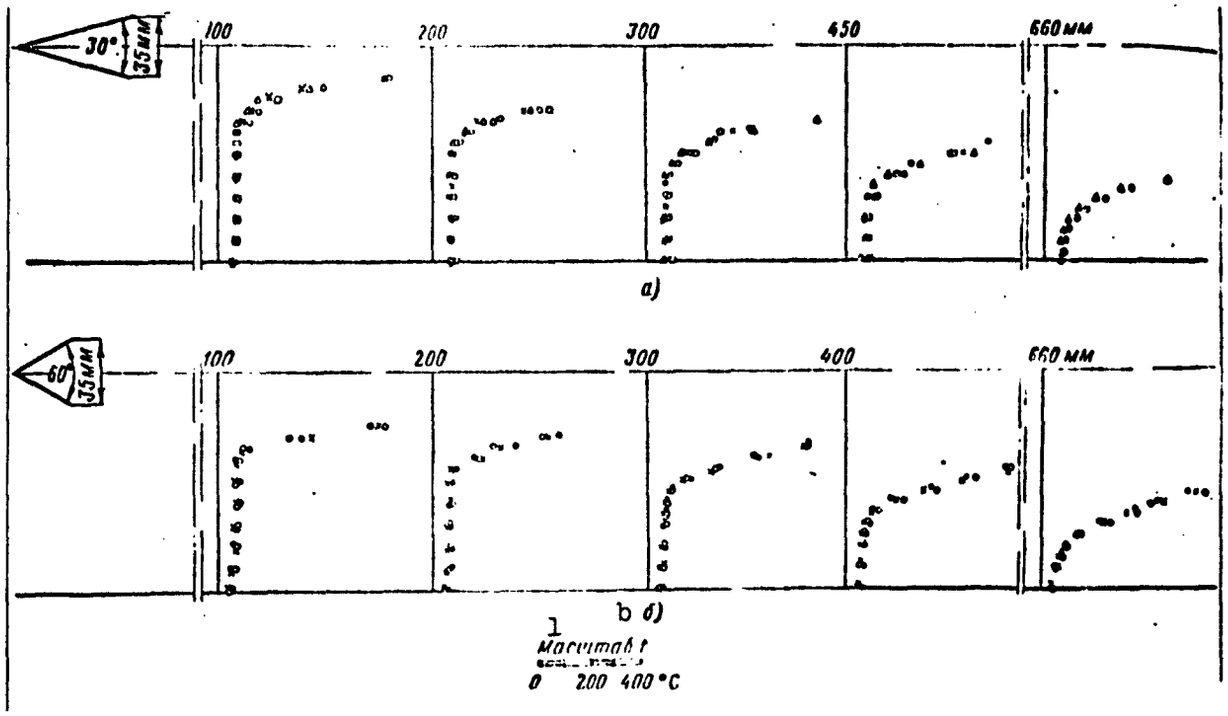

Fig. 11. Temperature fields.

а) $\alpha=1$ ○ □ $w=35$ м/сек; × △ $w=50$ м/сек; б) $\alpha=1{,}5$; ●—$w=35$ м/сек; ×—$w=50$ м/сек; ○—$w=70$ м/сек.
1 2

1) Scale of; 2) m/sec.

Consequently, the rate of propagation of the turbulent flame front is directly proportional to the first power of the pulsation velocity. It is interesting to note that this conclusion is valid independently of how the front position is determined, whether it be from the start of the change in temperature or from the start in the intense ionization.

Figure 13 shows the dependence of u_t on w', obtained as a result of processing the experimental data on the investigation of the combustion process behind stabilizers No. 1, 2, and 3. The determination of u_t and w' was carried out in sections located 200, 300, 450, and 660 mm away from the stabilizer. The position of the flame front was determined from the start of intense ionization.

It is seen from the figure that the experimental points cluster

with satisfactory accuracy along a straight line. The value of the proportionality coefficient B in the formula

$$u_t = Bw'$$

is found to be 1.21.

The results of an analogous processing, but for a front determined from the start of the temperature change, is shown in Fig. 14.

In the processing we used the data obtained behind stabilizers 1 and 2. In this case the points fitted satisfactorily a straight line, and the value obtained for the coefficient B equals 1.22.

With respect to the numerical value of the proportionality coefficient, a few remarks are in order.

When measuring the intensity of the turbulence by a thermoanemometer with a single-filament fitting, one determines in practice the longitudinal pulsational component of the velocity.

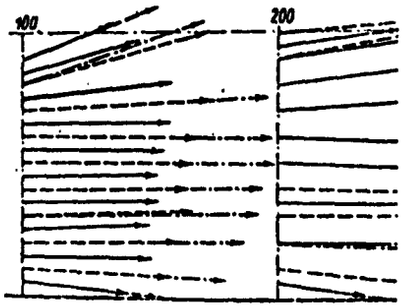

1 Масштаб w
0 20 40 м/сек

Fig. 12. Velocity fields. Stabilizer No. 1, $\alpha = 1.5$; —— w = 35 m/sec; ---- w = 50 m/sec; —·—· w = 75 m/sec. 1) Scale of.

In carrying out experiments in a stream with isotropic turbulence, measurement of the longitudinal pulsational velocity is equivalent to measurement of the transverse pulsational velocity and consequently the value of B calculated from the measured longitudinal pulsation velocity is the true value.

In investigations behind the stabilizer in a closed stream, the

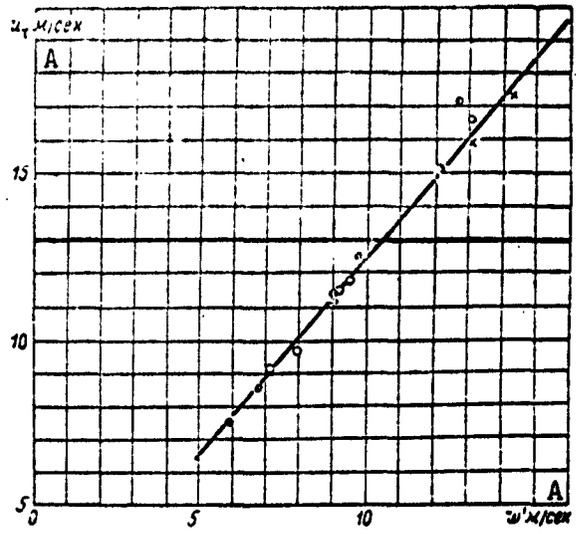

Fig. 13. Dependence of u_t on w' for different stabilizers. ●) Stabilizer No. 1, w = 35, 50, and 70 m/sec;
○) stabilizer No. 2
x) stabilizer No. 3
} w = 50 m/sec.
A) m/sec.

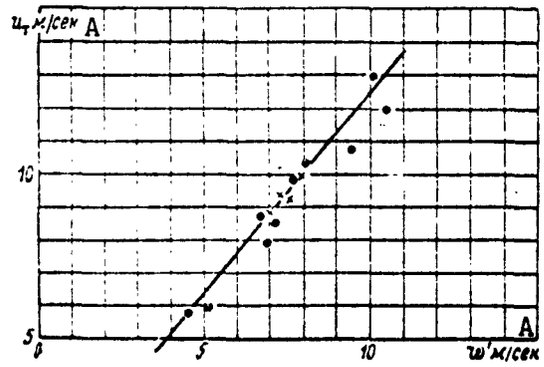

Fig. 14. Dependence of u_t on w' for different stabilizers. ●) Stabilizer No. 1; x) stabilizer No. 2.
A) m/sec.

turbulence cannot be assumed isotropic, and the most probable is a larger value of longitudinal component as compared with the transverse one, so that the obtained value of the coefficient B is smaller than the true one. This uncertainty in the numerical value of the propor-

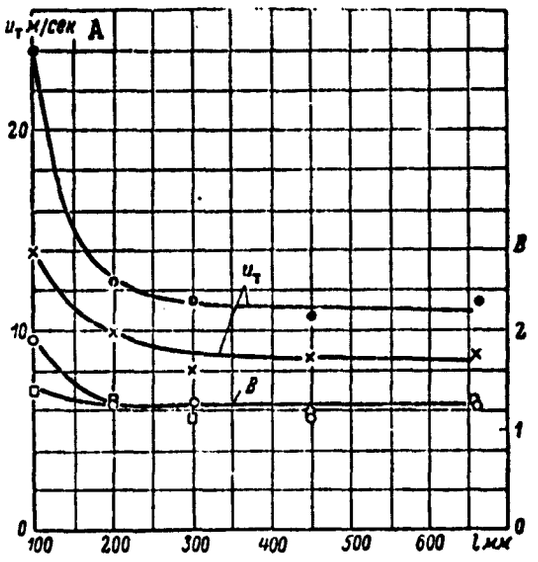

Fig. 15. Variation of u_t and B along the chamber. Stabilizer No. 1, w = 50 m/sec, α = 1.5.

X, □ } front determined from temperature;

●, ○ } front determined from ionization.

A) m/sec.

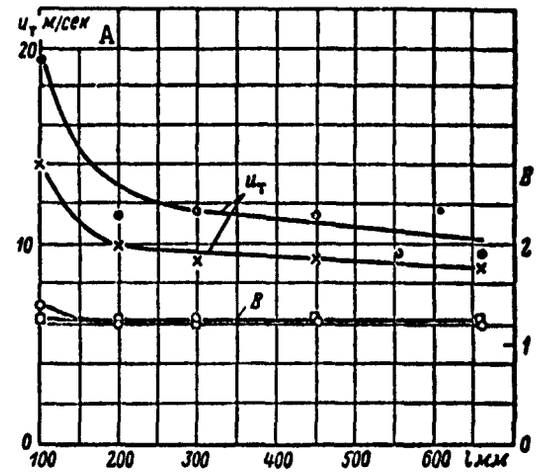

Fig. 16. Variation of u_t and B along the chamber. Stabilizer No. 2, w = 50 m/sec, α = 1.5.

X, □ } front determined from temperature;

●, ○ } front determined from ionization.

A) m/sec.

tionality coefficient may be significant in the development of a theory of turbulent flame front propagation. For practical purposes, for example for a determination of u_t in the chamber, it is more convenient to use a formula in which the coefficient B is determined from the longitudinal component, since it is simpler to measure than the transverse component.

To design the combustion chamber it is necessary to know the variation in the flame front propagation velocity along the chamber. These data are shown for stabilizer 1 in Fig. 15. The values of u_t and B were determined both from the temperature front and from the ionization front. In both cases the value of u_t corresponds to the velocity of flame propagation at the points of the leading front boundary. It is seen from the plot that the proportionality coefficient, starting with a distance of 200 mm from the stabilizer, remains constant along the chamber and is independent of which front was used to determine it. The character of variation of u_t along the chamber is the same whether u_t is determined from the ionization or from the temperature fronts. In both cases the flame front propagation velocity decreases noticeably at the distance from 100 to 200 mm from the stabilizer, and with increasing distance from the stabilizer it changes quite insignificantly. The constancy of the coefficient B in the interval 200-660 mm from the stabilizer indicates that a small decrease in u_t occurs in this interval because of the decrease in the pulsating velocity. The value of u_t determined from the ionization front, is somewhat higher than the value of u_t determined from the temperature front, owing to the larger pulsating velocity. Analogous results were obtained also in the investigation behind stabilizer No. 2 (Fig. 16).

An investigation of the influence of the turbulence scale on the rate of propagation of the turbulent flame front was carried out at a

stream velocity w = 50 m/sec and an excess-air coefficient $\alpha = 1.5$.

The average frequency of turbulent pulsations, which is proportional to the average turbulence scale, was changed by changing the form and dimension of the stabilizer.

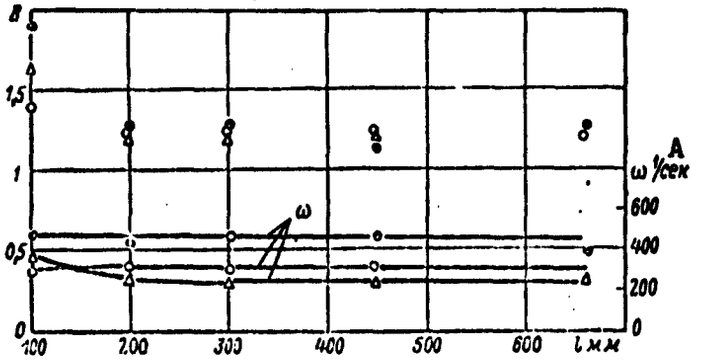

Fig. 17. Variation of B and ω along the chamber (w = 50 m/sec). ●) Stabilizer No. 1; O) stabilizer No. 2; Δ) stabilizer No. 3. A) sec.

The experiments were carried out behind stabilizers 1, 2, and 3.

Figure 17 shows the change in the proportionality coefficient B and in the average frequency of turbulent pulsations along the chamber. While the average frequency changes by a factor of two, the proportionality coefficient B remains practically constant. In addition, it was shown earlier that in plotting the dependence $u_t = f(w')$ the experimental points, obtained from the results of investigations made behind different stabilizers, fit satisfactorily one common straight line.

On the basis of these data we can conclude that the average frequency of the turbulent pulsations, and consequently also the turbulence scale, do not influence the rate of propagation of the turbulence flame front.

Influence of Turbulence Parameters on the Width of the Flame Front

In analyzing the frequency spectra obtained in the core of a free jet (see the first article of the collection) and behind a turbulizing

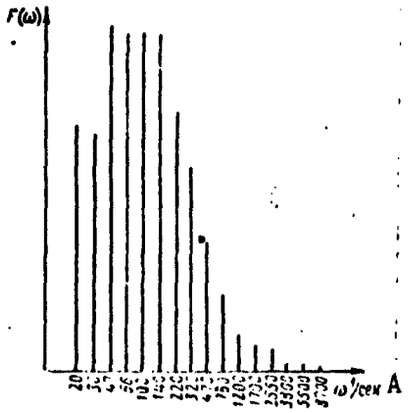

Fig. 18. Frequency spectrum (distance from turbulizing grid ø 10 is 450 mm, distance from the chamber wall is 50 mm). A) sec.

grid in a combustion chamber (Fig. 18), it is impossible to separate a definite frequency characterizing the given stream. The situation is different in the case of frequency spectra taken behind a stabilizer.

Figure 19 shows the frequency spectra obtained behind stabilizers 1, 2, and 3 at a stream velocity w = 50 m/sec. To each stabilizer corresponds its own characteristic pulsation frequency for a given stream velocity. Behind stabilizer No. 1, the presence of a characteristic frequency is less clear compared with the other stabilizers. This may be attributed to the fact that the filters had a narrow bandwidth and the characteristic frequency could lie between them. It must also be noted that a reduced value of the amplitudes of the characteristic frequencies could be obtained as a result of some disagreement between these frequencies and the frequencies to which the filters are tuned. From an examination of the spectra it is seen that an increase in the aperture angle of the stabilizer β and in the dimension 2h leads to a decrease in the characteristic frequency.

We can advance the hypothesis that vortices are produced behind the stabilizer, and that their dimension is determined by the dimension and form of the stabilizer. These vortices have the maximum energy compared with the vortex formations of other dimensions.

The variation of the frequency spectrum along the chamber section is shown in Fig. 20. The spectra were obtained in a section located 200 mm away from stabilizer No. 2. The variation of the frequency spec-

trum, brought about by the presence of a stabilizer in the chamber, is seen already at a distance of 5 mm away from the wall. This is manifest in the fact that pulsations with frequency of 320 cps begin to increase in amplitude. The increase in the amplitude of the 320-cps pulsations continues with increasing distance from the walls and reaches a maximum at approximately 50 mm away from it. With further increase in the distance from the wall the amplitude of the characteristic frequency decreases gradually and at 90 mm from the wall the curve of the spectral density becomes sufficiently smooth. At a distance of 100 mm from the stabilizer, at all points on the chamber cross section, one can separate in the frequency spectra the characteristic frequency of the turbulent pulsations (Fig. 21). The variation of the frequency spectrum along the chamber behind stabilizer No. 2 is shown in Fig. 22. For all the cross sections the frequency spectra were taken at the points at which the presence of the characteristic frequency was the most clearly pronounced. We can see from the figure how the amplitude of the characteristic frequency decreases with increasing distance from the stabilizer, something probably due to the gradual dissipation of energy of the vortices produced behind the stabilizer. In the 660-mm section behind the given stabilizer, the spectrum is practically equalized. An examination of the frequency spectra behind stabilizer No. 3 (Figs. 23 and 24) shows that the law governing their variation is analogous to that observed behind stabilizer No. 2, but in this case the characteristic frequency is quite clearly seen at a distance 660 mm from the stabilizer.

The variation of the average frequencies over the cross sections of the chamber, obtained by processing the frequency spectra behind stabilizer No. 1, is shown in Fig. 25. From an examination of the values of the average frequencies it follows that the average frequency

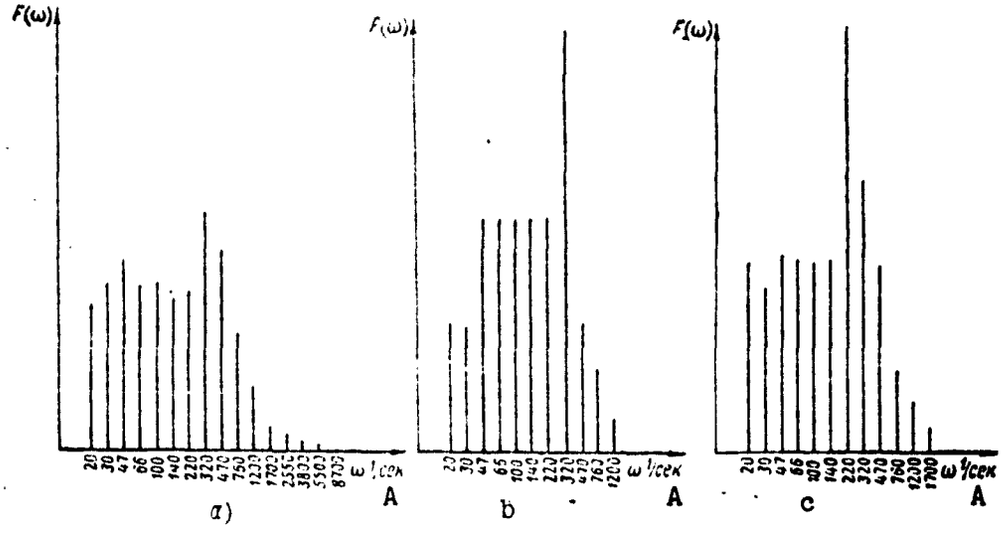

Fig. 19. Frequency spectra (section 100 mm). a) Stabilizer No. 1, 2h = = 35 mm, $\beta = 30^{\circ}$; b) stabilizer No. 2, 2h = 35 mm, $\beta = 60^{\circ}$; c) stabilizer No. 3, 2h = 70 mm, $\beta = 30^{\circ}$. A) sec.

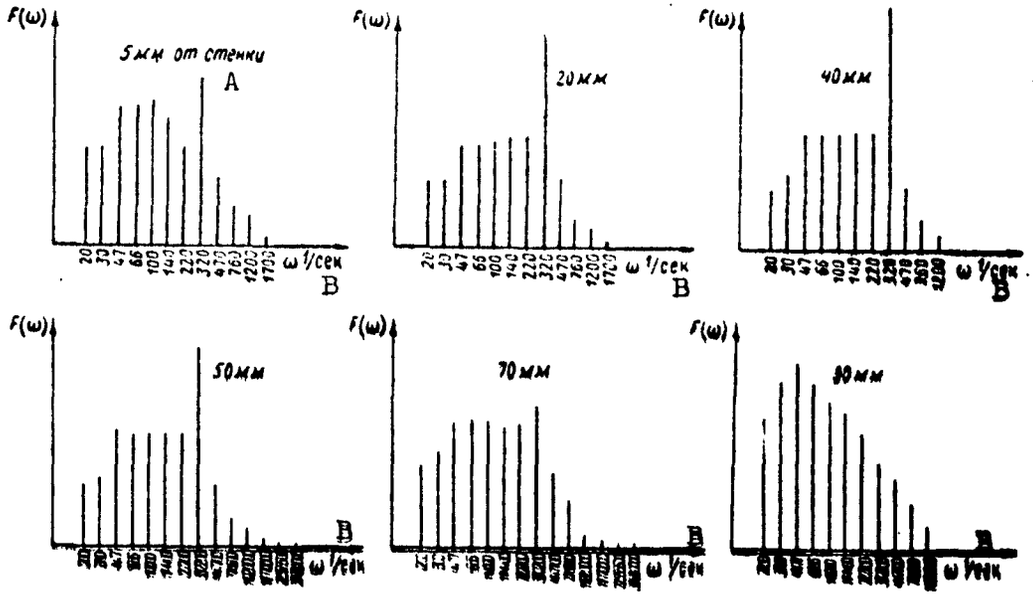

Fig. 20. Frequency spectra. Stabilizer No. 2, w = 50 m/sec, section 200 mm. A) From wall; B) sec.

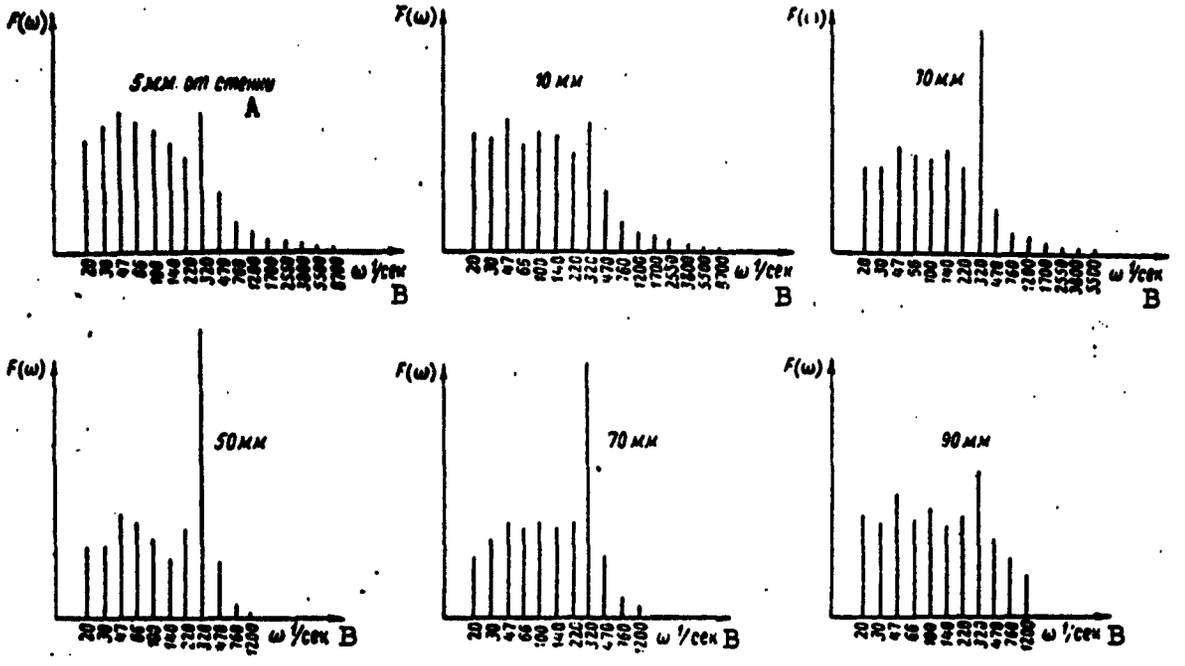

Fig. 21. Frequency spectra. Stabilizer No. 2, w = 50 m/sec, section 100 mm. A) From wall; B) sec.

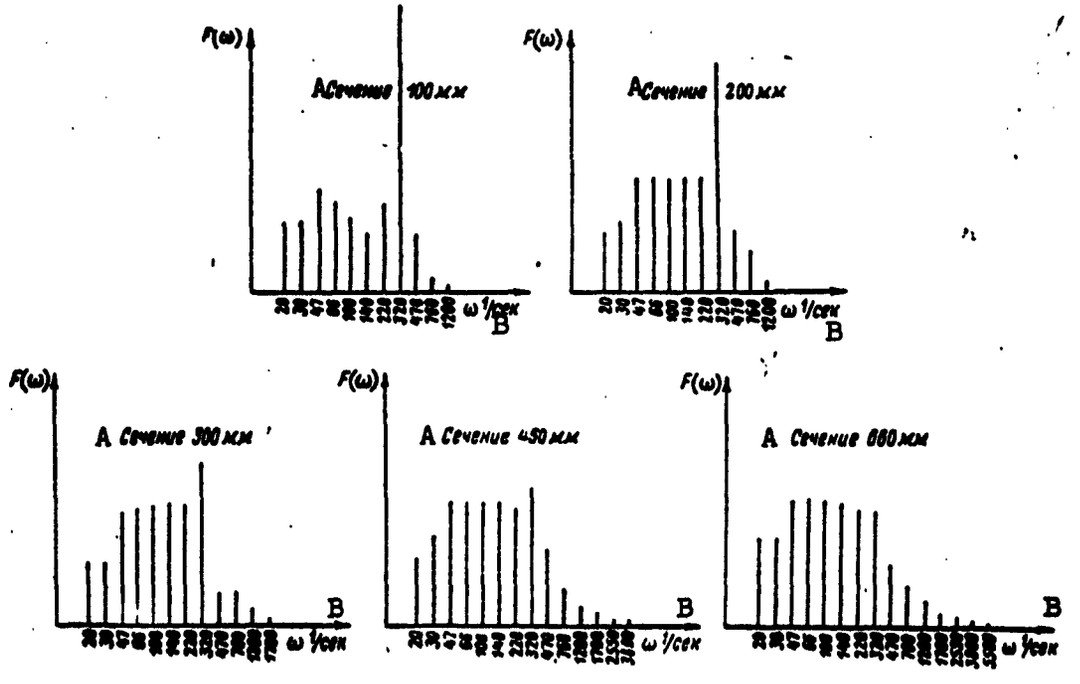

Fig. 22. Frequency spectra. Stabilizer No. 2, w = 50 m/sec. A) Section; B) sec.

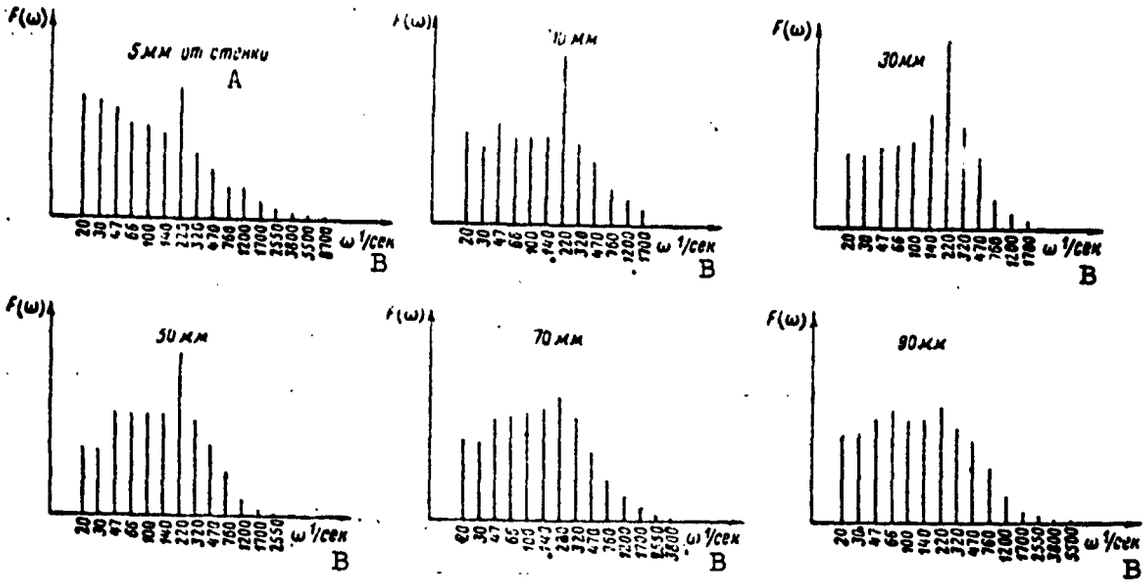

Fig. 23. Frequency spectra. Stabilizer No. 3, w = 50 m/sec, section 100 mm. A) From wall; B) sec.

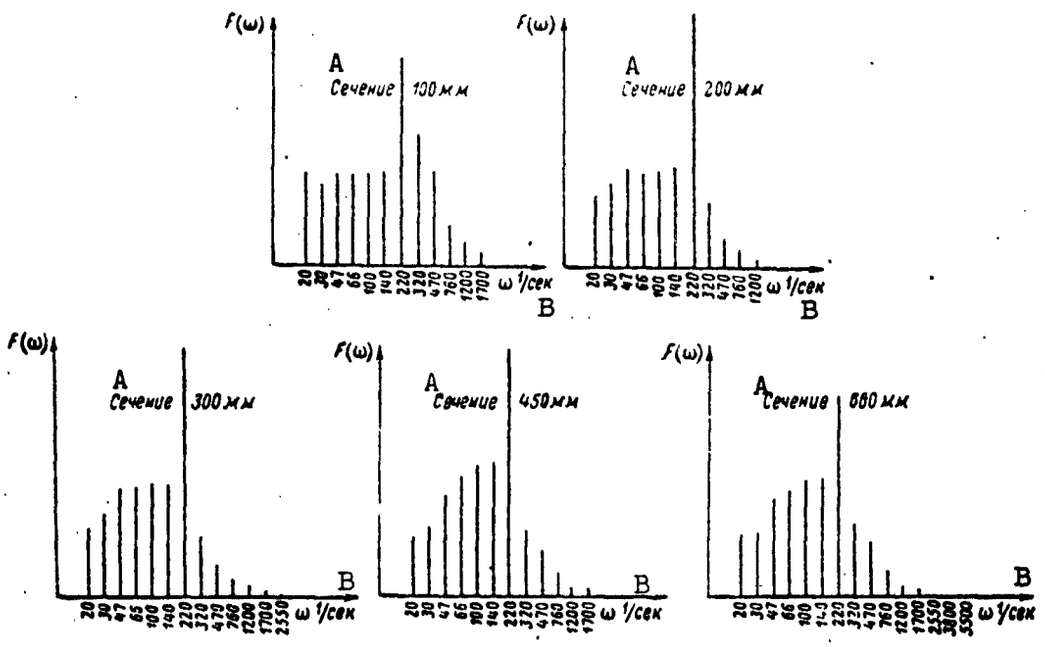

Fig. 24. Frequency spectra. Stabilizer No. 3, w = 50 m/sec. A) Section; B) sec.

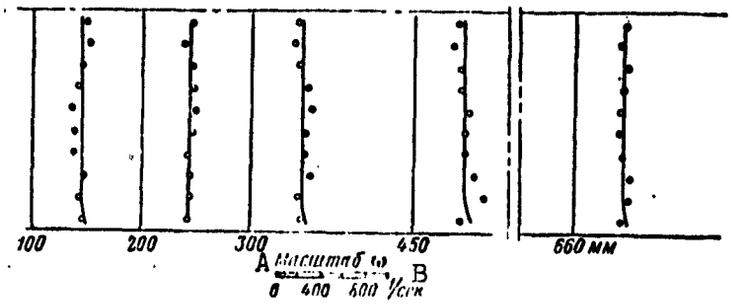

Fig. 25. Variation of the average frequency over the sections of the chamber. Stabilizer No. 1, w = 50 m/sec. A) Scale of; B) sec.

of the pulsations is practically constant both over the cross sections and along the chamber. Analogous results were obtained behind stabilizers No. 2 and 3 for the same stream velocity. A comparison of the values of the average frequencies shows that they depend both on the form and on the dimension of the stabilizer:

1 Стабилизатор	2 Средняя частота гц
№ 1 ($2h$=35 мм, β=30°)	460
№ 2 ($2h$=35 мм, β=60°)	310
№ 3 ($2h$=70 мм, β=30°)	240

1) Stabilizer; 2) average frequency, cps.

It is interesting to note that the values of the average and characteristic frequencies are quite close. Inasmuch as the average frequency characterizes the average turbulence scale, we can state that an increase in the aperture angle of the stabilizer by a factor of two increases the average turbulence scale by approximately one and a half times, and an increase in the dimension of the stabilizer by a factor of two leads to an increase in the scale by approximately a factor of two. An investigation of the influence of the velocity of the incoming stream on the value of the average frequency, carried out behind stabilizer No. 1 in the velocity range 35-70 m/sec (Fig. 26) shows that

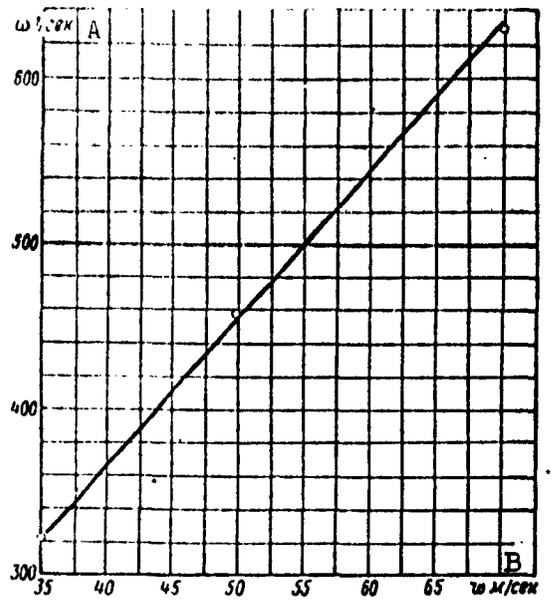

Fig. 26. Dependence of the average frequency on the stream velocity. A) 1/sec; B) m/sec.

the average pulsation frequency increases in proportion to the stream velocity, from which it follows that the ratio w_{sr}/ω_{sr} is constant.

It was indicated earlier that the following expression is valid for the turbulence scale:

$$l_{cp} = K\frac{w_{cp}}{\omega_{cp}}.$$

The constancy of the ratio w_{sr}/ω_{sr} as the stream velocity changes allows us to conclude that the turbulence scale behind the stabilizer is independent of the stream velocity. But from this it follows that the width of the flame front $\delta_t \sim \underline{l}/\varepsilon$ should not change with variation of the stream velocity, inasmuch as $\underline{l}$ and ε are constants for a given stabilizer. This conclusion is confirmed by the results of the investigation of the combustion process.

Figures 9 and 11 show that at different stream velocities the temperature curves coincide in all sections of the chamber, thus indicating that the width of the flame front is independent of the stream vel-

ocity.

Influence of Initial Turbulence on the Combustion Process

The turbulence of the stream ahead of the stabilizer was varied by installing turbulizing grids (see Fig. 4).

Figure 27 shows the temperature fields taken behind stabilizer No. 1 without a turbulizing grid in front of it and with a turbulent grid of 10 mm diameter installed at a distance 350 mm away from the stabilizer. With the initial turbulence increased, the rise in temperature in all the sections of the chamber begins earlier. The flame front spreads out and the combustion occurs in a larger volume, which leads to a more intense heat release along the chamber (Fig. 28).

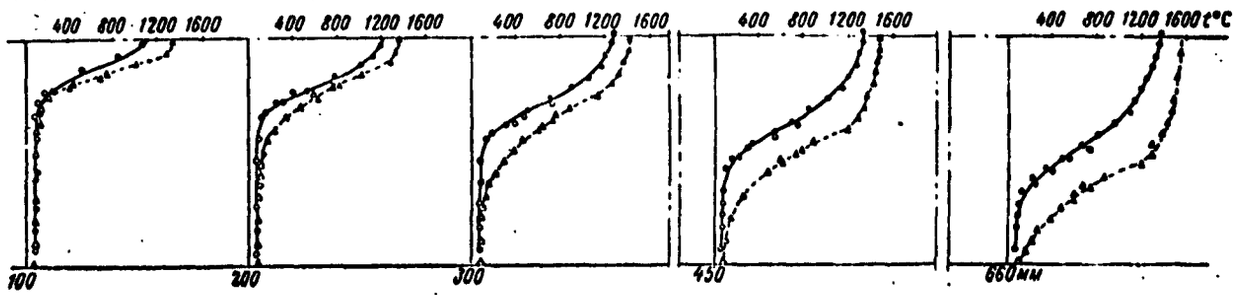

Fig. 27. Temperature fields. 1) Stabilizer No. 1, w = 50 m/sec, α = 1.5.
○) chromel-alumel thermocouple
●) platinum-platinum-rhodium thermocouple } without turbulizing grid;
△) chromel-alumel thermocouple
▲) platinum-platinum-rhodium thermocouple } with turbulizing grid.

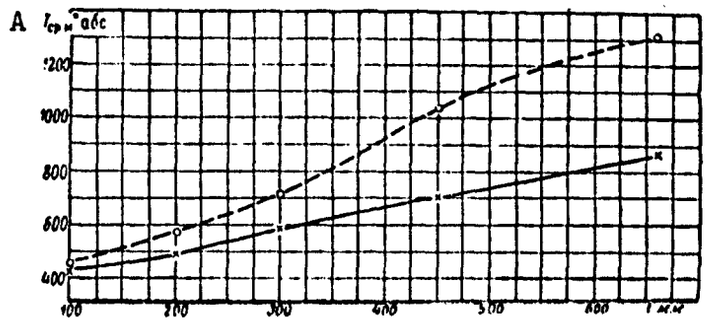

Fig. 28. Heat release along the chamber. Stabilizer No. 1, w = 50 m/sec, α = 1.5. x) Without turbulizing grid; ○) turbulizing grid Ø 10 mm at a distance 350 mm from the stabilizer; A) abs.

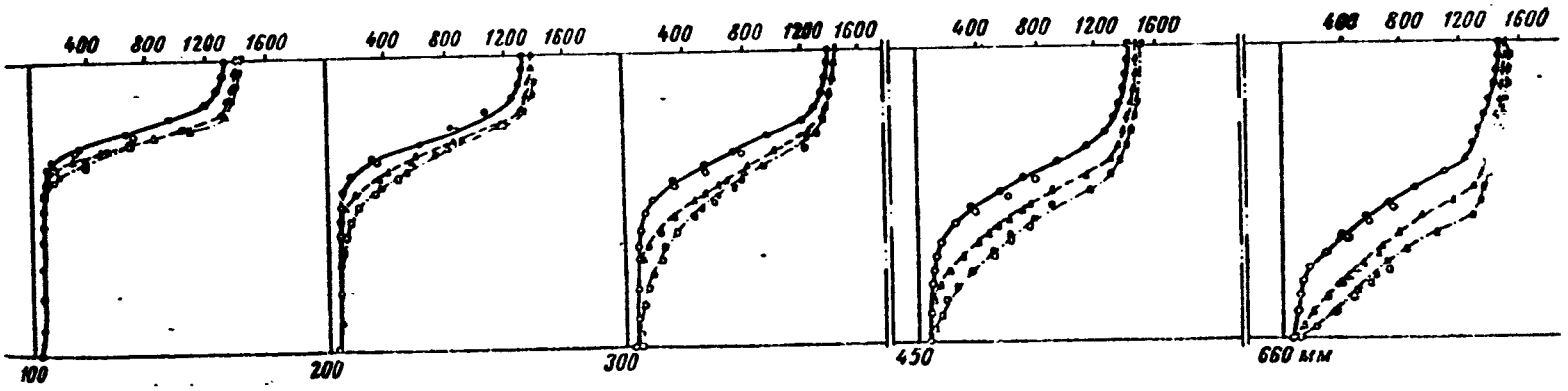

Fig. 29. Temperature fields. Stabilizer No. 2, w = 50 m/sec, α = 1.5.

○) chromel-alumel thermocouple
●) platinum–platinum-rhodium thermocouple
} without turbulizing grid;

△) chromel-alumel thermocouple
▲) platinum–platinum-rhodium thermocouple
} turbulizing grids Ø 15 mm at a distance 550 mm from stabilizer;

□) chromel-alumel thermocouple
■) platinum–platinum-rhodium thermocouple
} turbulizing grids Ø 15 mm at a distance 350 mm from stabilizer.

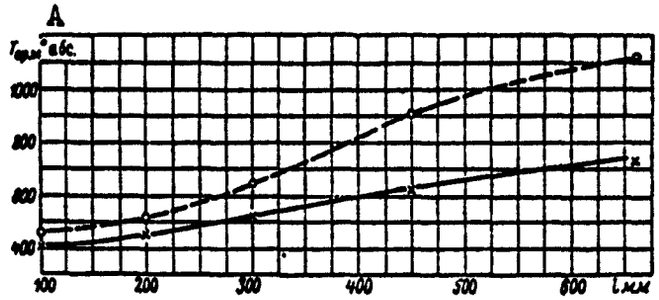

Fig. 30. Heat release along the chamber. Stabilizer No. 2, w = 50 m/sec, $\alpha = 1.5$. x) Without turbulizing grid; 0) turbulizing grids ø 15 mm at a distance 350 mm from stabilizer; A)°abs.

In the investigation carried out behind stabilizer No. 2, a grid 15 mm in diameter was installed ahead of it at distances 350 and 550 mm from the stabilizers. The results of these investigations are shown in Fig. 29. In both cases, in all sections of the chamber, the installation of the turbulizing grid leads to a spreading of the flame front, as can be seen from the start of the temperature change. Inasmuch as the intensity of the turbulence decreases with increasing distance from the turbulizing grid, it is natural that bringing the grid closer to the stabilizer will lead to a more noticeable spreading of the front. From the data shown in Fig. 30, it is seen that behind stabilizer No. 2 the heat release is also more intense when a turbulizing grid is installed ahead of it.

On the basis of these data we can conclude that for a better utilization of the volume of the combustion chamber it is convenient to increase the turbulence of the incoming stream.

Influence of the Form and Dimension of the Stabilizer on the Combustion Process

Figure 31 shows the variation of the intensity of the turbulence over the sections of the chamber behind the stabilizers No. 1, 2, 3, and 4. Behind stabilizer No. 2 with an aperture angle $\beta = 60^{\circ}$, the

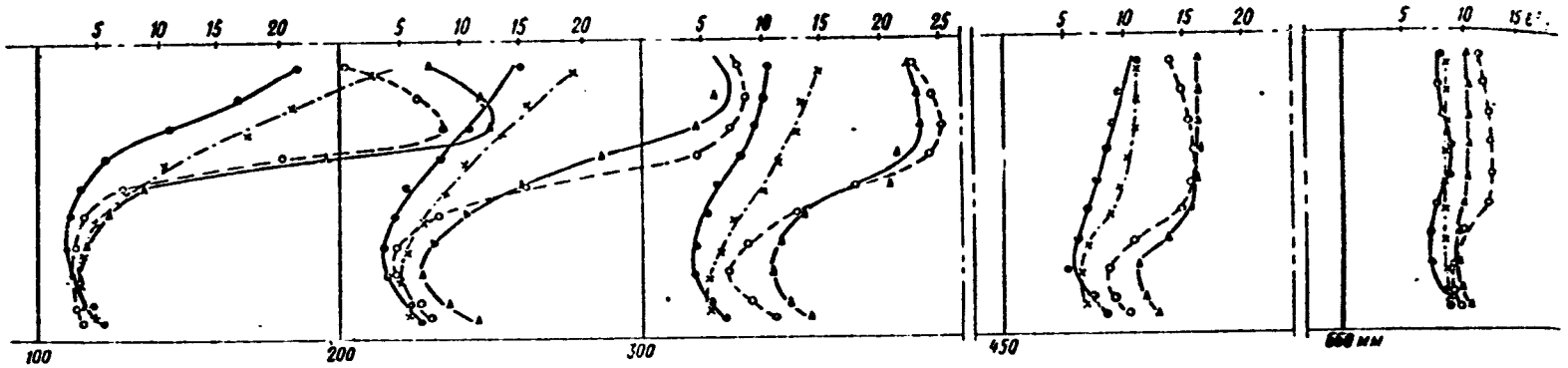

Fig. 31. Intensity of turbulence behind different stabilizers (w = 50 m/sec). ●) Stabilizer No. 1; x) stabilizer No. 2; ▲) stabilizer No. 3; 0) stabilizer No. 4.

values of the turbulence intensity in the initial sections of the chamber are somewhat higher than behind a stabilizer having the same dimension (No. 1) but a smaller aperture angle ($\beta = 30^{\circ}$). This difference decreases with increasing distance from the stabilizer and is practically missing in the section at a distance of 660 mm from the stabilizer. An increase in the dimension of the stabilizer (No. 3) leads to an appreciable increase in the maximum value of the turbulence intensity. Thus, in the section at a distance of 100 mm behind the stabilizer No. 3, we have $\varepsilon_{max} = 38\%$. Large values of ε are maintained also in the other investigated sections of the chamber.

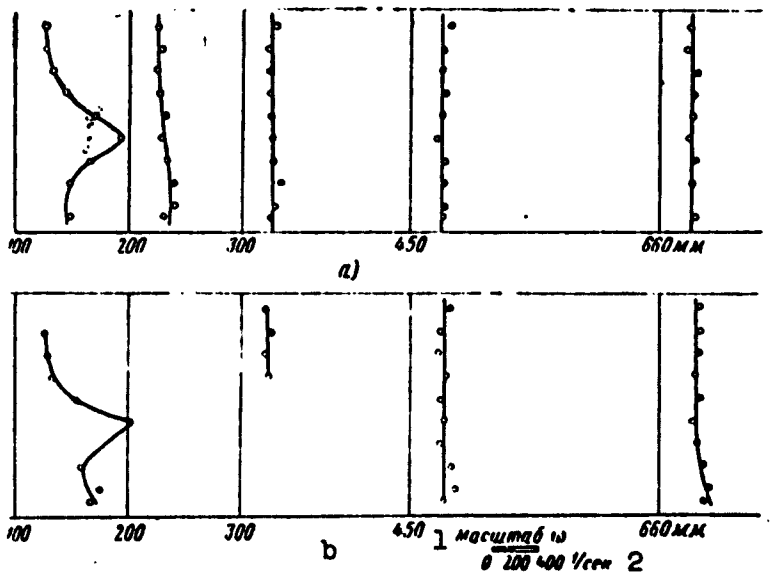

Fig. 32. Variation of the average frequency over the sections of the chamber (stabilizer No. 4, slotted, w = 50 m/sec). a) With stabilizing grid 25 mm in diameter at 550 mm from the stabilizer; b) without turbulizing grid. 1) Scale of; 2) sec.

Behind a slotted stabilizer, the maximum value of ε also noticeably exceeds the maximum value of ε behind stabilizers No. 1 and 2.

At a distance 200 mm from the slotted stabilizer No. 4, $\varepsilon_{max} = 33\%$, while behind stabilizer No. 2 $\varepsilon_{max} = 20\%$. In the section located 100 mm

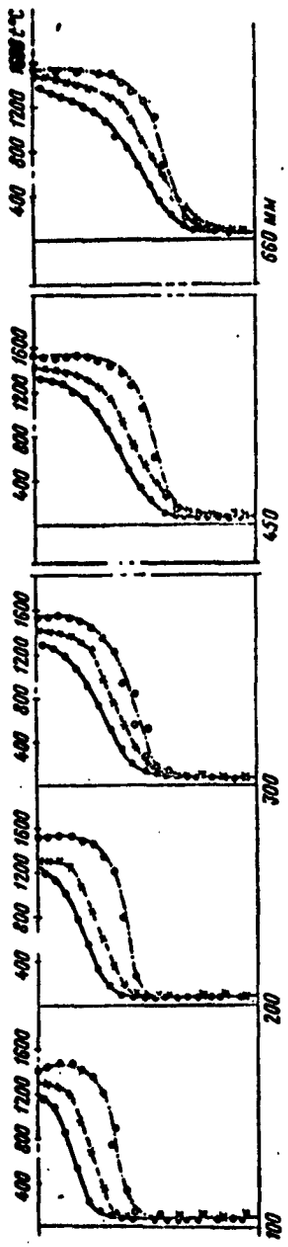

Fig. 33. Temperature fields. w = 50 m/sec, α = 1.5. ●) Stabilizer No. 1; x) stabilizer No. 2; ○) stabilizer No. 4.

away from the stabilizer, the maximum value of the turbulence intensity is attained at a distance 30 mm from the chamber axis. Greater values of ε compared with stabilizers No. 1 and 2 are retained in all the investigated sections of the chamber.

We note also that the presence of 10-mm bent plates in the slotted stabilizer leads to a noticeable increase in the average frequency in the initial sections of the chamber (Fig. 32).

At a distance of 100 mm from the stabilizer one observes a considerable unevenness in ω_{sr} over the cross section, but even at a distance of 200 mm from the stabilizer this unevenness drops out almost completely, and at 300 mm the average frequency becomes constant over the section of the chamber.

The influence of the form of the stabilizer on the combustion process was investigated by plotting the temperature fields behind stabilizers No. 1, 2, and 4. The results of the experiments are shown in Fig. 33.

From a comparison of the temperature fields, obtained behind stabilizers 1 and 2 with different aperture angles ($\beta = 30^{\circ}$

and $\beta = 60^{\circ}$) we see that the start of the rise of the temperatures behind the stabilizer with the larger aperture angle begins in all sections somewhat earlier. This result agrees with the data on the investigation of the turbulence intensity. The increase in the angle of the aperture of the stabilizer leads also to a certain increase in the temperature along the chamber axis.

Behind the slotted stabilizer one observes a small temperature gradient over the sections of the chamber. An analogous picture took place in the examination of the variation of the turbulence intensity behind this stabilizer. The maximum temperature on the chamber axis is reached behind a slotted stabilizer, in practice, at a distance of 200 mm away from it. In the 660-mm section the temperature on the axis was higher than in the 200-mm sections by merely 20°.

Furthermore, in the 200-mm section the temperature had a value which was not attained behind stabilizers No. 1 and 2 even at a distance of 660 mm.

All this indicates that the bent plates strongly intensify the burn-out process in the front. The intensification of the combustion process occurs both as a result of the increase in the intensity and as a result of the decrease in the turbulence scale at the initial sections. One must note, however, a smaller inclination of the front behind this stabilizer compared with the unslotted stabilizers, something which may be of importance in determining the necessary length of the combustion chamber.

Concluding the analysis of the data obtained, it is advisable to note the following main results of the investigation.

1) The direction of the velocity vectors, the intensity, and the turbulence scale are independent of the velocity of the incoming stream.

2) The position of the flame front and the width of the combustion

zone of a homogeneous mixture are independent of the velocity of the incoming stream in the investigated range of velocity (from 35 to 70 m/sec).

3) The rate of propagation of the turbulent flame front is directly proportional to the first power of the pulsational component of the velocity, is independent of the average frequency of the turbulent pulsations, and consequently also of the turbulence scale. The coefficient of proportionality in the formula for the rate of propagation of the flame front is the same for different stabilizers and, with the exception of the region close to the stabilizer, remains constant along the chamber.

4) The average frequency of the turbulent pulsations retains a constant value over the sections of the chamber on the investigated length at 660 mm from the stabilizer.

An increase in the aperture angle and in the stabilizer dimension lead to a decrease in the average frequency of turbulent pulsations and consequently to an increase in the turbulence scale. The average frequency is directly proportional to the velocity of the incoming stream.

5) The increase in the aperture angle of the stabilizer leads to an increase in the intensity of the turbulence and to a spreading of the flame front. The presence of bent plates in the slotted stabilizers leads to an increase in the intensity and to a decrease in the turbulence scale, something that intensifies noticeably the burn-out process in the front.

An increase of the initial turbulence of the stream contributes to a spreading of the flame front, to a more intense heat release along the chamber, and consequently to a better utilization of the chamber volume.

Manu-script Page No.	[List of Transliterated Symbols]
53	т = t = turbulentnyy = turbulent
58	ср = sr = av = average
63	т.п = t.p = toplivo, primes' fuel, additive
85	м = m = maksimal'nyy = maximum

COMBUSTION OF GASOLINE-AIR MIXTURE BEHIND STABILIZER SYSTEMS

Candidates of Technical Sciences V.P. Solntsev and V.A. Golubev

To effect stable combustion, poorly streamlined bodies or stabilizers are installed in combustion chambers.

The stabilizers are staggered in the chambers, and a considerable part of the fuel burns up upon interaction between the turbulent trails formed behind the poorly streamlined bodies. At the same time, it still is unclear what results from the interaction between the turbulent trails forming behind stabilizers of like and unlike forms and dimensions, and how the combustion process develops under these conditions.

1. PROBLEMS AND PROCEDURE OF THE INVESTIGATION

The present work is devoted to an experimental investigation of the combustion of fuel under conditions of interaction between turbulent trails that have both like and unlike turbulence parameters. In order to make the investigations approximate real conditions, the experiments were carried out in a closed stream. To exclude the influence of the physical and chemical properties of the fuel and the mixture-production factor, the development of the combustion process was investigated in a homogeneous gasoline-air mixture with an excess-air coefficient $\alpha = 1.5$. The velocity $\underline{w}$ and the temperature $\underline{t}$ at the inlet to the chamber were, respectively, $w = 50$ m/sec and $t = 120^{\circ}C$.

The experiments were carried out with the setup shown in Fig. 3 of the second article of the present collection.

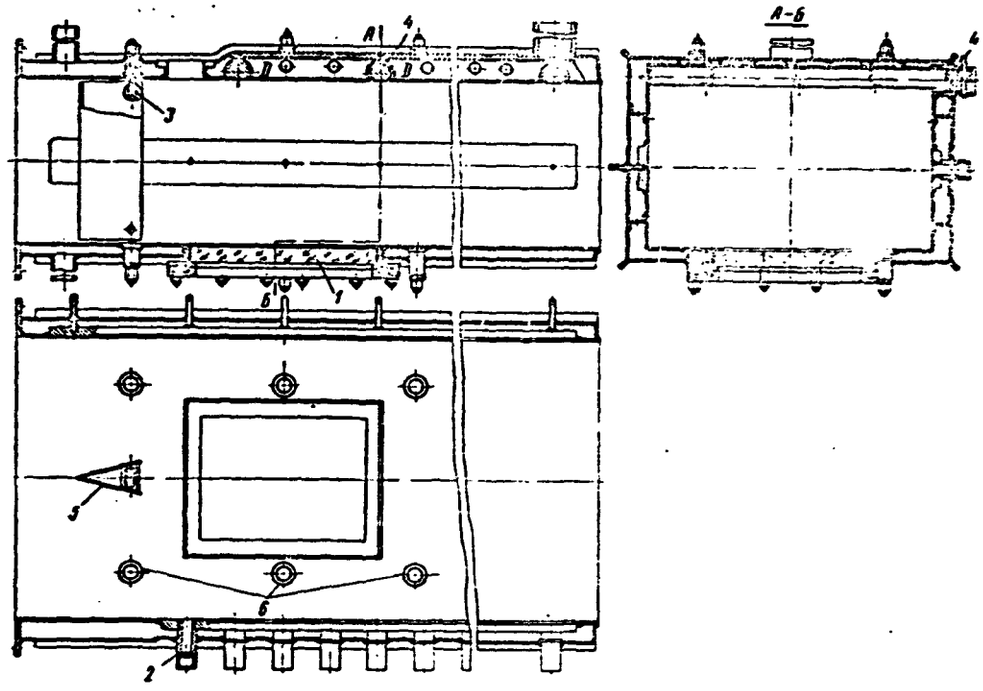

Fig. 1. Combustion chamber. 1) Viewing window; 2) pipe fitting for measurement; 3) units for mounting the stabilizer; 4) pipe fitting for "vertical" thermocouple; 5) central stabilizer; 6) locations where outer stabilizers were installed.

The combustion chamber (Fig. 1) was installed behind the transition cone and represented a tube of rectangular cross section 300 x x 175 mm, 1000 mm long.

Observation of the ignition and the combustion process was through quarts windows 1, installed in the lower part of the chamber. The chamber walls were water cooled. The measurement instruments were inserted into the chambers through connecting pipes 2, located distances 50 and 150 mm from one another. Either a single stabilizer or a system consisting of three stabilizers could be installed in the chamber. The construction of the chamber made it possible to displace the outside stabilizers at distances 150 and 300 mm relative to the central one. The stabilizers were made in the form of angles of different widths 2h (Fig. 2). The slotted stabilizer (see Fig. 2c) was made in the form of an angle the sides of which were slotted at intervals of 10 mm to a depth of 20 mm and bent perpendicular to the stream at the slots.

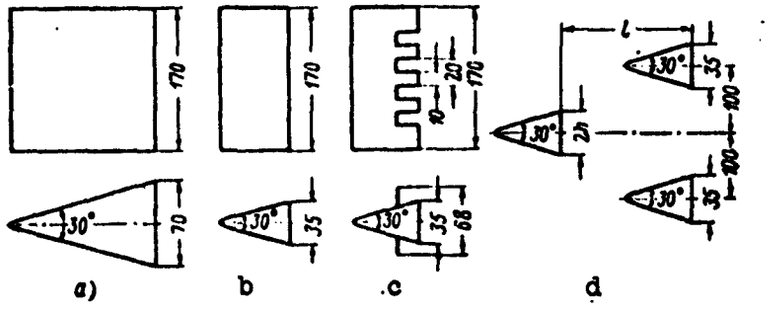

Fig. 2. Stabilizers and their arrangement. a) 2h = 70 mm, $\beta = 30^{\circ}$; b) 2h = 35 mm, $\beta = 30^{\circ}$; c) slotted stabilizer; d) stabilizers arranged together.

Measurements

The temperatures were measured in the flame front by means of platinum–platinum-rhodium thermocouples with open junctions, the use of which is subject to measurement errors resulting from heat conduction and radiation. The errors due to heat conduction increase with increas-

ing flame temperature gradient.

In a flat chamber and using flat stabilizers, the errors due to heat conduction can be reduced to a minimum by suitably locating the thermocouple.

If the stabilizers are vertically arranged and the temperature measured with a "horizontally placed" thermocouple, the latter is in a field with a considerable temperature gradient (Fig. 3a). The junction and the body of the thermocouple may be located at points in the stream whose temperatures differ by hundreds of degrees. Consequently, when measuring the temperature at point 1 (see Fig. 3a) the value obtained for it may be smaller than the real value, as a result of the heat diverted from the junction to the housing, while at points 2 and 3 the measured temperature may be higher than the real one. Behind different stabilizers, the temperature gradient in the transverse section of the torch may not be the same, and consequently the error due to the presence of heat conduction will vary.

In the present investigation the temperature fields represented the main data from which the analysis of the combustion process was made. The temperature fields were the basis for conclusions concerning the influence of the form and dimension of the stabilizer, and also concerning the presence or absence of mutual influence between the turbulent trails produced behind the stabilizers on the combustion process. In this connection, it was necessary to obtain the most reliable data when measuring the temperatures. To reduce the error due to the presence of heat conduction, it is desirable to install behind a flat stabilizer a thermocouple in vertical position (see Fig. 3b), for in this case the housing and the junction of the thermocouple are under identical temperature conditions. The construction of the "vertically placed" thermocouple employed is shown in Fig. 4.

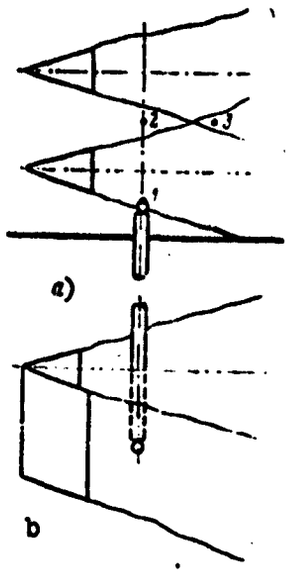

Fig. 3. Illustrating the measurement of the temperatures.

Thermocouple 1 is hinged to an internal cooled housing 3, which is located in an outer cooled housing 2. The outer housing has a longitudinal slot and can move relative to the inner one.

The thermocouple is placed in the combustion chamber (see Fig. 1) through a pipe fitting 4 in the upper part of the chamber, in a position indicated in Fig. 4c. When the outer housing 2 is moved relative to the inner housing 3 (Fig. 4b) and when the supporting pin 5 is moved out, the thermocouple 1 drops out of the outer housing under the influence of its own weight. Then the internal housing is moved forward and the thermocouple assumes the position indicated in Fig. 4a. The cold junction of the thermocouple is located inside the outer cooled housing. The wires to the measuring instrument are led out through the internal housing. In order for the hot combustion products not to enter the inner part of the outer housing, cold air is fed to the latter through tube 4 at a pressure somewhat in excess of the pressure in the combustion chamber.

Pins placed in flanges 6 prevented rotation of the internal housing relative to the external one, and also limited the longitudinal displacement of the internal housing. The thermocouple was prevented from rotating by lugs on the outer housing. These lugs slid freely in slots of a fork secured to the combustion chamber. Total pressures were measured in sections located 500-850 mm away from the stabilizer. In choosing the method for measuring the total pressures, velocity fields were plotted with the aid of a three-component fitting; an

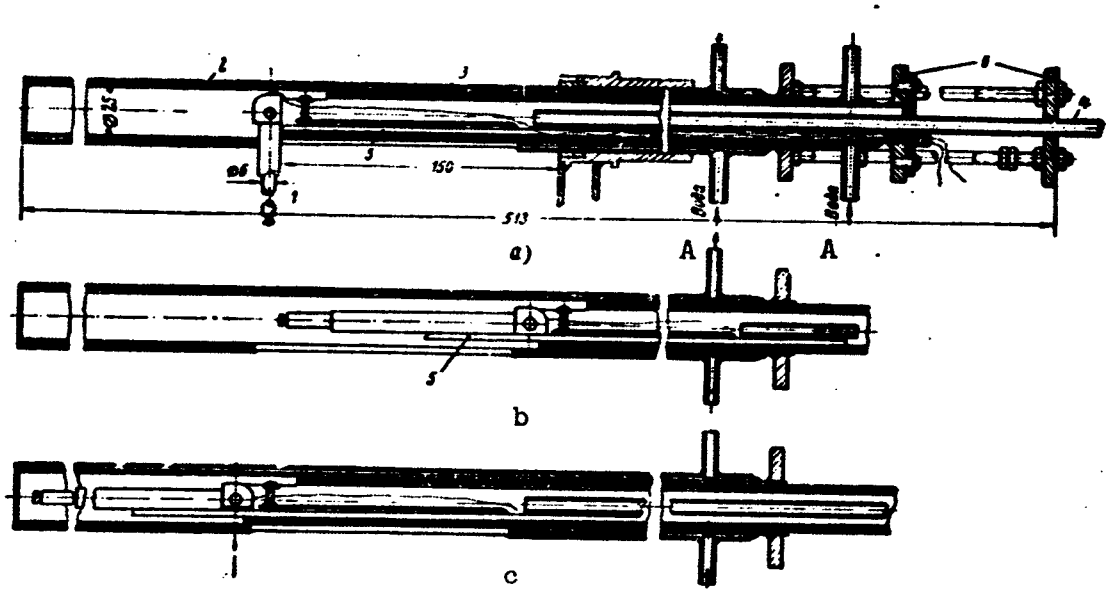

Fig. 4. "Vertical" thermocouple. 1) Thermocouple; 2) outer housing; 3) inner housing; 4) tube for air supply; 5) supporting pin; 6) flanges. A) Water.

analysis of these fields has shown that in the above-mentioned sections the deviation of the velocity vectors from axial direction is insignificant. In addition, a comparison of the total pressures, measured with L-shaped and three-component fittings, has shown that they practically agree. Therefore the total pressures were subsequently measured in all experiments with the aid of an L-shaped fitting.

Measurement of the turbulence intensity and of the average frequency of the turbulent pulsations is described in the first article of the present collection.

2. RESULTS OF THE EXPERIMENTS

Single Stabilizers

The change in the turbulence intensity over the sections and along the chamber was analogous to that observed behind similar stabilizers in a chamber of smaller dimensions and described in the fourth article of the present collection. In our case, too, the turbulence intensity depends appreciably on the form and dimension of the stabilizer. The average values of the turbulent-pulsation frequencies were obtained behind all the above-mentioned stabilizers. An analysis of the data shows that ω_{sr} depends both on the form and on the dimension of the stabilizer. An increase in the stabilizer dimension leads to a decrease in the average turbulent-pulsation frequency and consequently to an increase in the average turbulence scale.

The bent plates of the slotted stabilizer result in the appearance of high values of ω_{sr} behind such stabilizers, but the induced high frequencies attenuate rapidly.

Figure 5 shows temperature fields obtained behind the stabilizer with $2h = 70$ mm (mode II). It is seen from the presented temperature fields that the temperature gradient in the flame front is particularly large in sections close to the stabilizer, and consequently in

these sections the error obtained when the temperature is measured with a "horizontal" thermocouple can be a maximum. Measurements with a "horizontal" and "vertical" thermocouple, made at distances 250 mm away from the stabilizer, have shown that the start of the temperature rise and the temperature on the chamber axis, as registered by both thermocouples, practically coincide. But the process of temperature rise from minimum to maximum value is found to be different when measured with a "horizontal" and "vertical" thermocouple. The temperature gradient obtained with a "horizontal" thermocouple turns out to be smaller than the gradient obtained with a "vertical" thermocouple. This is most probably due to the error resulting from the presence of heat conduction, which occurs when the measurements are with a "horizontal" thermocouple which is subjected to a larger temperature gradient.

From the position of the forward boundary of the flame front, determined from the start of the temperature rise, it is seen that as the distance from the stabilizer increases the flame torch broadens, and that the aperture angle of the front decreases with increasing distance from the stabilizer. The reduction in the aperture angle of the flame front can be attributed both to the influence of the chamber walls and to the decrease in the turbulence intensity with increasing distance from the stabilizer. An analysis of the values of the temperatures in sections close to the stabilizer shows that even along the chamber axis the temperature does not reach its maximum value corresponding to complete combustion of the fuel. With increasing distance from the stabilizer a gradual rise in temperature takes place along the chamber axis. Furthermore, the temperature increase differs for different stabilizers (Fig. 6).

The observed drop in temperature in sections close to the stabil-

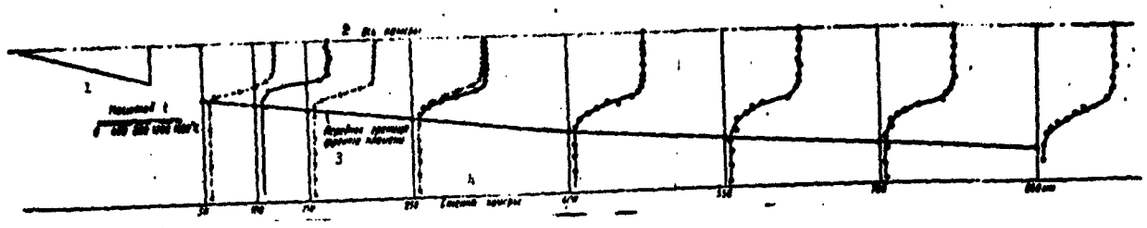

Fig. 5. Temperature fields. x) "Horizontal" thermocouple; 0) "vertical" thermocouple. 1) Scale of; 2) chamber axis; 3) forward boundary of flame front; 4) chamber wall.

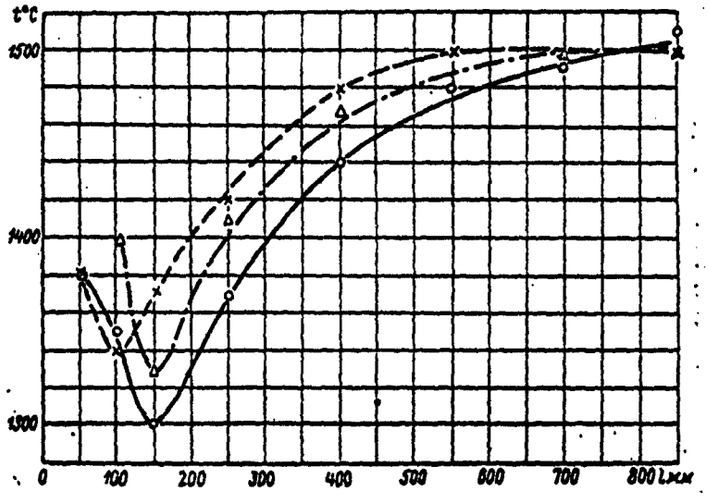

Fig. 6. Temperature variation along the chamber axis. 0) Mode I; Δ) mode II; x) mode III.

izers (for modes I and II up to $\underline{l}$ = 150 mm) is in all probability due to the presence of a backflow zone, in the center of which the temperature has a maximum value. With increasing distance from the central part of the backflow zone the temperature decreases, reaches a minimum value at the end of this zone, and then starts to increase as the combustion process develops in the active stream. The increase in temperature along the chamber axis behind the stabilizer with 2h = 35 mm (mode I) continues up to a section located 850 mm away from the stabilizer. The increase in temperature on the axis behind the stabil-

izer with 2h = 70 mm (mode II) practically terminates at a distance of 700 mm from the stabilizer, while behind the slotted stabilizer (mode III) it reaches a maximum value at a distance of 550 mm from the stabilizer. Furthermore, in all sections (starting with the section at 150 mm) the temperature on the chamber axis is higher behind the slotted stabilizer than behind all other stabilizers. Such an intensive combustion behind the slotted stabilizer can be attributed to the largest turbulence intensity ε (compared with other stabilizers) and to the smaller values of the turbulence scale l in the initial sections.

Stabilizer Systems

In analyzing the combustion process behind systems of stabilizers, it is advantageous to compare the turbulence parameters and the development of the combustion process behind each stabilizer in the system and behind the same stabilizer taken alone. Consequently, many figures show simultaneously with the results of the investigation obtained behind stabilizer systems also the data obtained in flow past single stabilizers.

The temperature fields plotted for stabilizer systems from data obtained behind single stabilizers were based on the assumption that there is no mutual influence of the turbulent trails formed by the stabilizers on the development of the combustion process. The deviation of the real fields from the temperature fields obtained in such a way indicates that such a mutual influence exists. The arrangement of the stabilizers in the various investigation modes is shown in Fig. 2d, while their data are presented in Table 1.

The values of the turbulence intensity, obtained behind a system of stabilizers with 2h = 35 mm, arranged in a single plane (mode IV), are shown in Fig. 7. In this case the turbulent trails, which had identical values of intensity and turbulence scale, interacted with one

TABLE 1

1 Режимы	2 Одиночные стабилизаторы				3 Система из трех стабилизаторов							
	I	II	III	IV	V	VI	VII	VIII	IX	X	XI	XII
2A	35	70	4 разрезной	35	35	35	70	70	70	4 разрезной		
l	—	—		0	150	300	0	150	300	0	150	300

1) Modes; 2) single stabilizers; 3) system of three stabilizers; 4) slotted.

another in the sections at 100 and 250 mm, the intensity of the turbulence behind the stabilizer system is somewhat higher than ε behind an identical stabilizer used alone (mode I).

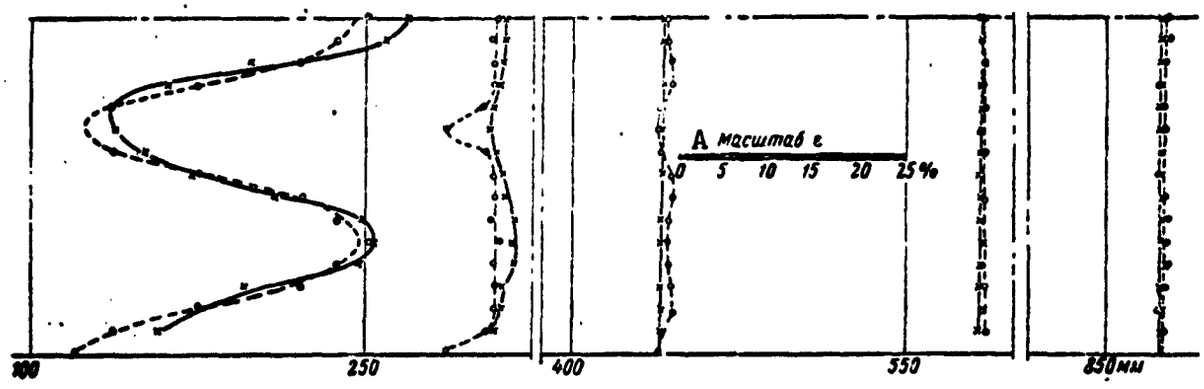

Fig. 7. Intensity of turbulence. o) Mode I; x) mode IV. A) Scale of.

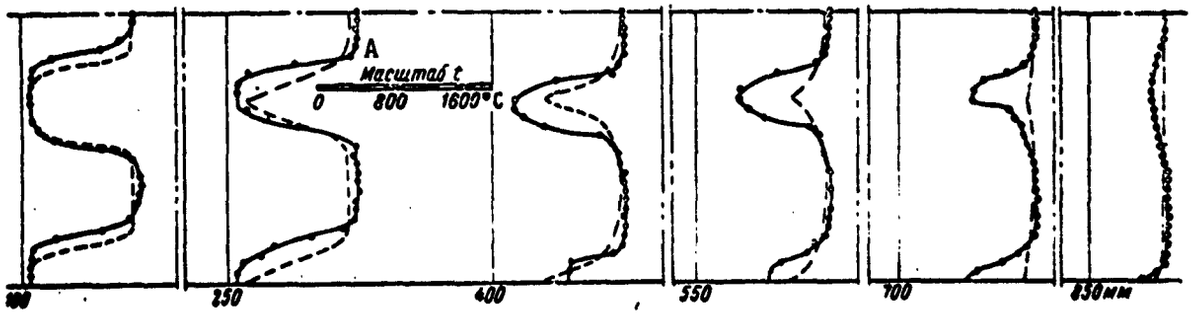

Fig. 8. Temperature fields. ---) Mode I; o) mode IV. A) Scale of.

Figure 8 shows the temperature fields measured behind the same stabilizer system. The dashed lines show the temperature fields from

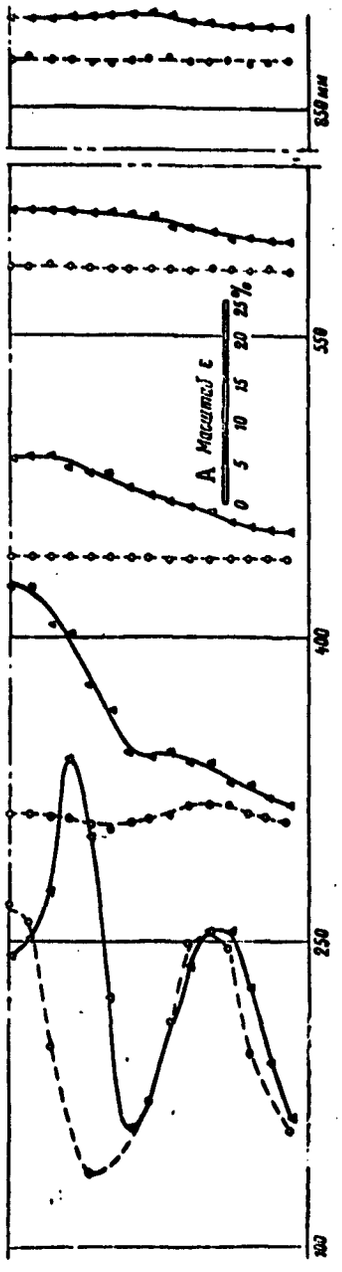

Fig. 9. Intensity of turbulence. O) Mode IV; Δ) mode X. A) Scale of.

data obtained in flow around single stabilizers. It is seen from these data that the flame torch behind either the central or the outer stabilizers is narrower than the flame torch behind a single stabilizer. Over a length of 250 mm, the temperature pattern corresponding to that of the cold mixture is maintained, indicating that the combustion process occurs not over the entire section of the chamber, whereas superposition of the temperature fields of the single stabilizers does not yield such a pattern.

It must be noted at the same time that inside the flame torches produced behind stabilizers that are part of a system, the combustion process is somewhat more intense and terminates 200 mm earlier along the chamber axis than behind a single stabilizer.

An analysis of the experimental data shows that the interaction between the turbulent trails with like turbulence parameters leads to a certain increase in the intensity and to a decrease in the turbulence scale, which in turn results in an insignificant intensification of the combustion process. Analogous investigations were carried out with a central

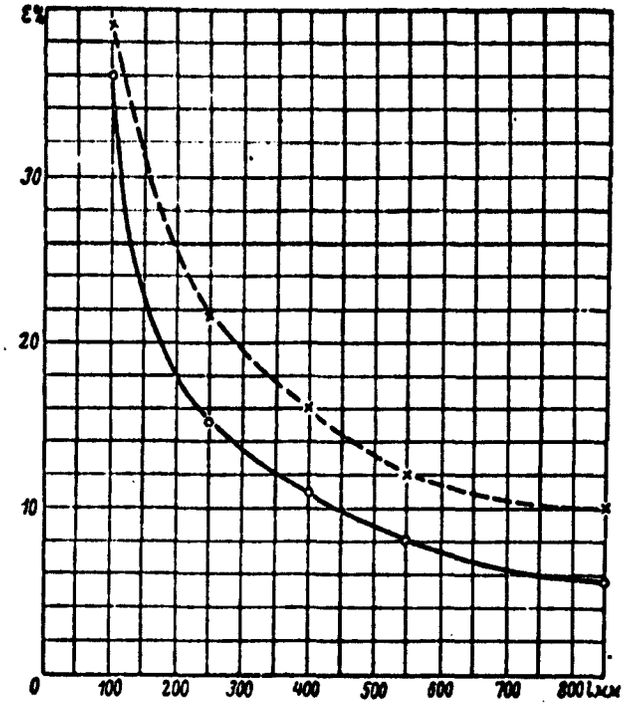

Fig. 10. Variation of turbulence intensity along the stabilizer axis. 0) Mode I; x) mode X (behind outer stabilizer).

slotted stabilizer (mode X) and with a stabilizer having 2h = 70 (mode VII).

In investigations with a central slotted stabilizer (mode X), the turbulent trails which had different values of intensity and turbulence scale interacted. Furthermore, in the first sections the turbulent trail of the central stabilizer had higher values of intensity and lower values of the turbulence scale, compared with the trail of the outer stabilizer.

Figure 9 shows for comparison the values of the turbulence intensity obtained behind stabilizer systems installed in a single plane and having central stabilizers of different forms (modes IV and X). The turbulence intensity behind a central slotted stabilizer was higher in all sections than behind a central unslotted stabilizer. Behind the outer stabilizers, up to a section 100 mm, the values of ε were prac-

tically the same in both systems. In this section one can still see a weak action exerted by the turbulent trail of the central stabilizer on the trail of the outer stabilizer. But already at 250 mm and beyond the influence of the trail of the central stabilizer manifests itself in full measure and the intensity of the turbulence behind the outer stabilizers, installed in conjunction with a central slotted stabilizer, noticeably exceeds the values of ε behind the lateral stabilizers of mode IV.

The variation of the turbulence intensity along the axis of the outer stabilizer (mode X) is shown in Fig. 10. The increase in intensity of turbulence without an accompanying increase, in this case, in the turbulence scale noticeably intensified the combustion process, which terminated on the axis of the outer stabilizer 500 mm away from the stabilizer, i.e., 300 mm earlier than behind a single stabilizer (Fig. 11).

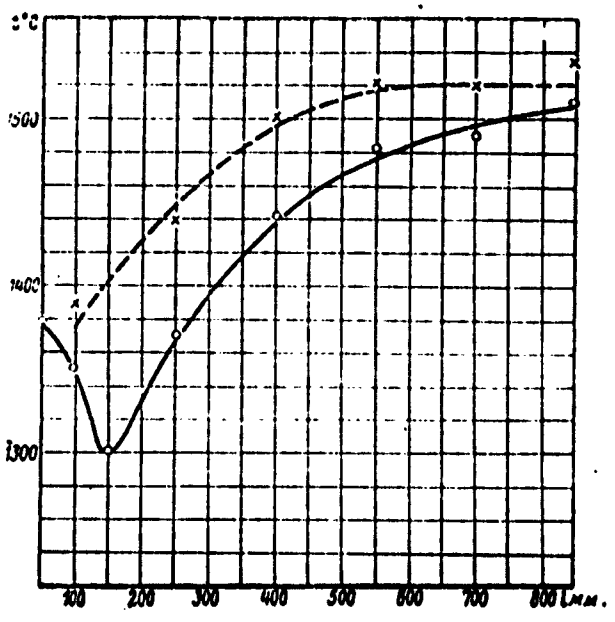

Fig. 11. Variation of temperature along the stabilizer axis. 0) Mode I;) mode X (behind outer stabilizer).

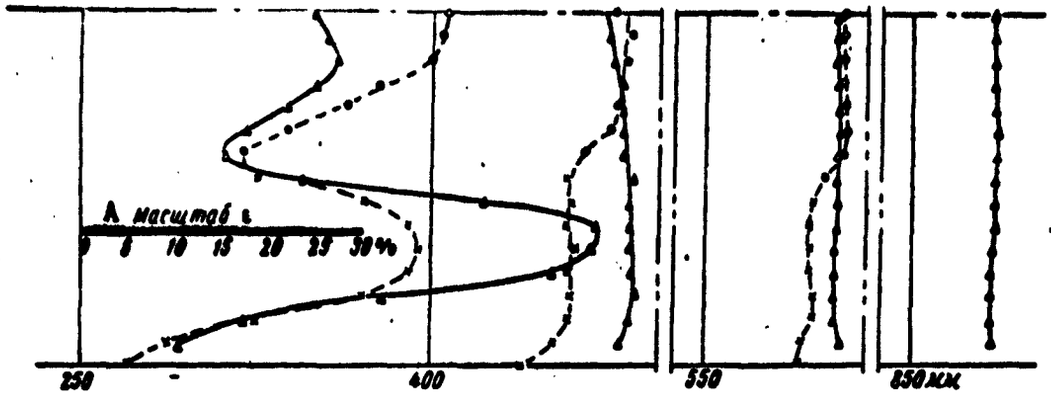

Fig. 12. Turbulence intensity. x) Mode I; O) mode III; Δ) mode XI. A) Scale of.

Figure 12 shows the variation of the turbulence intensity over the sections of the chamber, following a shift of the outer stabilizers by 150 mm relative to the central slotted stabilizer (mode XI). In this case the action of the trail of the central stabilizer leads to an appreciable increase in the value of ε behind the outer stabilizer even at a distance of 100 mm from the latter. As regards the intensification of the combustion process behind the outer stabilizers, the pattern observed in this case is analogous to that observed when the stabilizers were arranged in a single plane (mode X). An increase in the turbulence intensity behind the outer stabilizers is obtained also when a central stabilizer with 2h = 70 mm is used (Fig. 13a; mode VIII). But in the case of mode VIII one observes behind the outer stabilizers a reduction in the average frequency of the turbulent pulsations (see Fig. 13b) and consequently an increase in the average turbulence scale. The intensification of the combustion process due to the increase in ε is hindered by the increase in the turbulence scale, and this in turn, starting with the section at 400 mm, leads to a practical equality of the temperatures behind the extreme stabilizers and the single stabilizers (see Fig. 13c).

Figures 14, 15 and 16 show the effect of staggered side stabili-

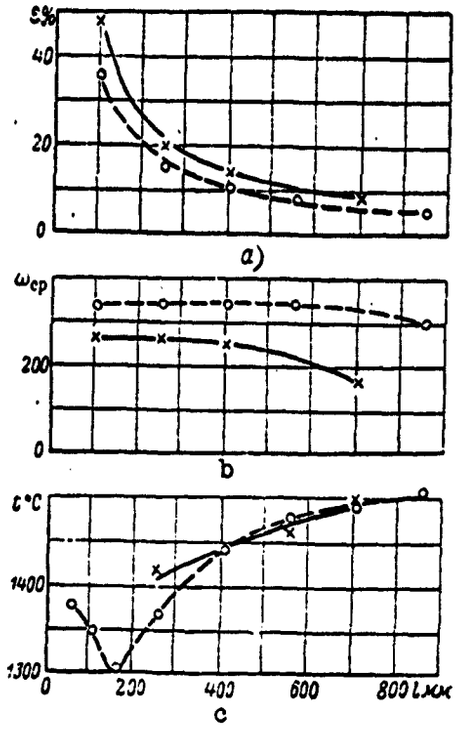

Fig. 13. Variation in the turbulence intensity ε, in the average turbulent pulsation frequency ω_{sr}, and in the temperature along the stabilizer axis. 0) Mode I; x) mode VIII (behind the extreme stabilizer).

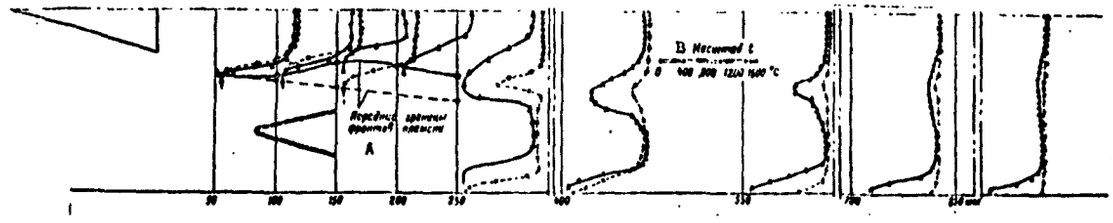

Fig. 14. Temperature fields. x) Mode I; 0) mode III; Δ) mode VIII. A) Forward boundaries of flame fronts; B) scale of.

zers on combustion behind central stabilizer.

Figure 14 shows the temperature fields plotted behind a system of

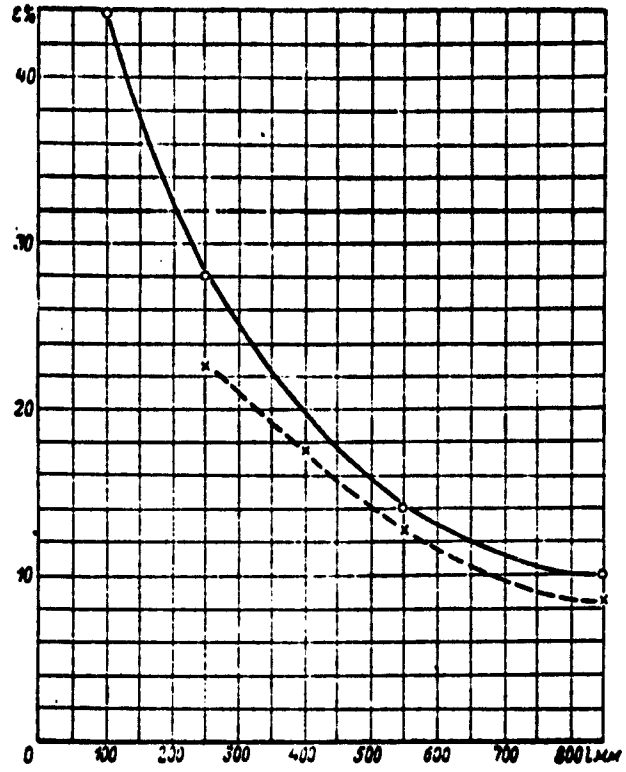

Fig. 15. Variation of turbulence intensity along the chamber axis. O) Mode III; x) mode VIII.

stabilizers, consisting of a central stabilizer with 2h = 70 mm and outer stabilizers with 2h = 35 mm, shifted by 150 mm (mode VIII). The temperature fields obtained behind this system and the temperature fields obtained behind single stabilizers were used to plot two corresponding flame fronts. The dashed line indicates the forward boundary of the flame front behind the single stabilizer. It is seen from this construction that the flame front behind the central stabilizer becomes noticeably narrower as a result of the tapering of the stream by the outer stabilizers. Thus, at a distance of 170 mm away from the stabilizer, the flame torch becomes narrower than at a distance of 70 mm. At the sections 200 and 250 mm, the area near the chamber axis where the temperatures are maximal at the given sections is practically

missing. The shift of the outer stabilizers gives rise to a certain dip in the temperature field even at a distance of 850 mm away from the central stabilizer, indicating that the combustion process is incomplete in this section.

Behind the central stabilizer one observes a decrease in the turbulence intensity (Fig. 15), which is most probably due to the formation of confusor flow behind the outer stabilizers. The reduction in ε leads to a slowing down in the development of the combustion process (Fig. 16). A noticeable decrease in temperature occurs already in the backflow zone. At a distance of 200 mm away from the stabilizer, the measured temperature turns out to be 140° lower than behind a single stabilizer. However, starting with this cross section, an intense increase in temperature along the chamber axis sets in, showing a rapid development of the combustion process.

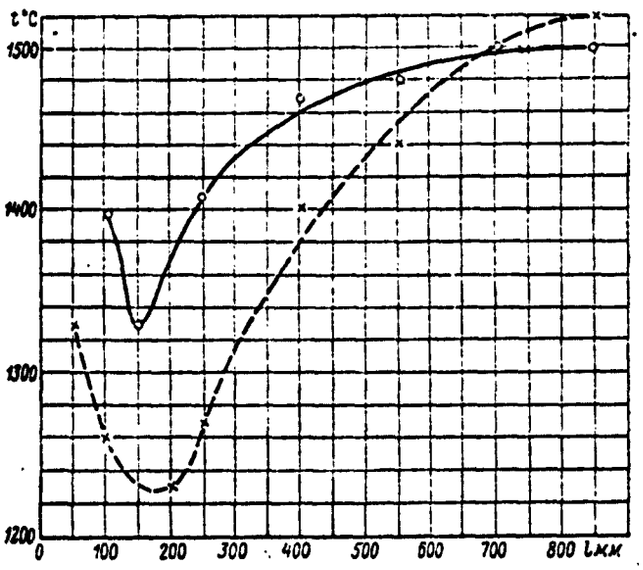

Fig. 16. Variation of temperature along the chamber axis. O) Mode III; x) mode VIII.

One can advance the hypothesis that the reduction in the temperature at the initial sections is both the result of a decrease in the

turbulence intensity and the result of a more intensified feeding of fresh mixture to the torch of the flame, owing to the tapering of the stream by the extreme stabilizers. The resultant rapid development of the combustion process is apparently due to the fact that batches of fresh mixture, penetrating deeper into the flame front, enter the zone with high temperature and with increased concentration of active centers.

Under these conditions the fresh mixture burns quite rapidly even under somewhat lower values of the turbulence intensity, and this leads to a more abrupt increase in the temperature as compared with the single stabilizer. This in turn causes the temperature along the chamber axis, behind the central stabilizer, which is appreciably lower in the 200-mm section, to turn out to be equal to the temperature behind a single stabilizer even at a distance of 650-700 mm. One must note the fact that the temperature drops in the backflow zone, and this can lead to a deterioration in the flameout characteristics of the central stabilizer.

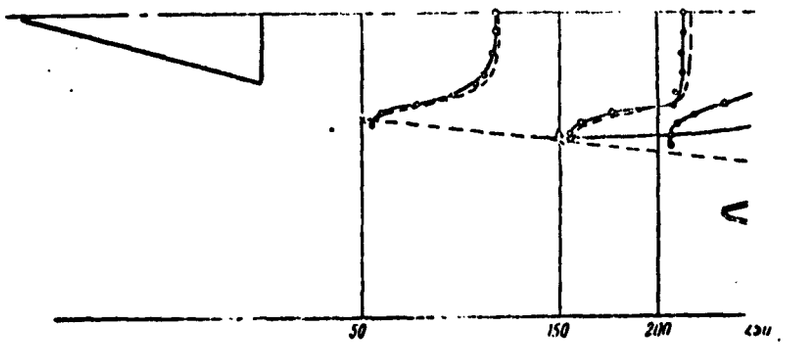

Fig. 17. Temperature fields. ---) Mode III; 0) mode IX. A) Forward boundaries of flame front; B) scale of.

The temperature fields and the position of the flame front when the outer stabilizers are shifted by 300 mm are shown in Fig. 17. The start of the narrowing down of the flame front behind the central sta-

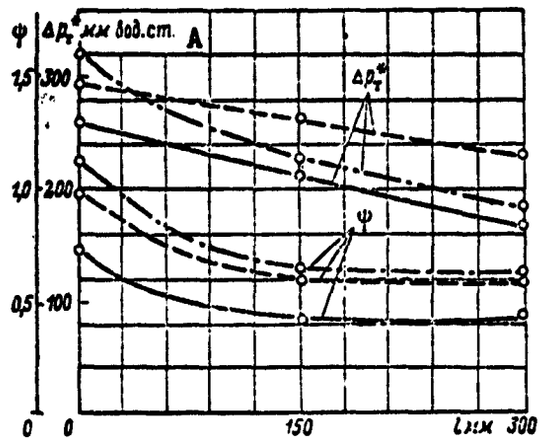

Fig. 18. Variation of Δp^*_t and ψ as functions of the stabilizer shift. —— Mode IV-V-VI; -·-·- mode VII-VIII-IX; ---- mode X-XI-XII.
A) Millimeters of water.

bilizer is observed in this case at a distance of approximately 150 mm from the stabilizer. The temperature fields at the 850-mm sections have an even larger dip than when the outer stabilizers are shifted by 150 mm. However, in the case of a 300-mm shift the temperature drop in the backflow zone is smaller than in the case of 150-mm shift. This may improve the flameout characteristics of the central stabilizer. Qualitatively analogous data were obtained in investigations of the combustion process behind a central stabilizer under conditions of modes V, VI, XI, and XII.

Figure 18 shows the variation of the quantity Δp^*_t, which is proportional to the heat released in the chamber, and of the hydraulic resistance caused by installation of different stabilizer systems, as functions of the shift of the outer stabilizers relative to the central one. The total-pressure loss was calculated in fractions of the velocity head at the inlet to the chamber

$$\psi = \frac{\Delta p^*_t}{\frac{\rho w^2}{2}},$$

where ψ is the coefficient of hydraulic resistance,

$$\Delta p^*_{kh} = p^*_n - p^*_k,$$

while p^*_n and p^*_k are the total pressure at the chamber inlet and outlet, respectively.

The quantity Δp^*_{kh} takes into account both the losses in the stabilizer region and losses due to the friction between the air and the walls of the chamber. Experiment has shown, however, that the friction losses do not amount to more than 2% of the total losses.

In investigations of the combustion process in the chamber, values $\Delta p^*_g = p^*_{n.g} - p^*_{k.g}$ were obtained. The quantity Δp^*_g takes into account both the hydraulic and the thermal losses occurring during combustion. Assuming arbitrarily that the losses caused by the stabilizer region during the combustion process in the chamber are equal to the same losses without combustion, we calculated the total pressure head losses due to the heat release:

$$\Delta p^*_t = \Delta p^*_g - \Delta p^*_{kh}.$$

The resultant value of Δp^*_t was assumed to be proportional to the heat release in the chamber.

From the data shown in Fig. 18 it follows that a sharp decrease in resistance is observed only at the start of the shift of the outer stabilizers. A shift larger than 150 mm does not lead in practice to a reduction in the chamber resistance.

It must be noted that for a more accurate plotting of the function $\psi = f(\underline{l})$ in the interval from 0 to 150 mm it is necessary to have additional experimental data. When the stabilizers are arranged in one plane the maximum heat release (Δp^*_t = 342 millimeters water) is obtained using a central stabilizer with 2h = 70 mm and $\beta = 30^\circ$. A somewhat smaller heat release is obtained with a system having a central slotted stabilizer (Δp^*_t = 295 millimeters water), and even less heat

is produced with a central stabilizer having 2h = 35 mm (Δp^*_t = 260 millimeter water).

A shift of the outer stabilizers by 150 mm, while causing an appreciable reduction in the hydraulic resistance, leads at the same time to a noticeable increase in the heat release in the chamber.

In the case of a system using a central stabilizer with 2h = 70 mm, the value of Δp^*_t decreases from 342 to 230 millimeters water. Such an appreciable reduction in the heat release can be attributed to the already indicated noticeable influence of the outer stabilizers on the central one (manifest in the narrowing down of the flame torch) and to the influence of the central stabilizer on the outer ones, behind which the combustion at the end of the chamber has not sufficient time to be completed even along the stabilizer axis, owing to the increase in the turbulence scale.

A noticeably smaller drop in the heat release is obtained in a system using a central slotted stabilizer. In this case Δp^*_t decreases from a value Δp^*_t = 295 to Δp^*_t = 262 mm H_2O. Consequently, when the outer stabilizers are shifted by 150 mm, the heat release behind a system with a central slotted stabilizer becomes larger than when using a central stabilizer with 2h = 70 mm. This is explained by the fact that in a system with a slotted stabilizer the combustion process behind the outer stabilizers develops quite intensely, and along the stabilizer axis, in spite of the shift, the combustion has time to terminate at the ends of the experimental chamber. At the same time, the influence of the outer stabilizers on the central one turns out to be somewhat smaller than in a system using a stabilizer with 2h = 70 mm.

Thus, in order to reduce the hydraulic resistance of the chamber it is advantageous to shift the outer stabilizers, but this leads to an increase in the necessary length of the combustion chamber. In ad-

dition, it must be borne in mind that in the case of a small shift a temperature decrease is obtained in the backflow zone of the central stabilizer, and this may deteriorate the breakaway characteristics of the latter. It must be noted that to obtain a more complete picture of the dependence $\psi = f(\underline{l})$ additional experimental material is necessary for different radial distances between stabilizers.

An analysis of the obtained experimental material shows that the combustion behind a single stabilizer differs from the combustion process behind a stabilizer which is part of a system. The interaction between the two turbulent trails, one of which has larger turbulence scale and intensity, leads to an increase in these parameters also in the second trail. Consequently, to intensify the combustion process behind a stabilizer it is advantageous to act on the turbulent trail produced behind the stabilizer, using a stream with larger values of intensity and smaller values of turbulence scale.

Manuscript Page No.

[List of Transliterated Symbols]

99 ср = sr = srednyy = average

112 т = t = teplovydeleniye = heat release

113 х = kh = [not identified in original]

113 г = g = goreniye = combustion

113 н = n = nachalo = beginning

113 к = k = konets = end

ON THE DESIGN OF THE SIMPLEST COMBUSTION CHAMBER OF THE RAMJET TYPE

Candidate of Technical Sciences K.P. Vlasov

The calculation of the processes that occur in a ramjet combustion chamber is a complicated problem.

Attempts to develop a procedure for such calculations were made both here ([5, 7]) and abroad ([1, 12, 13]).

Usually one determines the position of the flame torch, the pressure drop, and the variation of the completeness of combustion along the chamber as the flame propagates from a point-like ignition source. In many papers (for example [7]) this problem was solved for a flame front of finite width.

The most accurate mathematical solution was obtained by A.V. Talantov, who solved this problem, as is the case in other papers, using a whole series of simplifications (homogeneous mixture, point-like ignition source, constant turbulence parameters across and along the chamber, etc.). The simplifications assumed nevertheless do not make it possible to overcome the following difficulties:

1) the closure of the basic equations, necessary to obtain the solution, calls for introducing additional conditions, which are not always chosen with a sufficient degree of justification;

2) the exact dependence of the velocity of the turbulent propagation of the flame on the initial parameters (u', u_n, etc.) is not known;

3) there is no unified point of view with respect to the definition of the width of the turbulent-flame combustion zone (or the com-

bustion time). The experimental data on the determination of the width of the combustion zone are scanty and contradictory.

In this connection, the question arises of how to find a correct solution of this problem. The present article is devoted to this question.

1. SURVEY OF THE LITERATURE

The problem of the propagation of a flame in a cylindrical tube with ignition from a point source was solved in the papers of Ya.B. Zel'dovich, H. Tsien, G.I. Taganov, A. Scarlock, J. Fabri et al, and these authors solved this problem actually for a laminar flame (thickness of the flame front infinitesimally small, flame propagation velocity small compared with the velocity of the incoming stream). That is to say, the torch of the flame was regarded as a combustion-product zone, separated from the fresh mixture by an infinitesimally thin surface (the flame front), on which instantaneous release of heat is produced as a result of the combustion reaction; the temperature increases here abruptly by a factor of several times.

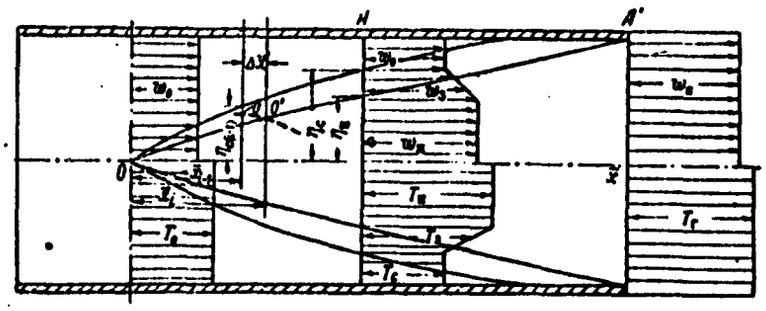

Fig. 1. Diagram of the flame torch in a tube.

Such a simplification is quite far from reality; indeed, the width of the combustion zone can be appreciable and cannot be neglected (see [4, 8]).

For a finite width of the combustion zone, such a problem was solved by B.P. Skotnikov and later by A.V. Talantov [7].

In the design of a combustion chamber, the problem is usually formulated as follows. The combustion chamber has a constant section. The mixture is ignited at a point on the stream axis. Before entering the chamber the stream is homogeneous. The static pressure is assumed constant over the transverse section of the chamber (Fig. 1). The laws governing the variation of the temperature and velocity in the combustion zone in a transverse direction are assumed specified. It is required to determine a method for calculating all the stream parameters in an arbitrary section i. The following quantities are determined: the velocity of the fresh mixture (w_s) and of the combustion products (w_p); the temperature of the fresh mixture (T_s) and of the combustion product (T_p), the pressure (p_{kh}), the ordinate of the initial flame front (y_s) and the end of the combustion zone (y_p). The solution is obtained by using the equations given below.*

The energy equation for the fresh-mixture stream:

$$c_p T_0 + A\frac{w_0^2}{2g} = c_p T_c + A\frac{w_c^2}{2g}, \qquad (1)$$

where T_0 and w_0 are the temperature and velocity of the stream at the inlet to the combustion chamber; alternately, after transformation:

$$\tau_c = 1 - \frac{k-1}{2} M_0^2 (u_c^2 - 1),$$

where

$$\tau_c = \frac{T_c}{T_0}; \quad u_c = \frac{w_c}{w_0};$$

where M_0 is the Mach number at the inlet to the chamber.

The adiabatic equation

$$\frac{T_c}{T_0} = \left(\frac{p_c}{p_0}\right)^{\frac{k-1}{k}},$$

or

$$\tau_c = \pi^{\frac{k-1}{k}}, \qquad (2)$$

where

$$\pi = \frac{p_n}{p_0}.$$

The energy equation for the stream of combustion products:

$$c_p T_0 + A\frac{w_0^2}{2g} + q = c_p T_n + A\frac{w_n^2}{2g},$$

or

$$\tau_n = \lambda_n - \frac{k-1}{2} M_0^2 (u_n^2 - 1). \qquad (3)$$

where

$$\tau_n = \frac{T_n}{T_0}; \quad u_n = \frac{w_n}{w_0}; \quad \lambda_n = 1 + \frac{q}{c_p T_0}.$$

The mass conservation equation for the entire stream:

$$\rho_0 w_0 F_0 = \rho_c w_c (F_0 - F_c) + \rho_n w_n F_n + \int_{F_n}^{F_c} \rho_s w_s \, dF, \qquad (4)$$

where ρ_0, ρ_s, and ρ_p are the densities in the initial section, in the fresh mixture, and the combustion products, respectively; ρ_z and w_z are the density and stream velocity of the mixture in the combustion zone; F_0 and F_p are the areas of the transverse section of the chamber and of the combustion-product stream; $F_s = F_0 - (F_p + F_z)$ is the area of the entire stream after subtracting the stream of the fresh mixture; alternately

$$1 = \frac{\pi}{\tau_c} u_c (1 - f_c) + \frac{\pi}{\tau_n} u_n f_n + \pi \int_{f_n}^{f_c} \frac{u_s}{\tau_s} df, \qquad (5)$$

where

$$f_c = \frac{F_c}{F_0}; \quad f_n = \frac{F_n}{F_0}; \quad u_s = \frac{w_s}{w_0}; \quad \tau_s = \frac{T_s}{T_0}.$$

The momentum equation is

$$p_0 F_0 + \rho_0 w_0^2 F_0 = p_\lambda F_0 + \rho_c w_c^2 (F_0 - F_c) + \rho_n w_n^2 F_n + \int_{F_n}^{F_c} \rho_s w_s^2 \, dF, \qquad (6)$$

or, after simple transformations

$$\frac{z}{2}+1=\frac{\pi}{\tau_c}u_c^2(1-f_c)+\frac{\pi}{\tau_n}u_n^2 f_n+\pi\int_{f_n}^{f_c}\frac{u_0^2}{\tau_0}df, \tag{7}$$

where

$$z=\frac{p_0-p_z}{\frac{\rho_0 w_0^2}{2}}=\frac{2}{kM_0^2}(1-\pi).$$

The mass-conservation equation for the fresh mixture:

$$\rho_{c(i-1)}(F_0-F_{c(i-1)})w_{c(i-1)}=\rho_{ci}(F_0-F_{ci})w_{ci}+\rho_{cp}u_\tau\Delta S, \tag{8}$$

where ρ_{sr} is the average density on the portion between the neighboring sections and ΔS is the area of the flame front between these sections, or, in dimensionless form

$$\pi_{c(i-1)}\frac{u_{c(i-1)}}{\tau_{c(i-1)}}(1-f_{c(i-1)})=\pi_{ci}\frac{u_{ci}}{\tau_{ci}}(1-f_{ci})+\frac{1}{2}\left[\left(\frac{\pi}{\tau_c}\right)_{i-1}+\left(\frac{\pi_c}{\tau_c}\right)_i\right]\bar{u}_\tau\Delta\bar{S}, \tag{9}$$

where $\bar{u}_t = u_t/w_0$ and $\Delta\bar{S} = \Delta S/F_0$.

Further, in order to solve this system of equations, it is necessary to introduce supplementary conditions. Different conditions were used in [7] and [11], so that in final analysis the results obtained are different.

In the work of A.V. Talantov, the lacking equations are obtained from the conditions that the "time consumed and available for the elementary jet must be equal." The available time on moving along the current line 00' (see Fig. 1) is

$$\Delta t_p=\frac{\Delta x}{w_{cp}}.$$

The time required to complete the combustion process can be determined if one knows the law governing the burning up of the mixture in the elementary jet in time:

$$\Delta t_n=t_n-t_{3(i-1)},$$

or

$$\frac{\Delta x}{w_{cp}} = t_n - t_{z(i-1)}, \qquad (10)$$

where Δx is the distance between neighboring sections; w_{gr} is the average velocity of motion of the mixture between these sections; t_p is the total time of combustion of the mixture in the elementary jet; and $t_{z(i-1)}$ is the time that the mixture stays in the zone, starting with the instant of crossing the initial torch boundary.

In addition, the author uses a supplementary approximate condition, first introduced by H. Tsien [9]. Equations (1) and (3) are used:

$$\frac{\tau_n}{\tau_c} = \frac{\lambda_n - \frac{k-1}{2} M_0^2 (u_n^2 - 1)}{1 - \frac{k-1}{2} M_0^2 (u_c^2 - 1)},$$

or approximately

$$\frac{\tau_n}{\tau_c} = \lambda_n. \qquad (11)$$

Finally, the fraction of the heat Q_v released in some section relative to the total heat Q_p possessed by the mixture (burnup) can be determined from the relation

$$r = \frac{Q_n}{Q_n} = \frac{\Sigma I_i - I_0}{Q_n}, \qquad (12)$$

where ΣI_i and I_0 are the total heat contents of the mixture in sections i and in the initial section, respectively. After transformations we obtain

$$r = \frac{1}{\lambda_n - 1}\left\{\left[\frac{\pi}{\tau_c} u_c (1 - f_c) + \frac{\pi}{\tau_n} u_n f_n - 1\right]\left(1 + \frac{k-1}{2} M_0^2\right) + \right.$$
$$\left. + \frac{\pi}{\tau_n} u_n f_n (\lambda_n - 1) + \pi \int_{f_n}^{f_c} u_s \, df + \frac{k-1}{2} M_0^2 \pi \int_{f_n}^{f_c} \frac{u_s^2}{\tau_s} \, df \right\}. \qquad (13)$$

The system is closed if the laws governing the variation of the parameters in the combustion zone are known and the integrals in Eqs. (5), (7), and (13) are evaluated. A.V. Talantov assumes a linear variation of the velocity and of the temperature in the zone.

The most doubtful in the calculation method of A.V. Talantov is the introduction of a characteristic combustion time in the turbulent stream. This combustion time is taken from the data of the author himself [8].

The question of the correctness of the employed measurement procedure and the results of the measurements of τ_{sg} are debatable. This question will be considered in greater detail below.

B.P. Skotnikov actually considered the same equations (1), (4), (6), (8).

The supplementary conditions for the solution of these equations were as follows:

1) a connection was found between u_s and u_{p0} (where u_{p0} is the velocity of the combustion products along the chamber axis) in the form of the relation

$$u_{s0} = \sqrt{1 + \tau(u_c^2 - 1)},$$

where τ is the degree of heating and

$$\rho_s/\rho_p = \tau;$$

2) a parabolic variation of the velocity profile over the section of the chamber was specified (and a similar density profile);

3) the dependence of the width of the combustion zone in the radial direction ($\delta_t = \eta_s - \eta_p$) was specified in the form $\delta_t = f(\eta_s)$, for which experimental data were used.

Here η_s is the radius of the initial boundary of the torch and η_p is the radius of the boundary of the combustion products of the torch.

The calculation of B.P. Skotnikov is also not fully correct. It is incorrect to specify $\delta_t = f(\eta_s)$, since δ_t depends not on η_s, but on $\bar{x}$, the distance from the point of ignition of the combustible mixture, and therefore the author's calculation data are valid only for one particular case, when $w = \text{const}$, $\alpha = \text{const}$, $\varepsilon = \text{const}$, $\bar{x} = \text{const}$ [the

variation of $\underline{w}$, α, ε, and other parameters changes also the dependence of $\delta_t = f(\eta_s)$].

Yu.A. Shcherbina [11] proposed a method of calculating the burnup behind one or several sources of the ignition. On the basis of this calculation one can plot the temperature fields at any distance from the ignition sources. It is assumed that the flame front fluctuates in random fashion about some average position $\underline{a}$, with some mean-square deviation σ from this average position. The value of σ can be obtained from Taylor's equations for specified $\underline{l}$, ε, and $\underline{x}$.

At the present time u_t cannot be determined analytically and therefore the author obtains an empirical dependence $u_t = f(u_n, w, \sigma)$. Knowing u_t, it is possible to find the value of $a = f(x)$ and consequently calculate the temperature profile and the completeness of combustion in a given section of the combustion chamber. With regard to [11], the following remarks can be made.

The author actually does not take into account at all the influence of the chamber walls on the development of the combustion and formation of the flame torch. Therefore this calculation is valid only for several particular cases, for which the dependence $a = f(\overline{x})$ has been obtained.

Satisfactory agreement was obtained between the calculation results and the experimental data of other authors (to be sure, all these experiments pertained either to conditions of semiopen combustion chambers or to relatively short chambers when the influence of the walls is insignificant). Such an agreement is not surprising, since the author uses an empirical relation $u_t = f(u_n, w, \sigma)$, which is obtained from the very same experiments. Actually, the author specified the position of the torch in the combustion chamber $\eta_s = f(x)$, i.e., the dependence which has to be determined as a result of the calculations.

2. PRELIMINARY REMARKS

Before we proceed to describe the proposed method of designing the combustion chamber, let us dwell in greater detail on some characteristics without which any chamber design is impossible. We have in mind two principal characteristics: the rate of propagation of the turbulent flame u_t, and the width of the combustion zone of the turbulent flame δ_t (or a quantity which is analogous to it in meaning, namely τ_{sg}, the combustion time).

At the present time it is impossible to calculate theoretically the value of u_t. There are several experimental researches on the determination of u_t in an open stream of homogeneous combustible mixtures. The question of how to determine u_t is debatable (see [2, 3, 9, 10]), but the results of the experimental determination of u_t also depend on this fact, and consequently different authors obtained values which differed quite strongly from one another. Whereas the dependences $u_t = f(u', u_n, p)$ obtained by various authors are more or less close to one another [3], the absolute values of u_t differ appreciably [thus, $u_t \approx (1\text{-}6)u'$]. On the other hand a change in the absolute value of u_t greatly influences the results of calculation of η_s and $r = f(\bar{x})$. In addition, no measurements of u_t in the combustion chamber were made. Therefore, in order to solve this problem, we undertook to determine the values of $\bar{u}_t$ from results of reduction of experimental data on burnup in a combustion chamber.

Even more debatable is the question of the determination of δ_t or τ_{sg}.

A.V. Talantov [8] derived the theoretical relations $\tau_{sg} = f(\underline{1}, w, w', u_n)$ and compared this relation with the experimental results. The derivation of these theoretical relations, carried out by the author, is far from obvious, and the experimental determination of τ_{sg} raises

many objections.

The author calculates the combustion time in the following manner: he considers the combustion of an individual source of fresh mixture, cut off by turbulent pulsations from the initial flame surface and surrounded by combustion products. This assumption is not obvious. Further, A.V. Talantov proposes that such a source of fresh mixture burns from the surface at the initial time with velocity

$$u_n = u_n + K_{\mu 0} w'_0 \frac{l}{l_0},$$

where $K_{\mu 0}$ is a coefficient that takes into account the efficiency of the action of the pulsational velocity (the value of this coefficient is not determined); w'_0 and $\underline{l}_0$ are the initial values of the pulsational velocity and the dimension of the elementary source; and $\underline{l}$ is the running dimension of the elementary source, which burns with velocity $u_m = u_n$.

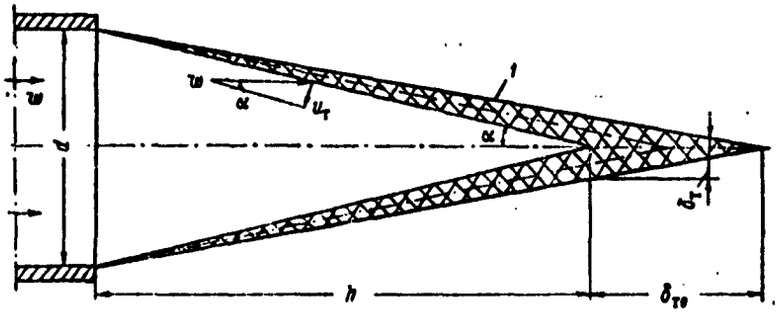

Fig. 2. Schematic representation of the direct cone of the flame. 1) Combustion zone.

No account is taken here of the increase in the normal velocity when the elementary source has small dimensions, i.e., when its surface has large curvature.

Writing the combustion equation in the form

$$d\underline{l} = u_m d\tau$$

and integrating it, the author obtains a final equation in the form

$$\tau_{sg} = \frac{l_0}{w_0} \ln\left(1 + \frac{w_0'}{u_t}\right);$$

it is assumed here that $K_{\mu 0} = 1$.

The entire derivation is based on many assumptions which are made a priori, so that these results cannot be regarded as proved.

To determine τ_{sg}, the width of the combustion zone δ_{t0} was measured along the axis of the direct cone of the flame. In many investigations (see, for example, [4]) it has been shown that the value of δ_{t0} depends on the distance $\bar{x}$ to the ignition source (the latter was not taken into account at all by A.V. Talantov). Such a result can be obtained from an elementary analysis (see Fig. 2):

by definition we have

$$\tau_{cr} = \frac{\delta_{t0}}{w};$$

we can assume approximately that

$$\delta_{t0} \approx \delta_t \frac{w}{u_t} \text{ and } \frac{u_t}{w} \cong \frac{d}{2x},$$

where $\underline{x}$ is the distance from the vertex of the flame cone to the base of the burner; $\underline{d}$ is the diameter of the burner, and δ_t is the width of the combustion zone along the radius.

Hence

$$\tau_{cr} = \frac{\delta_t}{u_t}.$$

As will be shown later, assuming D = const = u'$\underline{l}$', we get

$$\delta_t = A\underline{x} \quad \text{for small } \underline{x}; \qquad (*)$$

$$\delta_t = A\sqrt{2\underline{l}_0 x} \quad \text{for large } \underline{x}. \qquad (**)$$

Since u_t is independent of $\underline{x}$, in both cases [(*) and (**)] the value of τ_{sg} will depend on the distance to the ignition source. This factor was not accounted at all by A.V. Talantov, let alone the fact that generally the characteristic of τ_{sg} is quite arbitrary.

Actually, however, the combustion time in a turbulent flame is

determined just as in a laminar one:

$$\tau_{sg} = 1/u_n^2.$$

According to modern notions concerning turbulent combustion, found for example in [14, 15] and others, and based on the physical model of K.I. Shchelkin, the width of the combustion zone of a turbulent flame is determined by the depth of the bends produced in the flame front under the influence of turbulent pulsations. These bends, and also the pulsations of the flame front, are determined by the statistical value of the mean-square displacement of the flame dimension $\sqrt{\overline{Y}^2}$, which as before leads to the inequality $\delta_t \approx \sqrt{\overline{Y}^2}$.

The quantity $(\overline{Y}^2)^{1/2}$ can be calculated theoretically if we disregard the influence of the normal velocity and autoturbulization (the normal velocity decreases the value of $(\overline{Y}^2)^{1/2}$ as a result of the smoothing effect, which in some cases is justified):

$$(\overline{Y}^2)^{1/2} = \varepsilon x \text{ for } x \leqslant \frac{l_0}{\varepsilon}; \qquad (14)$$

$$(\overline{Y}^2)^{1/2} = \sqrt{2\varepsilon l_0 x} \text{ for } x > \frac{l_0}{\varepsilon}. \qquad (15)$$

To determine the value of $\delta_t \sim (\overline{Y}^2)^{1/2}$, it is thus necessary to reduce statistically a large number of instantaneous positions of the flame front.

In practice, however, to determine the width of the combustion zone, one usually resorts to a measurement of the flame temperature with the aid of thermocouples or other inertial measurement methods.

Of certain interest can be data on the width of the combustion zone, obtained with the aid of ionization transducers, since this method of measurement is sufficiently sensitive and makes it possible to fix individual oscillations of the flame.

In [4] the width of the combustion zone was determined with the aid of ionization transducers which crossed the flame torch rapidly

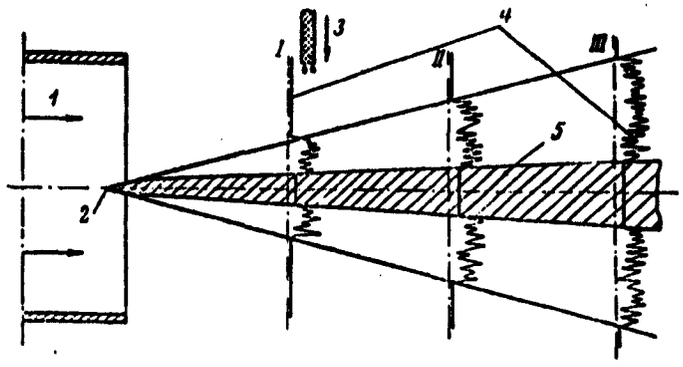

Fig. 3. Determination of the flame boundary with the aid of an ionization transducer. 1) Homogeneous gasoline-air mixture; 2) source of mixture ignition; 3) direction of motion of ionization transducer in crossing the flame torch; 4) typical patterns of the distribution of the ionization current; 5) products of total combustion of the mixture.

(Fig. 3) in an open stream and using a cylindrical combustion chamber. The rate of crossing such a flame was about 0.5 m/sec, whereas the velocity of the incoming stream was $\geq$50 m/sec. By the same token, what was actually plotted was not the instantaneous distribution of the ionization current over the transverse cross section of the flame torch, but the time-averaged pattern.

As is well known, in the zone of chemical transformations, for example of a laminar flame, one observes increased ionization, which makes it possible to separate the region of chemical transformations from the region of the total-combustion products of the turbulent flame torch.

The width of the combustion zone δ_{t_u} obtained in [4] (along the radius of the flame torch) should, starting from the probability-theory relations, amount to (assuming the measurement error to be ~1%)

$$\delta_{\tau_u} \approx 4{,}6\,(\overline{\gamma^2})^{1/4}. \qquad (16)$$

In order to verify the correctness of this relation, the results of the experiments of [4] were reduced in the form of a relation

$$\bar{\delta}_t = f(\bar{x}),$$

where $\bar{\delta}_t = \delta_t / 4.6$ and $\bar{x} = 2x/d$.

On the other hand, Relations (14) and (15) are known.

As can be seen from Fig. 4, the obtained values of $\delta_t/4.6$ and $(Y)^{1/2}$, calculated from Eqs. (14) and (15), practically coincide. The velocity of the incoming stream, the composition of the combustible mixture (meaning also u_n) did not influence the value of δ_t. The value of δ_t likewise was independent of the conditions under which it was determined – in an open stream or in a cylindrical combustion chamber. The results obtained are confirmed also by the data of [11].

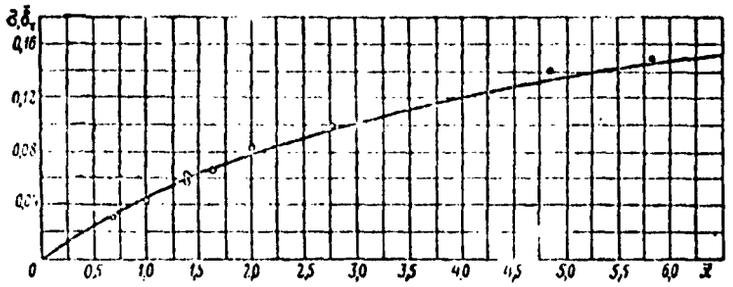

Fig. 4. Dependence of the mean-square displacement of the flame on the relative distance to the ignition source. ——) Calculated values of mean-square displacement σ; O) experimental values of $\bar{\delta}_t$, obtained in open-stream installations (w = 35-50 m/sec; α = 0.5-1.3); ●) values of $\bar{\delta}_t$ in cylindrical chamber ∅ 145 mm (w = 35-75 m/sec; α = 0.7-1.3).

3. PROPOSED CALCULATION PROCEDURE

The foregoing analysis demonstrates the principal feasibility of designing the combustion chamber. As in many of the papers considered above, one can use Eqs. (1), (4), (6), and (8) as a basis. One can also use, as was done by A.V. Talantov, the condition of H. Tsien [9] in order to close the system of equations. Finally, the last equation necessary for the calculation will be the relation

$$\delta_r \sim (\overline{Y^2}) = f(\bar{x})$$

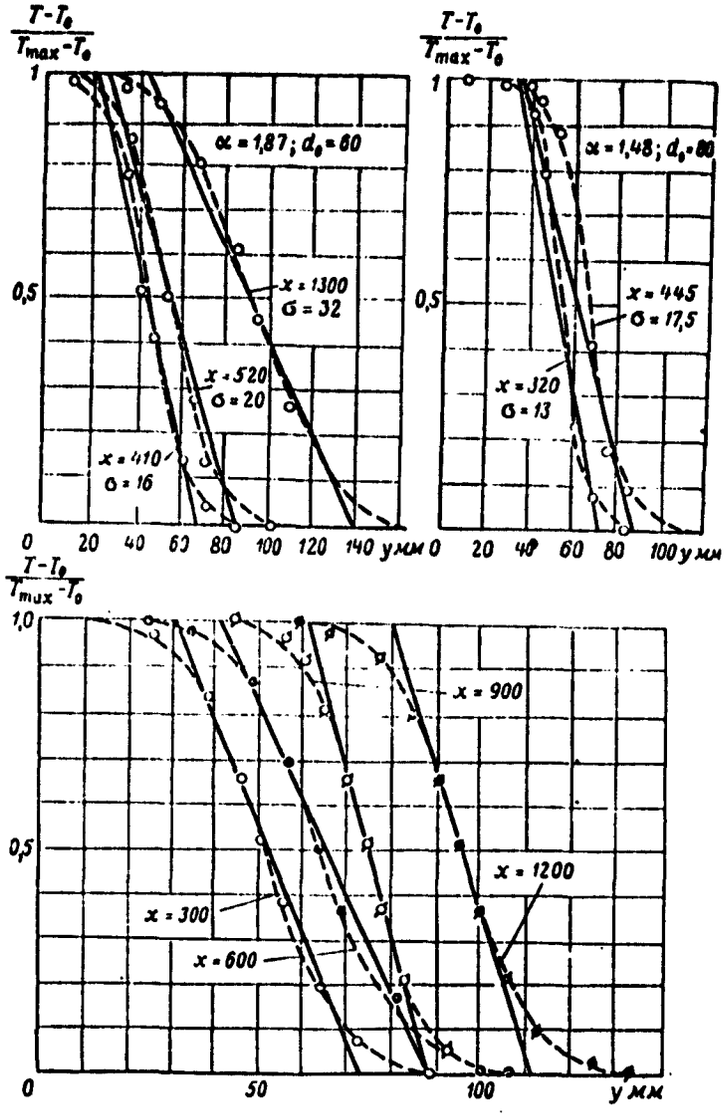

Fig. 5. Experimental and theoretical dimensionless temperature profiles behind a single stabilizer (a linear temperature variation — solid lines — was assumed in the work).

[see Eqs. (14) and (15)].

To calculate the position of the flame boundary and the burnout boundary it is necessary to know not so much the values of δ_t or τ_{sg}, as the variation of the velocity and temperature in the transverse cross section of the flame torch. As shown by a reduction of the experimental results, the temperature profile along the flame torch is

rather complicated (Fig. 5). As shown in [11], the temperature profile can be defined by means of a relation of the type

$$p_2 = \frac{\overline{T} - T_0}{T_{max} - T_0} = \frac{1}{2}[1 - \Phi(t)],$$

where $t = \frac{y - a}{\sigma}$;

$\Phi(t)$ is the tabulated Gauss integral.

However, such a law for the temperature variation does not make it possible to integrate (6) (numerical integration leads to exceedingly complicated expressions).

An analysis of the available experimental material makes it possible to obtain a simpler solution, namely to represent the temperature variation by a linear law. All the change in the temperature from T_0 to T_{max} occurs within a zone having a depth

$$\delta_T = 3\sigma \left(\sigma = \sqrt{\overline{Y^2}}\right).$$

The coefficient "3" is the result of processing numerous experiments (see Fig. 4). [Incidentally, in other works (for example [6]), the law governing the temperature and velocity variation was assumed linear, but over a depth ~6σ.]

We thus put

$$\tau_3 = \frac{\tau_1 - \tau_{in}}{\tau_{ic} - \tau_{in}}(\tau_c - \tau_n) + \tau_n.$$

The variation of the velocity over the depth δ_t of the zone is also assumed linear:

$$u_3 = \frac{\eta - \eta_n}{\tau_{ic} - \tau_{in}}(u_c - u_n) + u_n.$$

After all these simplifications, the system of equations for the determination of $\eta_s = f(\overline{x})$ is written in the form

$$\tau_n = \lambda_n \tau_c; \tag{17}$$

$$u_c = \sqrt{\frac{1 - \tau_c}{\frac{k-1}{2} M_0^2} + 1}; \tag{18}$$

$$u_n = \sqrt{\frac{\lambda_n - \tau_n}{\frac{k-1}{2} M_0^2} + 1}; \tag{19}$$

$$\pi = \tau_c^{k/k-1}; \tag{20}$$

$$\delta_\tau = 3\sigma = f(x); \quad 3\sigma = \eta_s - \eta_n; \tag{21}$$

$$\Delta x = \sqrt{\left\{\frac{2\left[\left(\frac{\pi}{\tau_{c(i-1)}}\right)(1-\eta^2_{c(i-1)})u_{c(i-1)} - \left(\frac{\pi}{\tau_{ci}}\right)(1-\eta^2_{ci})u_{ci}\right]}{\left[\left(\frac{\pi}{\tau_{c(i-1)}}\right) + \left(\frac{\pi}{\tau_{ci}}\right)\right](\eta_{c(i-1)} + \eta_{ci})\bar{u}_\tau}\right\}^2 - (\eta_{ci} - \eta_{c(i-1)})^2}, \tag{22}$$

$$\eta_c = -\frac{P}{2A} + \sqrt{\frac{P^2}{4A^2} - \frac{Q}{A}}, \tag{23}$$

where

$$P = \frac{2\sigma}{\tau_c - \tau_n}\left(u_c - u_n\frac{\tau_c}{\tau_n}\right);$$

$$A = \frac{u_n}{\tau_n} - \frac{u_c}{\tau_c};$$

$$Q = \frac{u_c}{\tau_c} - \frac{1}{\pi}.$$

The quantities to be determined are: τ_s, τ_p, u_s, u_n, π, σ, η_s, $\Delta\bar{x}$. The known quantities are: M_0, λ_p, $\underline{k}$, $\bar{u}_t$, w_0, u_n.

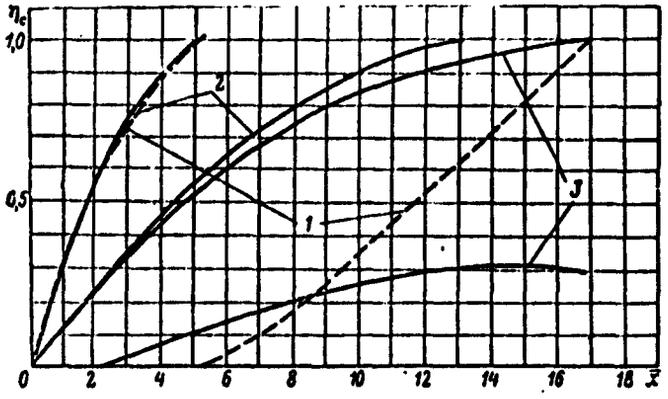

Fig. 6. Position of the flame boundary as calculated by A.V. Talantov (1) and as calculated by the proposed method (2) [3 – results of calculation by the proposed method if one assumes that u_t = = 2.26 m/sec (curves 2 are obtained for w = 50 m/sec, u_t = 10 m/sec, T_0 = 288° abs)].

The number of unknowns is eight and the number of equations is seven, but one of the unknowns is the argument (for example τ_s or $\Delta\bar{x}$),

so that there are enough equations to obtain the solution.

These equations enable us to complete the calculation, going from section to section, by successive approximations.

In order to compare this method of calculation with the calculation as given by A.V. Talantov, we calculated the example given in [9] for the following initial conditions: $w = 50$ m/sec, $u_t = 10$ m/sec, and $T_0 = 288^\circ$ abs. It must be noted that the chosen value of u_t in this example is highly exaggerated. Under ordinary conditions with $\varepsilon = 0.05$ the values of u_t, as will be shown later on, are noticeably smaller than those specified. The results of such a calculation are shown in Fig. 6. It can be seen that, as expected, both methods give approximately the same initial front position, but the final position of the front differs greatly from that calculated by A.V. Talantov. For a more correct comparison of both methods, it is necessary to take account of the fact that the values of u_t used by A.V. Talantov differ greatly from the real values (this is due to determining u_t from the forward boundary of the flame, which is incorrect, see [2]). Indeed, as follows from the calculation based on our experimental data (which should yield the true value of u_t), we have $u_t = 2.26$ m/sec for $\varepsilon = 0.05$; $\alpha = 1.2$. For the same conditions and even for somewhat smaller values of u_n, we obtain from A.V. Talantov's equations [7]: $u_t = 5.3(u')^{0.7}(u_n)^{0.3} = 7.7$ m/sec. If we take $u_t = 2.26$ m/sec, calculate the position of the flame boundaries in accordance with the proposed method, and compare with the calculations of A.V. Talantov, we obtain a considerable disparity in the results (see Fig. 6).

In order to calculate the total length of the combustion chamber, it is necessary to obtain a method for determining the coordinate η_p in the sections of the chamber where $\eta_s = 0$.

In this case it is recommended that the following obvious rela-

tion be used:

$$L_{z.r} = \delta_t \frac{u_{cp}}{u_t} = 3\sigma \frac{u_{cp}^2}{u_t u_0},$$

where $L_{z.g}$ is the width of the combustion zone along the current line, u_{sr} is the average stream velocity at the center of the combustion zone $L_{z.g}$, and

$$u_{cp} = \frac{u_{c0} + u_{n.k}}{2}.$$

In many cases it is possible to put approximately $u_{sr} \approx u_n$, and then we obtain finally

$$L_{z.r} = 3\sigma \frac{u_n^2}{u_t u_0}.$$

In many approximate calculations, when the form of the curve $\eta_s = f(x)$ can be neglected, the calculation of the position of the flame boun dary [$\eta_s = f(x)$] greatly simplifies. Here the total length of the cold part of the chamber (until the torch touches the chamber walls, $\eta_s = 1.0$) remains practically constant. In this case the entire calculation can be carried out by assuming the flame front to be infinitesimally thin, i.e., determine the curve $\eta_s = f(x)$ and then find the value $\delta_t = 3\sigma$ for each value of x. The calculation is carried out in accordance with the following scheme.

The specified quantities are: M_0, k, λ_p, τ_s, and we determine: τ_p, u_s, u_p, π, η_s.

$$\tau_n = \lambda_n \tau_c; \quad \lambda_n = 1 + \frac{\eta_n}{c_p T_0};$$

$$u_c = \sqrt{\frac{1 - \tau_c}{\frac{k-1}{2} M_0^2} + 1}; \quad u_n = \sqrt{\frac{\lambda_n - \tau_n}{\frac{k-1}{2} M_0^2} + 1};$$

$$\pi = \tau_c^{k/k-1}; \quad \eta_s = \sqrt{\frac{1}{\pi} \frac{\pi/\tau_c - u_c}{(u_n/\tau_n - u_c/\tau_c)}}.$$

In view of the great interest that attaches to data on the absolute values of u_t, it is interesting to calculate the values of u_t as obtained from ordinary results of combustion-chamber tests [for exam-

ple, from the variation of the static pressure along the combustion chamber $z = f(x)$]. Such a calculation scheme can be readily set up on the basis of the equations given above. The calculation sequence will be as follows:

$$\pi = 1 - \frac{kzM_0^2}{2}; \tag{24}$$

$$\tau_c = \pi^{\frac{k-1}{k}}; \tag{25}$$

$$\tau_n = \lambda_n \tau_c; \tag{26}$$

$$u_c = \sqrt{\frac{1 - \tau_c}{\frac{k-1}{2} M_0^2} + 1}; \tag{27}$$

$$u_n = \sqrt{\frac{\lambda_n - \tau_n}{\frac{k-1}{2} M_0^2} + 1}; \tag{28}$$

$$u_\tau = \sqrt{\frac{\left\{2\left[\left(\frac{\pi}{\tau_{c1}}\right)\left(1 - \eta_{c1}^2\right) u_{c1} - \left(\frac{\pi}{\tau_{c2}}\right)\left(1 - \eta_{c2}^2\right) u_{c2}\right]\right\}^2}{\left\{\left[\left(\frac{\pi}{\tau_{c1}}\right) + \left(\frac{\pi}{\tau_{c2}}\right)\right](\eta_{c2} + \tau_{c1})^2 [\Delta x^2 + (\eta_{c2} - \tau_{c1})^2]\right.}}; \tag{29}$$

$$\tau_{ic} = -3sp + \sqrt{9s^2p^2Q}; \tag{30}$$

$$p = \frac{u_c - u_n \frac{\tau_c}{\tau_n}}{(\tau_c - \tau_n)\left(\frac{u_n}{\tau_n} - \frac{u_c}{\tau_c}\right)};$$

$$Q = -\frac{\pi^{\frac{u_c}{\tau}} - 1}{\pi\left(\frac{u_n}{\tau_n} - \frac{u_c}{\tau_c}\right)}.$$

Let us proceed now to an examination of the experimental results of the investigation of burnup in a combustion chamber.

In the present work we investigated a combustion chamber of very simple type, with diameter 150 mm and length of the hot portion L_g = = 720 mm. The ignition and stabilization source was a conical stabilizer 12 mm in diameter. The static pressures were sampled along the chamber (Fig. 7). The following conditions were varied: the velocity of the incoming stream and the mixture composition α. The experimental results were obtained in the form a dependence $z = f(\bar{x})$ for various initial conditions.

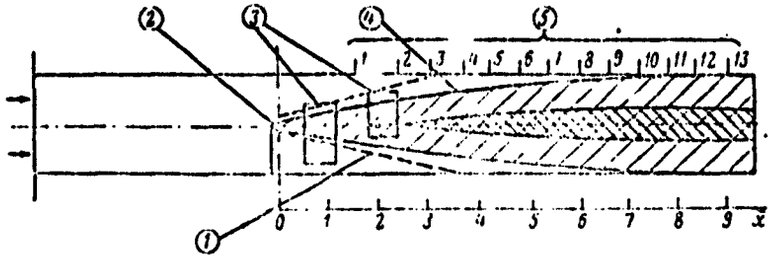

Fig. 7. Schematic representation of the configuration and of the measurement system for a combustion chamber. 1) Location of turbulizing grids; 2) flame stabilizer; 3) transparent windows; 4) flame torch; 5) sampling of static pressure.

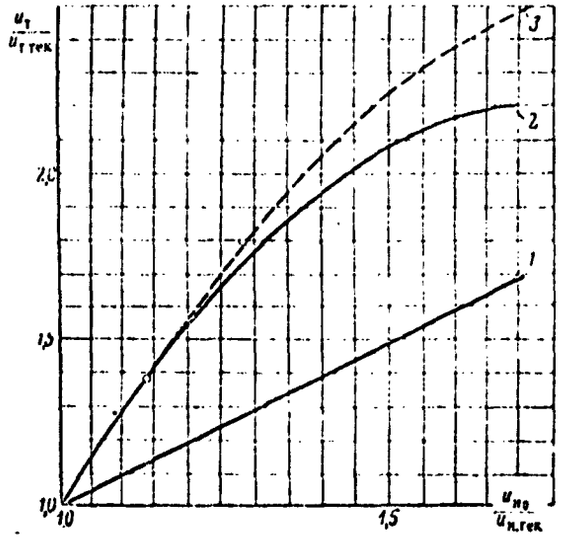

Fig. 8. Relative variation of rate of turbulent combustion as a function of the normal combustion velocity. 1) Dependence $u_t/u_{t.tek} = u_n/u_{n.tek}$; 2) dependence $u_t/u_{t.tek} = u_n/u_{n.tek} \times T_2/T_{2tek}$; 3) results of calculation from the experimental data for the conditions $w_0 = 50$ m/sec; $\alpha = 1\text{-}1.6$.

Knowing from experiment the value

$$\zeta = \frac{\Delta p}{\rho_0 \frac{w_0^2}{2}}$$

in a given section of the combustion chamber, it is possible to deter-

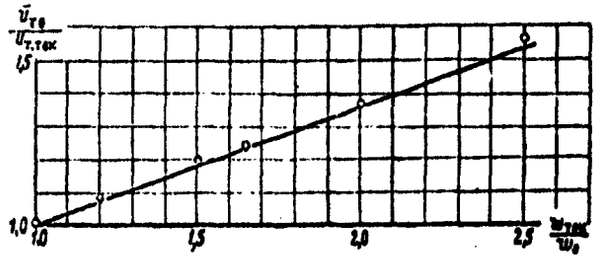

Fig. 9. Relative variation of the rate of turbulent combustion with increasing stream velocity.

mine the current values of η_s, η_p, u_t, etc. The quantities Δx and σ are known (we assumed in this work $\varepsilon = 0.05$; for these conditions σ is determined from Fig. 4).

The values of $\bar{u}_t$ were determined for individual portions Δx of the combustion chamber, after which the average value of $\bar{u}_t$ was determined. The results of the calculation are shown in Figs. 8 and 9.

The order of the obtained values of u_t amounts to $0.5\text{-}1.5\bar{u}'$, which is in good agreement with present-day notions concerning turbulent combustion (see [14, 15]). The dependence obtained $u_t \approx (u')^{0.5\text{-}0.6}$ and $u_t \approx u_n$ (in the region $\alpha \geq 0.9$) is in good agreement with the known experimental results, which yield the dependence $u_t = f(u', u_n)$ (see [15]), taking into consideration the errors of the calculation.

A somewhat stronger influence of u' (via the action of $\underline{w}$) and of u_n on the value of u_t than in Reference [15] can be attributed to the influence of the ignition source. In the case of small ignition-source dimensions the completeness of combustion near the source along the stream axis, as is well known, can be considerably smaller than the usual value 0.95-0.98. In this case the start of ignition of the combustible mixture occurs not near the edges of the stabilizer, but fur-

ther downstream, something not taken into account in the present calculation.

It must be noted that inasmuch as the flame front does not touch the chamber walls in the majority of modes ($\eta_s < 1.0$), a correction was introduced in the calculation of $u_t = f(u_n)$ for the expansion of the combustion products, as was done in the paper by Yu.A. Shcherbina [11].

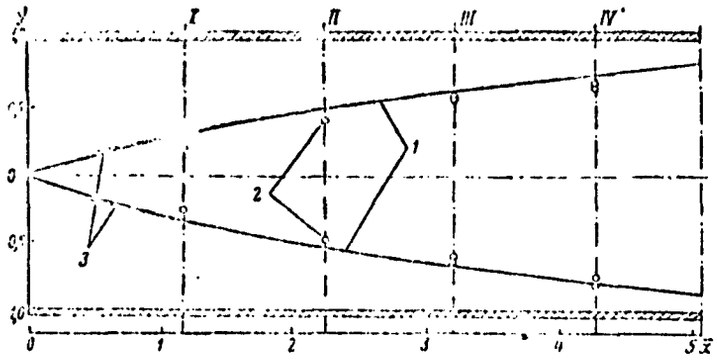

Fig. 10. Position of boundaries of the flame torch. 1) Calculated; 2(0)) experimental points obtained by the ionization-transducer method; 3) boundaries obtained by the method of direct photography.

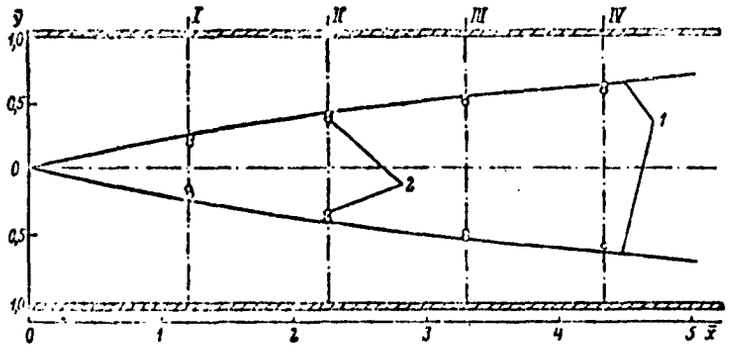

Fig. 11. Position of boundaries of the flame torch. 1) Calculated; 2(0)) experimental points obtained by the ionization-transducer method.

Thus, we can finally assume in first approximation

$$\bar{u}_t = u_{t0}\left(\frac{\dot{w}}{\dot{w}_0}\right)^{0,6}\left(\frac{\varepsilon}{\varepsilon_0}\right)^{0,2}\left(\frac{u_n}{u_{n0}}\right)\left(\frac{T_{max}}{T_{max0}}\right),$$

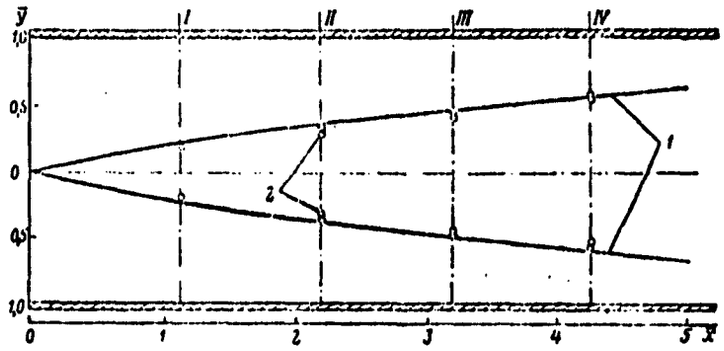

Fig. 12. Position of boundaries of the flame torch. 1) Calculated; 2(0)) experimental points obtained by the ionization-transducer method.

where $u_{t0} = 0.092$; $w_0 = 30$ m/sec; $u_{n0} = 81$ cm/sec; $T_{max0} = 2400^\circ$ abs; $\varepsilon_0 = 0.05$.

In the case when the flame torch touches the walls of the combustion chamber we have

$$\frac{T_{max}}{T_{max0}} = 1.0.$$

We also compared the flame boundaries in a cylindrical chamber as determined by the calculation method and as determined by the ionization-transducer method [2], and also by photography through the window of the combustion chamber. As can be seen from Figs. 10-12, good agreement with the calculation data was obtained.

CONCLUSION

A method was proposed for the design calculations of a very simple ramjet combustion chamber, consisting of closing the fundamental gasdynamic equations for the flow of a combustible mixture in a cylindrical tube with a pointlike ignition source, by introducing a supplementary condition whereby the width of the combustion zone depends on the distance to the ignition source.

The results of the calculation were compared with some experimental data. Good agreement between calculation and experiment was demon-

strated.

Manuscript Page No.	[Footnote]
118	We present below all the fundamental equation, without which any calculation of the combustion chamber is impossible.

Manuscript Page No.	[List of Transliterated Symbols]
116	н = n = normal'nyy = normal
117	с = s = smes' = mixture
117	п = p = produkt = product
117	г = g = goreniye = combustion
117	з = z = zona = zone
118	х = kh = [not identified]
120	ср = sr = srednyy = average
121	п = p = polnoye = total
121	в = v = vydelivshiysya = released
122	сг = sg = sgoraniye = combustion
124	т = t = turbulentnyy = turbulent
124	м = m = [maksimal'nyy = maximum]
134	з.г = z.g = zona goreniye = combustion zone
134	п.к = p.k = produkty, konets = products, end
135	г = g = gorvachiy = hot
136	тек = tek = tekushchiy = current, present

DISTRIBUTION LIST

DEPARTMENT OF DEFENSE	Nr. Copies
HEADQUARTERS USAF	
AFCIN-3D2	1
ARL (ARB)	1
OTHER AGENCIES	
CIA	1
NSA	6
[illegible]	9
AID	2
OTS	2
AEC	2
[illegible]	1
NASA	1
ARMY (FSTC)	3
NAVY	3
NAFEC	1
	12
[illegible]	1
SPE[illegible]	1

MAJOR AIR COMMANDS	Nr. Copies
AFSC	
SCFDD	1
DDC	25
TDBTL	5
TDBDP	5
AEDC (AEY)	1
SSD (SSF)	2
BSD (BSF)	1
AFFTC (FTY)	1
ASD (ASYIM)	1